BOSTON UNIVERSITY

SCHOOL OF MEDICINE

Dissertation

DEAMIDATION AND RELATED PROBLEMS IN STRUCTURAL ANALYSIS OF PEPTIDES AND PROTEINS

by

NADEZDA P. SARGAEVA

B.S., St. Petersburg State Polytechnical University, 2002

M.S., St. Petersburg State Polytechnical University, 2004

Submitted in partial fulfillment of the

requirements for the degree of

Doctor of Philosophy

2012

Approved by

First Reader _____

Peter B. O'Connor, Ph.D.

Associate Professor of Biochemistry

Second Reader _____

Cheng Lin, Ph.D.

Assistant Professor of Biochemistry

Dedications

I dedicate this thesis to my Family

Acknowledgments

I would like to express my deepest gratitude to my advisor, Prof. Peter B. O'Connor. We met in St. Petersburg, Russia in 2004 and you believed in my abilities and you gave me an opportunity to be a part of such a great mass spectrometry program. I also want to thank you for your support and your guidance throughout my Ph.D. studies. Thank you for pushing me to achieve my goals of learning and becoming a better scientist, and for the opportunity you gave me to build up my professional and scientific network. Your help, your advice, and your encouragement in building up my professional career are very much appreciated.

Prof. Cheng Lin, thank you for being my second reader and mentor. Working with you has always been a pleasure – I highly value your well thought out ideas, your constant use of the scientific principle, and your willingness to follow up regarding the data, the future directions, etc. I truly appreciate your attention to details, your regular availability and willingness to help me hands on. Thank you for mentoring me not just throughout the program but also regarding the life journey I'm about to embark on.

Peter and Cheng, you are the two most influential people that helped me achieve my goals and I thank you very much from the bottom of my heart.

I would like to express my gratitude to the other members of my thesis advisory committee: Prof. Carmela Abraham, Prof. Matthew Nugent, Prof. Mark E. McComb, and Prof. Joseph Zaia for spending your valuable time serving on my committee and giving me constructive criticism and advice. Special thanks to Mark (along with Nancy Leymarie), for spending a lot of time with me working on the last challenging project – your contribution is very much appreciated.

I am sincerely thankful to Prof. Catherine E. Costello. Your wealth of experience and, more importantly your willingness to share it, have been very important to my development. Thank you for your valuable advice and your contribution to my studies.

The research groups of Prof. Dieter Seebach, Prof. Sam Gellman, Prof. Kaj Blennow, and Prof. Mikhail Gorshkov are highly appreciated for their great collaborations and inimitable samples.

My dear fellow former and present students and colleagues, it was a pleasure to get to know you and work with you. Special gratitude goes to Dr. Chunxiang Yao, Dr. Weidong Cui, Amanuel Kehasse, Dr. Nancy Leymarie, and Dr. Sandrine Voillard Bourgoin. Dr. Jason Cournoyer, Dr. Cheng Zhao, Dr. Vera Ivleva, and Dr. David Perlman thank you for your immense help during my initial stages of the program. Dr. Konstantin Aizikov, Prof. Alexander Ivanov, Dr. Bogdan Budnik, and Prof. Eugene Moskovets, thank you for your friendship and your willingness in help through all the years of my Ph.D. studies. Eugene, I truly appreciate your help well before and throughout the program; you are always ready with scientific advice and life guidance.

Most importantly, my wonderful family and friends, I'm so blessed to have all of you in my life. My beloved husband, Alexander Cherkassky, I would not be able to go through the obstacles, especially during the last months, without your endless help, moral support, and infinite love. I'm very lucky to deserve all the kindness and unconditional love of your wonderful family, especially, your Mother, Polina, and your sister, Rimma. To the best possible parents in life, my Mother, Alla, and my Father, Pavel, and to my dearest sister, Olga - I never feel that we are across the ocean; you are always here with me in my heart. I can't be thankful enough for you being there for me at all times – the day or the night.

DEAMIDATION AND RELATED PROBLEMS IN STRUCTURAL ANALYSIS OF PEPTIDES AND PROTEINS

(Order No.)

NADEZDA P. SARGAEVA

Boston University School of Medicine, 2012

Major Professor: Peter B. O'Connor, Ph.D., Associate Professor of Biochemistry

ABSTRACT

Electron capture dissociation (ECD) and electron transfer dissociation (ETD) can generate unique fragments and preserve post-translational modifications (PTMs), enabling their detection in biological samples. They have been used to differentiate isomeric aspartic (Asp) and isoaspartic acids (isoAsp) produced upon non-enzymatic deamidation of asparagine (Asn) – a frequently occurring PTM. IsoAsp formation was detected in amyloid-β (Aβ) peptides in the specimens of Alzheimer's disease (AD) patients, and is a potential biomarker for AD if it can be detected early in biofluids of live individuals. Synthetic isoAsp-containing Aβ fragments were studied using ECD to test the method's applicability. IsoAsp-7 and -23 were detected in top-down analysis of the 4.5kDa Aβ42 protein and in Aβ17-28 peptide. Further, a related method, electron ionization/impact dissociation (EID), was successfully applied to Asp/isoAsp differentiation for the first time. High-performance liquid chromatography (HPLC) is a powerful technique for the separation of complex mixtures. HPLC separation of Asp- and isoAsp-containing peptides revealed inconsistent elution orders, especially when isoAsp was located at the N-terminus, requiring ECD for identification. New diagnostic

fragments were proposed for N-terminal isoAsp based on the ECD and ETD results. Challenges in detection of such fragments were improved by supplemental activation and chemical modifications. Furthermore, a model for retention time prediction was applied to isoAsp-containing peptides and suggested for their improved identification in HPLC-MS/MS approach. IsoAsp is a β-amino acid, which distinctively contains an additional methylene group in the backbone, forming a C_α-C_β bond. Cleavage of this bond provides diagnostic fragments for isoAsp by ECD. The same was proposed for other β-amino acids. However, the C_α-C_β bond cleavages were rare due to the instability of the C_β radical. Alternatively, in-source decay (ISD) fragmentation during matrix-assisted laser desorption/ionization (MALDI) process can produce abundant ECD-like fragmentation. It was proposed that use of hydrogen-accepting matrices may lead to C_α-C_β bond cleavage in β-amino acids, because the resulting radical would be stabilized by the carbonyl group. To test this, β-amino acid-containing peptides were analyzed by MALDI-ISD using 5-nitrosalicylic acid matrix. The C_α-C_β bond cleavages were observed. Overall, new and improved methods were implemented allowing better characterization and differentiation of β-amino acids.

Table of contents

Title page……..i

Reader's approval page……ii

Dedications……...…… iii

Acknowledgements..……iv

Abstract……...vi

Table of contents.....viii

List of Tables..... xiv

List of Figures..... xv

List of Abbreviations..... xx

Chapter 1 **1**

Introduction **1**

1.1 Introduction to Mass Spectrometry in the Analysis of Biomolecules.....1

1.2 Introduction to Mass Spectrometry 2

1.2.1 Ionization Techniques and Ionization Sources.....3

1.2.2 Mass Analyzers 10

1.2.3 Tandem Mass Spectrometry 29

1.2.4 ESI QqQ-FTICR mass spectrometer.....37

1.2.5 Bruker Daltonics solariX FTICR MS 40

1.3 High Performance Liquid Chromatography (HPLC).....42

1.3.1 Reversed Phase High Performance Liquid Chromatography (RP-HPLC) 44

1.3.2 On-line and off-line Liquid Chromatography Mass Spectrometry.....48

1.4 Introduction to deamidation and isomerization of peptides and proteins 49

1.4.1 Deamidation and isomerization of peptides and proteins 49

1.4.2 Biological importance of deamidation and isomerization 51

1.5 Introduction to β-peptides 53

1.6 Thesis overview 56

Chapter 2 **57**

Identification of isoAsp in Amyloid β Peptides by Tandem ExD MS/MS **57**

2.1 Introduction 57

2.1.1 Amyloid β in Alzheimer's disease. 57

2.1.2 Isoaspartic acid formation 58

2.1.3 IsoAsp in Alzheimer's disease 58

2.1.4 IsoAsp detection methods 60

2.2 Experimental section 62

2.2.1 Peptides and reagents 62

2.2.2 Sample preparation 62

2.2.3 Mass Spectrometry 64

2.3 Results and Discussion 64

2.3.1 Distinguishing the isomers 64

2.3.2 ECD of the full length Amyloid beta protein fragment 1-40 67

2.3.3 Detecting isoAsp in Amyloid beta 1-42 69

2.4 Conclusion 73

Chapter 3 **74**

The analysis of isoAsp, Asp, and Asn containing peptide variants by Liquid Chromatography **74**

3.1 Introduction 74

3.2 Experimental section 76
3.2.1 Peptides and reagents 76
3.2.2 Liquid Chromatography 76
3.2.3 Mass spectrometry 77
3.2.4 RT prediction 77
3.3 Results and Discussion 78
3.3.1 RP-HPLC separations of isoAsp-peptides 78
3.3.2 Predictive chromatography 83
3.4 Conclusion 86
Chapter 4 **88**
Differentiating N-terminal Asp and isoAsp residues in peptides **88**
4.1 Introduction 88
4.2 Experimental section 89
4.2.1 Peptides and reagents 89
4.2.2 Deamidation 90
4.2.3 Chromatography 90
4.2.4 Mass Spectrometry 91
4.3 Results and Discussion 92

4.3.1 Diagnostic fragments for the N-terminal Asp/isoAsp.....92

4.3.2 Analysis of the deamidation products of Aβ1-10 (N1N7) by off-line RP-HPLC followed by ECD 94

4.3.3 Peak interference.....98

4.3.4 N-terminal acetylation 98

4.3.5 Analysis of the N-terminal isoAsp by ETD 100

4.3.6 The effect of ion activation 102

4.4 Conclusions.....104

Chapter 5 **105**

Detection of IsoAsp in Amyloid β Peptides From CSF **105**

5.1 Introduction.....105

5.2 Experimental section 106

5.2.1 Standard peptides.....106

5.2.2 Immunoprecipitation of Amyloid β peptides from human CSF 106

5.2.3 On-line nanoLC - ETD MS 107

5.3 Results and Discussion 108

5.3.1 NanoESI of Aβ standards.....108

5.3.2 On-line nanoLC - ETD MS analysis of the standards 109

5.4 Future concepts.....112

Chapter 6 **113**

β-Peptide analysis by ExD tandem MS **113**

6.1 Introduction.....113

6.2 Experimental section 114

6.2.1 Peptides and reagents 114

6.2.2 Sample preparation 115

6.2.3 Mass Spectrometry 115

6.3 Results and Discussion 116

6.3.1 Q_{06} beta peptide $_{\beta 2}V_{\beta 2}A_{\beta 2}L_{\beta 3}V_{\beta 3}A_{\beta 3}L$. 116

6.3.2 Charge increase 118

6.3.3 ETD of Q_{06} beta peptide 120

6.3.4 Modified Substance P 122

6.3.5 Puma BH_3 protein analogues 125

6.3.6 Proposed mechanism 128

6.4 Conclusion 134

Chapter 7 **136**

In-Source Decay for β-Peptide Analysis **136**

7.1 Introduction 136

7.2 Experimental section 138

7.2.1 Peptides and reagents 138

7.2.2 Sample preparation 138

7.2.3 Mass Spectrometry 138

7.3 Results and Discussion 139

7.3.1 Diagnostic fragments for the C_α-C_β bond cleavage 139

7.3.2 Advantages and disadvantages of the proposed method 142

7.4 Conclusion 143

Chapter 8 **144**

Conclusion and Future Perspective **144**

8.1 Conclusion 144

8.2 Future Perspective 147

Bibliography 149

Curriculum vitae 176

List of Tables

Table 3.1 The elution order results for peptides containing Asn, Asp, and isoAsp residues.....82

Table 4.1 The effect of additional energy input on the diagnostic fragment formation. Relative intensity (Rel. Int.) was calculated as the absolute intensity of the diagnostic fragment divided by the sum of the absolute intensities of all *c* and *z* fragments. 102

List of Figures

Figure 1.1 The electrospray ionization process. 6

Figure 1.2 The MALDI process. 9

Figure 1.3 The schematic of a closed cylindrical ICR cell. Ions are trapped along the axis by the trapping potential applied to the trapping plates. Cyclotron motion of the ions is indicated, which is perpendicular to the magnetic field ***B***. 19

Figure 1.4 Ion motions in an ICR cell. The axis and the magnetic field face the paper. Reproduced from Kolhinen, V. S.; et al, Commissioning of the double Penning trap system MLLTRAP, *Nuclear Instruments & Methods in Physics Research Section a-Accelerators Spectrometers Detectors and Associated Equipment*, 2009, 600, 391-397, with permission. 23

Figure 1.5 Excitation and detection of trapped ions in an ICR cell. 24

Figure 1.6 A schematic representation of the orbitrap mass analyzer. The outer electrodes form the shape of a barrel (a). Ions (*i*) move in spirals around the central spindle-shaped electrode (*b*) while oscillating back and forth along the *z* axis. 28

Figure 1.7 Peptide ion fragmentation nomenclature. 31

Figure 1.8 The ESI qQq-FTICR mass spectrometer. Reproduced (modified) from O'Connor, P. B. *et al*., Rapid Communications in Mass Spectrometry, *20*, 259-266, 2006, with permission. 38

Figure 1.9 The solariX^{TM} FTICR mass spectrometer (Bruker Daltonics). 41

Figure 1.10 Isomerization of aspartic acid and deamidation of asparagine via a succinimide intermediate. 50

Figure 1.11 β-Peptide nomenclature. 54

Figure 2.1 The ECD major pathway to produce *c* and *z* fragment ions (a); proposed ECD mechanism for formation of diagnostic fragment ions (b). 63

Figure 2.2 ECD of Aβ17-28 (a), ECD of isoAβ17-28 (b), and EID of isoAβ17-28 (c). 65

Figure 2.3 ECD of Aβ40. 69

Figure 2.4 ECD of Aβ42 deamidated at Asn7 and Asn27. 72

Figure 3.1 IsoAsp position affects the peptide elution order. 79

Figure 3.2 Chromatograms of Ang II peptide variants. 80

Figure 3.3 N-terminal acetylation preserves the elution order of isoAsp modified peptides. 81

Figure 3.4 Improved sequence identification (ID) 84

Figure 3.5 Correlation between the predicted and the experimental retention time: Ang II variants separated in FA (a) experiment and (b) correlation; synthetic variants separated in TFA (c) experiment and (d) correlation. 85

Figure 3.6 Improved identification of modified peptides. 86

Figure 4.1 ECD spectra of the Angiotensin II (a) and its modified variant with isoAsp at the N-terminus (b). Insets show side-chain losses from the charge-reduced species $[M + 2H]^{+\bullet}$. IsoAsp specific fragment $[M + 2H - 74]^{+\bullet}$, produced as a result of the C_α - C_β

bond cleavage within the N-terminal isoAsp residue, is present in the modified variant only, (b) inset. 94

Figure 4.2 Chromatogram of the peptide mixture, generated by partial deamidation of the Aβ1-10 (N1N7) peptide (top panel). Each chromatographic peak labeled based on ECD results. ECD spectra shown correspond to the VIII-XI fractions with the isoAsp specific fragments indicated in the insets. 96

Figure 4.3. ECD spectra of chromatographic peaks I, IV-VII from the partially deamidated Aβ1-10 (N1N7) peptide mixture. 97

Figure 4.4 ECD spectra of the synthetic peptide variants with Asp (a) and isoAsp residues (b) amidated at the C-terminus and acetylated at the N-terminus. IsoAsp1 and isoAsp5 specific fragments, $[M + 2H - 116]^{+\bullet}$ and $z_6^{\bullet} - 57$, are observed only for the isoAsp-peptide variant. Asp side-chain losses are also indicated, (a) inset. 100

Figure 4.5 N-terminal isoAsp residue diagnostic fragment peak $[M + 2H - 74]^{+\bullet}$ detection for the Aβ1-10 peptide variant (**iD**AEFRH**iD**SGY, fraction XI in the Figure 4.4, top panel) by: (a) ETD on LTQ-Orbitrap, with supplemental activation energy parameter 15; and (b) ECD on SolariX. Insets show diagnostic peaks and their S/N ratios. 101

Figure 4.6 N-terminal isoAsp residue diagnostic fragment peak $[M + 2H - 74]^{+\bullet}$ detection using ETD without (a) or with SA (b) for the modified Ang II peptide variant (**iD**RVYIHPF). Both spectra were acquired on Orbitrap. Insets show the S/N ratio of the $[M + 2H - 74]^{+\bullet}$ peak and the appearance of additional side-chain losses upon SA (His and Tyr). 103

Figure 5.1 NanoESI mass spectrum of the Aβ40 standard peptide. Note the presence of the Aβ26-40. 109

Figure 5.2 LC-MS run of Aβ40, 200 fMol injected. On top is the total ion chromatogram (TIC). In the middle is the base peak chromatogram for the 707.90-707.92 *m/z* region, corresponding to the doubly charged ions of Aβ26-40 peptide as confirmed by ETD, which is shown on the bottom. 111

Figure 5.3 Hydrophobicity index of the Aβ40 peptide, generated by GPMAW 5.02.....112

Figure 6.1 Q_{06} beta peptide $_{\beta 2}V_{\beta 2}A_{\beta 2}L_{\beta 3}V_{\beta 3}A_{\beta 3}L$: a) ESI, b) IRMPD, c) EID. Asterisk indicates noise peaks. 118

Figure 6.2 ECD of Q_{06}•cholamine. 119

Figure 6.3 ETD of Q_{06} β_2/β_3-peptide.....121

Figure 6.4 ECD of Substance P: a) unmodified, b) modified at Q_5 and L_{10} to β_3-type amino acids. 123

Figure 6.5 ECD mechanism within α- vs. β-amino acid residues. 124

Figure 6.6 ECD of Puma BH_3 protein analogue I. 126

Figure 6.7 ECD of Puma BH_3 protein analogue II. 127

Figure 6.8 ECD cleavage scheme of Puma BH_3 protein analogues I and II. 127

Figure 6.9 ECD mechanism for β-amino acid residues. 129

Figure 6.10 ECD of triply charged substance P $[M+3H]^{3+}$: a) unmodified, b) modified at Q_5 and L_{10} to β_3-type amino acids. 131

Figure 7.1 Formation of the ISD fragments: (a) *c/z*-type via hydrogen attachment and (b) *a/x*-type via hydrogen abstraction. 137

Figure 7.2 MALDI-ISD-FTICR mass spectrum of modified substance Pusing 5-NSA matrix. Data was acquired at the Bruker Daltonics facility, Billerica, MA. 139

Figure 7.3 MALDI-ISD-FTICR mass spectrum of the β-Q06 peptide. Insets show the diagnostic ions for β_2-valine-1, and β_3-leucine-5 amino acids with corresponding region of a blank matrix as a control on top. * indicates abundant matrix cluster ions, ** indicates unidentified chemical noise peaks. 140

Figure 7.4 Upon the loss of a hydrogen, amide nitrogen radical would cleave the C_α-C_β bond producing diagnostic *a*-14 and $x^{\bullet}$+14 in the case of the β_3-type amino acid (a) and *a*-[side chain] and $x^{\bullet}$+[side chain] in the case of the β_2-type amino acid (b). 142

List of Abbreviations

1,5-DAN	1,5-diaminonaphtalene
2,5-DHB	2,5-Dihydroxy benzoic acid
2-AA	2-aminobenzoic acid
2-AB	2-aminobenzamide
3D	three dimensional
5-FSA	5-formylsalicylic acid
5-NSA	5-nitrosalicylic acid
Å	angstroms
AA	acetic acid
ABC	Ammonium Bicarbonate
AC	alternating current
ACN	acetonitrile
AD	Alzheimer's disease
AI-ECD	activated-ion ECD
AI-ECD	activated ion electron capture dissociation
Ala	alanine
Ang II	angiotensin II
APCI	atmospheric pressure chemical ionization
APP	amyloid precursor protein
APPI	atmospheric pressure photoionization
Arg	arginine
Asn	asparagine

Asp	aspartic acid
Aβ	amyloid beta
BioLCCC	liquid chromatography of biomacromolecules at critical conditions
BUDA	Boston University Data Analysis
CAD	collisionally activated dissociation
CHCA	α-Cyanohydroxy cinnamic acid
CI	chemical ionization
CID	collisionally induced dissociation
CSF	cerebrospinal fluid
DC	direct current
DE	delayed ion extraction
DMSO	dimethyl sulfoxide
DNA	deoxyribonucleic acid
ECD	electron capture dissociation
EDD	electron detachment dissociation
EI	electron ionization
EID	electron ionization dissociation
ESI	electrospray ionization
ESI qQq-FTICR MS	hybrid electrospray triple quadrupole FTICR mass spectrometer
ETD	electron transfer dissociation
eV	electron volts
ExD	electron activated dissociation
FA	formic acid

FL	Lorentz force
FTICR	Fourier transform ion cyclotron resonance
FWHM	full width at half maximum
GAGs	glycosaminoglycans
GC/MS	gas chromatography mass spectrometry
Gly	glycine
HBTU	hexafluorophosphate
HCAD	high energy CAD
hDM2	human oncogene product double minute 2
HFBA	heptafluorobutyric acid
HILIC	hydrophilic interaction liquid chromatography
His	histidine
HOBt	1-Hydroxybenzotriazole
hotECD	hot electron capture dissociation
HPLC	high performance liquid chromatography
ICR	ion cyclotron resonance
ID	inner diameter
iD	isoaspartic acid
ID	identification
IEM	inborn errors of metabolism
IgG	immunoglobulin gamma
Ile	isoleucine
IP	immunoprecipitation
IRMPD	infrared multiphoton dissociation

ISD	in-source decay
isoAsp	isoaspartic acid
isoD	isoaspartic acid
IVR	intramolecular vibrational energy redistribution
kDa	kilodalton
keV	kiloelectron volts
LC	liquid chromatography
LC-MS	liquid chromatography-mass spectrometry
Leu	leucine
m/z	mass-to-charge ratio
mAb	monoclonal antibody
MALDI	matrix assisted laser desorption ionization
MeOH	methanol
Met	methionine
MRM	multiple reaction monitoring
MS	mass spectrometry
MS/MS	tandem mass spectrometry
MS2	tandem mass spectrometry
MSn	tandem mass spectrometry
nanoESI	nanoelectrospray ionization
nCI	negative CI
NP-HPLC	normal phase HPLC
OR	orifice
PA	picolinic acid

PA	protective antigen protein
PIMT	protein L-isoaspartyl O-methyltransferase
ppm	parts per million
Pro	proline
PSD	post source decay
PTM	post translational modifications
Q-o-TOF	quadrupole orthogonal time-of-flight
QqQ	triple quadrupole mass spectrometer
QTOF	quadrupole – TOF
Rel. Int.	relative intensity
re-TOF	reflectron-TOF
RF	radio frequency
RGB	Arg-Gly-isoAsp
RGN	Arg-Gly-Asn
RNA	ribonucleic acid
RNG	ring electrode
ROP	retinopathy of prematurity
RP	reversed phase
RP-HPLC	reversed phase high performance liquid chromatography
RT	retention time
S/N	signal to noise ratio
SA	supplemental activation
SD	smart decomposition
SEC	size exclusion chromatography

Ser	serine
SK	skimmer
SORI-CAD	sustained off-resonance irradiation collision activated dissociation
SRM	selected reaction monitoring
ST	stubbies
T	Tesla
TEA	triethylamine
TFA	triflouroacetic acid
TOF	time-of-flight
TOF/TOF	time-of-flight/time-of-flight tandem mass spectrometer
TQMS	triple quadrupole mass spectrometer
Trp	tryptophan
Tyr	tyrosine
UHV	ultrahigh vacuum
UPLC	ultra performance liquid chromatography
UV	ultraviolet
UVPD	ultraviolet photodissociation

Chapter 1

Introduction

1.1 Introduction to Mass Spectrometry in the Analysis of Biomolecules

Understanding the biological machinery of living organisms is the key to unveil the cause of and to cure and prevent diseases. Studying the structure and function of biomolecules can shed important light on life and disease. Mass spectrometry (MS) has become one of the most powerful tools to address this challenge in biomedical research because of its high sensitivity, specificity, speed and accuracy.

Mass spectrometry is an analytical technique that measures the mass-to-charge ratio of the molecule. The history of MS began a century ago, when the first spectra of chemical elements or ions of single atoms and their isotopes were recorded. With advances of MS technologies, it is now possible to measure the molecular mass of metabolites, proteins and protein complexes, complex carbohydrates, oligonucleotides, lipids, and even whole viruses.

Biomolecules, such as proteins, appear to have distinct structures. The function, activity, and stability of a protein are determined by its structure, which is defined by its sequence, and possible post translational modifications (PTMs). Tandem mass spectrometry is a technique that allows gas-phase fragmentation of biomolecules such as proteins, providing accurate characterization of the protein structure. With tandem MS, the protein sequence, type(s) of modifications as well as their locations within the molecule can be determined, thus allowing better understanding of its biological activity.

The power of MS was greatly enhanced when combined with liquid chromatography (LC), a technique that allows for separation of various molecules. LC - MS is a very powerful method for quantitative and qualitative analysis of complex mixtures. It is routinely applied to analyze clinical samples for known disease biomarkers, as well as for new biomarker discovery in various biofluids.

In this thesis, ion-electron and ion-ion reaction based fragmentation techniques are used in tandem MS experiments to study two common post-translational modifications - asparagine deamidation and aspartic acid isomerization, as well as the related problem of β-peptide characterization. This chapter includes an introduction to MS and LC. Various ionization methods, mass analyzers, fragmentation techniques, and LC separation methods are discussed, followed by a detailed description of the instruments used in this work. This chapter continues with an explanation of protein deamidation and isomerization, and concludes with an introduction to β-peptides.

1.2 Introduction to Mass Spectrometry

In a mass spectrometry experiment, analytes must be vaporized and ionized first, before they could be separated in electric and/or magnetic fields according to their mass-to-charge ratio (*m/z*), and detected. Therefore, all mass spectrometers contain the following major modules: an ionization source, a mass analyzer, and a detector. The mass analyzer and the detector could be a single unit as in the case of the Fourier transform ion cyclotron resonance (FTICR) MS. A fragmentation module may be added for tandem MS analysis performed tandem in space, which requires the use of two physically distinct mass analyzers. Alternatively, tandem MS analysis could be

performed in time inside of a single mass analyzer. This section will describe major types of each module that are commonly used for biomedical research.

1.2.1 Ionization Techniques and Ionization Sources

Ionization refers to the process of ion production and an ionization source is a mechanical mass spectrometer component where ionization takes place. The ionization method/sources described below work by converting a neutral molecule into an ion through electron capture, electron ejection, cationization, protonation, or deprotonation.

Conventional ionization techniques, such as electron ionization (EI), were limited to small molecule analysis because of their requirement on sample volatility and thermal stability. In EI, the harsh ionization condition (high energy electrons ~70 eV) may also lead to extensive analyte fragmentation, which further limits its application to analysis of large biomolecules. The development of new soft ionization techniques such as matrix assisted laser desorption ionization (MALDI)[1-3] and electrospray ionization (ESI)[4-6] has made possible the analysis of large intact biological molecules such as peptides and proteins, which brought mass spectrometry to a revolutionary stage in biological research. Currently, MALDI and ESI are the preferred techniques for ionization of biomolecules, as these “soft” techniques possess the appropriate sensitivity, mass range and general performance for biomolecular mass spectrometric analysis.

Electron Ionization (EI)

Electron ionization (EI, formerly referred to as electron impact) is an ionization method in which high energy electrons interact with gas phase compounds to produce ions.[7] The sample for EI has to be delivered in a gas form, which is achieved by either introducing the sample in a gas form via a capillary or “boiling off” liquid or solid sample

via thermal desorption. In many instances, before the sample is introduced into the mass spectrometer via gas capillary, gas chromatography is utilized to provide the desired analyte separation prior to MS detection (GC/MS). The typical ionization mechanism involves irradiating analytes with 70 eV electrons, which eject an electron from the molecule, leading to analyte ionization:

$$M + e^- \text{ (fast)} \rightarrow M^{+\bullet} + 2\,e^- \qquad (1.1)$$

Because an EI source employs thermal desorption of liquid and solid samples, followed by passing the sample through an electron beam, EI is considered a hard ionization technique. EI typically results in extensive fragmentation of precursor ions. Additionally, the effectiveness of EI decreases for molecules above 350-400 MW because of the necessity of thermal desorption. The issues associated with the thermal desorption are typically manifested via the involatility of larger compounds, excessive fragmentation or thermal breakdown.[8]

Chemical Ionization (CI)

In chemical ionization (CI), the ions are produced by colliding the analytes with reagent gas ions that are present in the ion source via ion-molecule reaction. Some commonly used reagent gases are: isobutene, methane and ammonia. Inside the CI source, the reagent gas is present in large excess compared to the analyte. The chemical ionization process starts with the ionization of reagent gas by electron impact. This is followed by the reaction between reagent gas ions and reagent gas neutrals to form an ionization plasma. The products of these ion-molecule reactions will react with analyte molecules to generate analyte ions. The mechanism can be depicted as follows (methane is used as an example of reagent gas):

$$CH_4 + e^- \rightarrow CH_4^{+\bullet} + 2e^- \qquad (1.2)$$

$$CH_4^{+\bullet} + CH_4 \rightarrow CH_5^+ + CH_3^\bullet \quad (1.3)$$

$$CH_5^+ + M \rightarrow MH^+ + CH_4 \quad (1.4)$$

Both positive and negative ions can be generated by reactions with this ionization plasma. Chemical ionization is a lower energy process than electron ionization, which yields less fragmentation, and usually generates a simpler mass spectrum. CI is more likely to produce the molecular ion than EI.[9]

Electrospray Ionization (ESI)

Electrospray ionization (ESI) is an important mass spectrometry ionization technique often used in biomolecular analysis. While first electrospray experiments were performed in as early as 1930's, it was not until 1989 when John Fenn's work led to the development of the modern day technique of electrospray mass spectrometry and its applications to biomolecular analysis.[5] Fenn's electrospray work was recognized with the Nobel Prize in Chemistry in 2002.

Electrospray ionization is a technique that produces gaseous molecular ions from a liquid solution under atmospheric pressure.[10] Analytes are dissolved in a solution that allows for dissolution as well as easy evaporation (e.g. a 50:50 mixutre of methanol or acetonitrile and water plus 0.1 % of formic acid). The solution is pumped through a capillary, and a strong electric field (1-5 kV) is applied between the capillary and the MS instrument inlet, often referred as the orifice. As a result, charge accumulates on the surface of the liquid forming a "Taylor cone" at the tip of the capillary.[11] When charge repulsion becomes stronger than liquid surface tension, highly charged droplets tear off the cone peak. As a droplet travels towards the MS inlet, solvent molecules evaporate, and the radius of the droplet shrinks and eventually reaches the Reyleigh limit, when Coulombic repulsion exceeds surface tension, ultimately leading to "Coulombic

explosion" and formation of smaller droplets. Drying gas and heat are often applied to help the solvent evaporation process to rid off the solvent molecules and other neutrals. This process continues on until the unsolvated charged molecular ions are generated and enter the mass spectrometer vacuum system. The process described above results in the formation of positive ions and is illustrated in Figure 1.1. In order to generate and detect negative ions, the polarity of the electric field is switched and a base instead of an acid is added to the solvent.

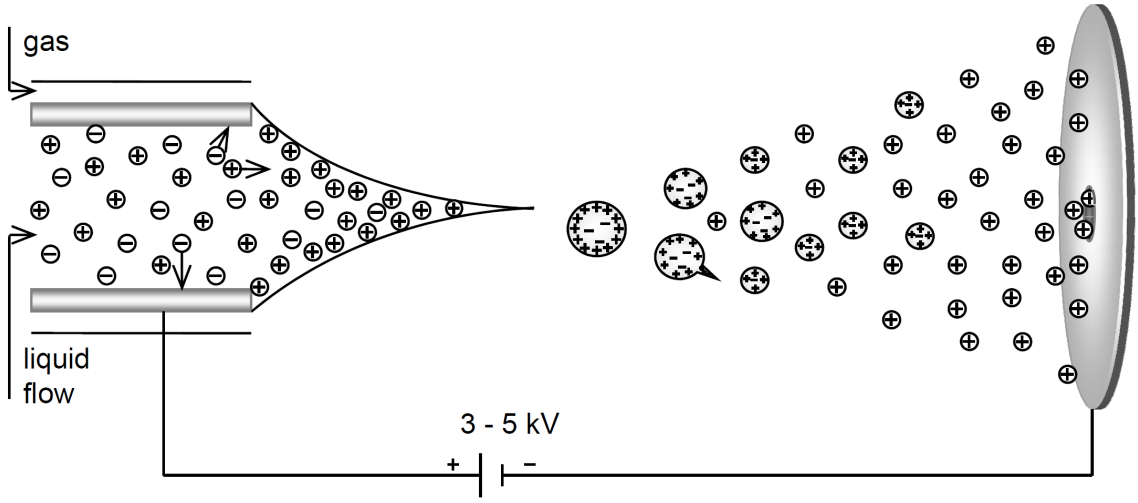

Figure 1.1 The electrospray ionization process.

ESI is a very soft ionization technique that allows observing biologically native non-covalent interactions.[12] ESI often generates multiply-charged ions allowing analysis of large molecules in a small *m/z* range (up to 3000). The presence of multiple charge states for one molecule complicates the analysis of spectra, especially with complex mixtures; fortunately modern software packages can mitigate this issue. ESI does not suffer from matrix interference, but ion suppression can limit the analysis of complex mixtures. ESI requires very clean samples and it is salt intolerant; thus, when analyzing biological samples, a careful sample cleaning is required.

Nanoelectrospray ionization (nanoESI) is an electrospray ionization variant, where a capillary with a much smaller diameter is utilized and the sample is delivered without external force at a very low flow rate (nl/min vs. µl/min in ESI). The much lower flow rate becomes essential when analyzing biological samples with limited volumes. Additionally, nanoESI generates much smaller droplets, thus reducing the necessary evaporation to generate ions. As a result, nanoESI is slightly more tolerant of salts and other impurities (less evaporation means that salt/impurities are concentrated down less during the nanoESI process).

Electrospray ionization is a powerful technique that is routinely used to analyze peptides, proteins, lipids, oligonucleotides, carbohydrates, various polymers and small molecules. ESI is a particularly powerful technique when on-line high performance liquid chromatography is coupled to a mass spectrometer providing analyte separation, sample clean up, and added specificity to biomolecular analysis.

Atmospheric-pressure chemical ionization (APCI)

Atmospheric-pressure chemical ionization (APCI)[9, 13] can be thought of as a hybrid ionization technique between ESI and CI. Similar to ESI, sample in a liquid form is delivered straight into the ionization source. However, the sample droplets are not charged (as is the case for ESI), but are simply vaporized by heat application. Similar to CI, solvent molecules are excited and ionized, followed by frequent collisions with the analytes. Consequently, the analytes become charged via proton transfer or proton loss, resulting in the formation of positive or negative ions, respectively. The differences between APCI and CI are that APCI happens at atmospheric pressure and solvent molecules are ionized by corona discharge rather than by electron irradiation.

APCI is amendable to on-line HPLC-MS systems to allow for analyte separation, sample cleanup and improved specificity. APCI typically generates singly charged ions due to its more energetic ionization process compared to ESI. APCI is particularly useful for mass analysis of non-polar compounds with moderate molecular weight up to 1.5 kDa.

Matrix Assisted Laser Desorption Ionization (MALDI)

Matrix Assisted Laser Desorption Ionization (MALDI), like ESI, is an important mass spectrometry ionization technique often used in biomolecular analysis. MALDI was first introduced through the works of Tanaka, Karas, Hillenkamp and colleagues.[1, 3] For his work, Tanaka shared the 2002 Nobel Prize in Chemistry with Fenn.

In order to perform MALDI mass spectrometry experiments, the analyte is first mixed with the matrix (typically weak organic acid, 10^2-10^6 times in excess) and crystallized on a metal plate. The surface of the crystal is then irradiated with a pulsed laser beam, which initiates matrix/sample ablation. As a result, the hot plasma plume of matrix ions and analyte neutrals is created. In this cloud of desorbed particles, multiple reactions can occur and the analyte molecules get ionized presumably via proton transfer from the protonated matrix ions (a.k.a. gas phase protonation model) or by preserving their charges from solution (a.k.a. lucky survivor model).[14, 15] Once in the gas phase, the desorbed ions are guided by electrostatic forces into the mass analyzer. The ionization process described above is demonstrated in Figure 1.2.

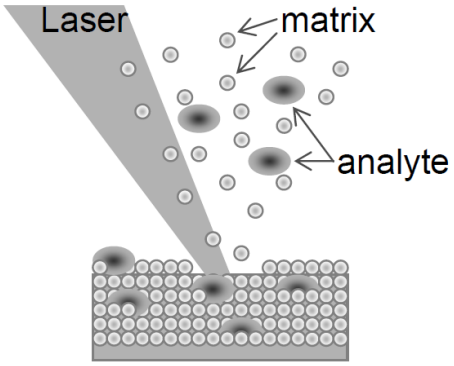

Figure 1.2 The MALDI process.

MALDI sources typically employ ultraviolet (UV) lasers, such as nitrogen lasers operated at 337 nm.[14] The matrix serves as an intermediate compound which indirectly transfers the energy from the laser to the analyte, preserving it in a non-fragmented state. This is the reason MALDI is also considered a soft ionization technique.

The matrix is often an easily crystallized small aromatic compound that readily absorbs most of the photons, thus minimizing potential sample damage. There is a great variety of matrices available for different types of analytes.[16] The most frequently used matrices for the analysis of peptide mixtures are α-Cyanohydroxy cinnamic acid (CHCA) and 2,5-Dihydroxy benzoic acid (DHB), and sinapinic acid for proteins.

Since its introduction, MALDI has become a widespread ionization technique for analysis of peptides, proteins, oligonucleotides, carbohydrates, lipids, and other biomolecules. MALDI's value for biomolecular analysis is manifested by its ability to generate molecular weight information for intact compounds. MALDI produces mostly singly charged protonated ions $[M+H]^+$, but can also generate metal-adducted ions $[M+Me]^{n+}$ (Me = K, Na, Ca, and others) if small amount of salt is present in the sample (MALDI can be tolerant to salts up to millimolar concentrations). MALDI is practical and applicable for compounds with molecular weight up to 300,000 Da and provides

relatively simple spectra, which is advantageous for heterogeneous samples. Moreover, the pulsed nature of MALDI makes it well suited for the time-of-flight (TOF) mass analyzer.

MALDI has some disadvantages as well. One of its major drawbacks is the presence of abundant matrix clusters in the low *m/z* range of the spectra, which limits the analysis of molecules with *m/z* below 500-1000. Additionally, the possibility of photo-degradation of analytes of interests by laser ablation exists. Finally, singly charged ions that are generated by MALDI might preclude certain tandem MS methods, such as those requiring multiply charged precursor ions (*vide infra*).

1.2.2 Mass Analyzers

The ionized analytes can be separated according to their *m/z* as they now can be manipulated by the electrical and magnetic field. A mass spectrum can then be recorded to provide the *m/z* information to the user. The first MS instrument was called a mass spectrograph, because the spectrum of the *m/z* values was recorded as a photograph. When the mass measurement was recorded as electronic signal, the instrument's name became the mass spectrometer.

There are many types of mass analyzers available today. They differ by their principles of operation and the following important properties: the mass range limit, the dynamic range, the mass accuracy, the resolving power (a.k.a. the resolution), the sensitivity, the scanning speed, tandem MS analysis capabilities, and cost. These characteristics are described below and throughout each subsection within this chapter.

The *mass range* limit is the *m/z* range between the low and the upper thresholds that could be measured by the mass analyzer.

The *dynamic range* is a measure of the detection range of a detector, which is characterized by the ratio of the largest to the smallest detectable signals (related to the number of ions that can be detected).

The *mass accuracy* is the ratio of the experimental *m/z* error to the theoretical *m/z* value, which is usually measured in parts per million (ppm). Mass accuracy is linked to the resolving power of the analyzer: low resolving power analyzers cannot provide high mass accuracy.

The *resolving power*, or resolution, is the ability of a mass analyzer to distinguish signals for two distinct ions with close *m/z* values. It can be calculated as

$$R = M/\Delta M \tag{1.5}$$

where,

$$M = ((m/z)_1 + (m/z)_2)/2 \tag{1.6}$$

$$\Delta M = |(m/z)_1 - (m/z)_2| \tag{1.7}$$

The resolving power can also be determined with a single peak, where ΔM is its full width at half maximum (FWHM).

The mass spectrometer's *sensitivity* is the lowest amount of sample that could be detected. In the ideal case, it would a single ion. The sensitivity depends on the efficiency of ion transmission though the mass spectrometer, defined as the ratio of the number of ions reaching the detector to the number of ions generated in the ion source.

The *scan speed* is the rate at which the analyzer measures over a particular mass range.

Tandem mass spectrometric analysis refers to the process where specific ions (often referred to as parent ions or precursor ions) were separated and selected for fragmentation (via collision with inert gas or by other techniques) to generate secondary

ions (often referred to as product ions, fragment ions, or daughter ions) whose *m/z* values are then measured. Tandem mass analysis provides additional specificity to the measurement of unknown analytes. Tandem mass spectrometry is described in more details in Chapter 1.2.3.

The cost of the instrument depends on the combination of various modules which comprise the mass spectrometer.

Quadrupole Mass Analyzer

Quadrupole mass analyzers have been utilized with EI sources since 1950's and are the most widespread mass analyzers today.[9] Since late 1980's and early 1990's, quadrupole analyzers have been utilized with ESI and APCI ionization sources. There are a few factors that led to quadrupole analyzers being the most common mass analyzers. One of these factors is their low cost. Secondly, quadrupole analyzers can operate at a relatively high vacuum pressure, which makes them compatible with high flow-rate liquid-based ionization sources, such as ESI and APCI. Additionally, quadrupole mass analyzers possess wide *m/z* range of up to 4 kDa.

The quadrupole analyzer, as its name implies, consists of four parallel metal rods. Ions are constrained within the boundary of the quadrupole under influence of a combined direct current (DC) and radio frequency (RF) potentials applied to the rods. This spatial quadrupole arrangement generates an oscillating electric field, which only allows ions with specific *m/z* to travel the entire length of the quadrupole mass analyzer, whereas other ions are filtered out.

Quadrupole mass analyzers have poor mass accuracy of ~100 ppm, limited resolution of ~4000, wide mass range of up to 4000 *m/z*, and slow scan speed (about a second for the entire mass range).

Quadrupole mass analyzers are amendable to performing tandem mass spectrometry experiments when three such analyzers are placed sequentially. Such a tandem mass spectrometer instrument is referred to as a triple quadrupole MS (QqQ, or TQMS). The first quadrupole, Q1, scans and selects the ion of interest (a.k.a. the parent or precursor ion). The second quadrupole, q2, or the collision cell, is where the selected parent ion is transmitted to and undergoes collisions with an inert gas (e.g. Argon) to induce collisionally activated dissociation (Chapter 1.2.3). The third quadrupole, Q3, is utilized to scan and analyze the resultant fragment ion(s). ESI/APCI QqQ instruments are the mass spectrometers of choice for small- and medium-sized analyte quantification in biomedical and *in vitro* diagnostics fields. Isotope dilution mass spectrometry technique is often used with these instruments for accurate quantitation of various biomarkers in order to screen for or to diagnose various disorders in clinical diagnostics laboratories.

Quadrupole Ion Trap Mass Analyzer

Ion trap mass analyzer was invented by Wolfgang Paul who later received the Nobel Prize in Physics in 1989 for this work. Following the invention of the ion trap analyzer, work by Stafford *et al.* resulted in the first commercially available ion trap mass analyzers.[17] A quadrupole ion trap operates on the similar principle as a quadrupole mass analyzer; however, the ions are trapped in the ion trap mass analyzer instead of passing through it as in the quadrupole mass analyzer. An ion trap consists of two hyperbolic endcap electrodes and a ring electrode in between the endcap electrodes. Ions are trapped in this three dimensional (3D) space by applying oscillating RF voltages to the ring electrode and non-oscillating, static DC voltage to the end cap electrodes to create a 3D quadrupolar electric field. By changing the radio frequency of

the auxiliary alternating current (AC) electric field applied to the end cap electrodes, the ions are ejected through a small hole in the endcap electrode and towards the detector.[17] In addition to 3D ion traps, there are also linear ion traps. A linear ion trap utilizes the quadrupole arrangement with sectioned quadrupoles, and uses two dimensional RF field to trap the ions.[18] A linear ion trap can be used as a selective ion filter or an actual ion trap. Linear ion traps have higher ion capacity than 3D traps, thus higher dynamic range.

Ion traps have very similar performance to quadrupole mass analyzers. Ion traps have poor mass accuracy of ~100 pm, low resolution of ~4000, wide mass range of up to 4000 *m/z*, and slow scan speed (about a second for the entire mass range). Similar to quadrupoles, ion traps are low-cost instruments. Ion traps in theory have higher analytical sensitivity than quadruples due to their ability to accumulate ions.

Ion traps are also amendable to tandem mass spectrometry, but it is not performed tandem in space (as is the case with quadrupoles), but in time. This is achieved because of the ability of an ion trap to select a single ion species of interest, while ejecting all other ions, with gas pulsing into the ion trap chamber to facilitate collisions between the selected ions and gas molecules, which subsequently results in formation of fragment ions. Moreover, the resultant fragment ions can be isolated by the same process as described above, and further fragmented to generate secondary fragment ions. This process of multiple tandem mass spectrometry analysis is known as the MS^n. Additionally, ion traps can be used to perform tandem mass analysis by electron transfer dissociation (ETD) to generate complementary *c* and *z* fragment ions.[19] This technique will be described later.

Ion traps with ESI or MALDI sources are utilized for a number of biomolecular applications such as protein characterization by MS and MS^n analysis of proteolytic digests, carbohydrate characterization and analysis as well as small molecule analysis.

Time-of-Flight Mass Analyzer (TOF)

A time-of-flight (TOF) mass analyzer is the simplest analyzer based on its physical design. The origin of TOF analyzers goes back to 1946 through the work of Stephens.[20] In a TOF mass analyzer, a cluster of different ions is accelerated through a flight tube at 10^{-7} Torr vacuum by an electric field of a constant, known strength. Because the accelerating potential is constant, all ions have the same kinetic energy when they exit the source; however, lighter ions will have higher velocities and thus reach the detector first, whereas heavier ions will reach the detector at later times. Therefore, as its name implies, a TOF analyzer measures the time it takes for an ion to reach the detector, which is subsequently converted to its *m/z* value.

Simple linear TOF analyzers such as one described above, have reasonable performance characteristics, but have been enhanced over the years to perform modern day biomolecular mass analysis. Linear TOFs have infinite *m/z* range in theory, poor mass accuracy of ~200 ppm, moderate mass resolution of ~8000 and fast scan speed (in the millisecond scale). These analyzers are generally of low cost and cannot be utilized for tandem mass spectrometry analysis. More recently, TOF analyzers have been improved to deliver much better performance for biomolecular analysis. Specifically, reflectron-TOF (re-TOF) and delayed ion extraction (DE) for MALDI sources have been at the forefront of the TOF performance enhancement.

Early MALDI-TOF instruments suffered from poor mass resolution and subsequently poor mass accuracy. This was due to the fact that ions were accelerated

instantaneously in the MALDI source into the flight tube. This resulted in ions with the same mass hitting the detector at slightly different times due to the fact that ion plasma plume formation by laser ablation and desorption is not an instantaneous, but rather a timed process lasting a finite time period, leading to the temporal spread of the originally formed ion packet. Moreover, the ion kinetic energy spread resulted in further degradation of the TOF resolution. This shortcoming of MALDI-TOF systems was overcome by an innovation known as the delayed extraction.[21] DE works by allowing for cooling and focusing of the ions prior to ion acceleration, which takes about 200 nanoseconds, thus the delayed extraction. Physically, this is achieved by pulsating high voltage to the extraction plate (between the MALDI target plate and the drift tube entrance) on a nanosecond scale in unison with MALDI laser pulses. This causes the ions that are further from the drift tube entrance being accelerated more towards the entrance and the ions that are closer to the entrance being accelerated less. In turn, the net result is an ion packet with narrower kinetic energy distribution prior to their entrance into the flight tube, ultimately resulting in tighter temporal and spatial ion distribution hitting the detector, thus the increased resolution.

Another important innovation that led to TOF being a major tool for biomolecular analysis was re-TOF.[22] Re-TOF combines the time-of-flight concept with an electrostatic mirror. The purpose of the electrostatic mirror is to reflect (hence the name) the ions towards the ion detector while improving the mass resolution. The electrostatic field allows separation of the ions that have the same *m/z* ratio, yet different kinetic energies, by increasing the amount of time it takes ions to reach the detector: higher energy ions penetrate more deeply into the reflectron, thus spending more time inside the reflectron, which partially offset their shorter flight time outside of the reflectron. Therefore, re-TOF

improves the mass resolution by improving the kinetic energy focusing and by increasing the ion path length; however, the benefit of re-TOF drops off above 5,000 *m/z*. Re-TOFs have a mass range up to 10,000 *m/z*, are fairly accurate at ~10 ppm or better, with a high mass resolution of ~15,000 or much better (e.g. the latest commercial Bruker Daltonics ultrafleXtreme TOF has a claimed 1 ppm mass accuracy and 40,000 mass resolution) and fast scan speed in the millisecond scale. These analyzers are moderately priced and can be utilized for tandem mass spectrometry analysis. Further, modern day TOF mass spectrometers can utilize not only MALDI sources, but also ESI and nano-ESI sources.

Tandem mass spectrometry experiments are possible with re-TOF mass analyzer via a technique known as the Post Source Decay (PSD). PSD is a process in which a parent ion dissociates into fragment ions after it leaves the ionization source and travels through the flight tube. Because PSD occurs in the flight tube where the ion velocity has already been established, the parent and the fragment ion(s) have the same velocity, and would arrive at the detector at the same time in linear TOF instruments, making them indistinguishable from each other. In re-TOF instruments, however, parent and fragment ion(s) have different kinetic energies, and will penetrate the reflectron to different depths, thus producing the parent and fragment ion spectra. Alternatively, fragmentation can take place inside the ion source, a process known as the in-source decay (ISD), which will be described in details later.

There are two tandem mass spectrometers utilizing TOF mass analyzers: the quadrupole – TOF (QTOF) and the TOF/TOF instruments. QTOF tandem mass spectrometry is conceptually similar to QqQ described above. The first mass analyzer, a quadrupole, scans, selects and guides the parent ions into a collision cell. The resultant

product ions are then analyzed by a TOF reflectron mass analyzer. A QTOF instrument can provide much higher mass accuracy and mass resolution than a QqQ instrument.

The MALDI-TOF/TOF instrument is another tandem mass spectrometer utilized for biomolecular analysis.[23] For these types of experiments, the first TOF analyzer (with a linear flight tube) is used to select the parent ions, and the second TOF analyzer is a reflectron used to detect and analyze the fragment ions. The generation of fragment ions is facilitated by PSD, by colliding with gas molecules in the collision cell, and by ultraviolet laser irradiation.[24]

Fourier Transform - Ion Cyclotron Resonance Mass Analyzer

The Fourier transform - ion cyclotron resonance (FTICR) mass analyzer was first introduced for the mass spectrometry analysis in 1974 by Comisarow and Marshall.[25] Among all different types of mass analyzers, the FTICR is capable of achieving the highest performance in terms of resolving power and mass accuracy, yet it is a complicated and an expensive system. The FTICR mass analyzer is an electromagnetic trap, known as the Penning trap, which uses a combination of an electric and a magnetic field to trap ions inside the ICR cell.

The ICR cell. The ICR cell is one of the main components of an FTICR mass analyzer, where mass analysis takes place. It is positioned inside a homogeneous magnetic field. Many different geometries of ICR cells have been implemented over years, including the cubic cell, the Infinity cell, the open and closed cylindrical cells, the three-sectioned cell, cell with hyperbolic electrodes, cell with hemisphere end caps, dual cells, the elongated cell, and others.[26, 27] One example cell geometry is schematically shown in Figure 1.3. This is a closed cylindrical ICR cell. The cylinder consists of two pairs of electrodes – one for ion excitation and the other for detection of the image

current . End cap electrodes are used to trap ions along the magnetic field axis. The principles of ion motion and detection are explained below.

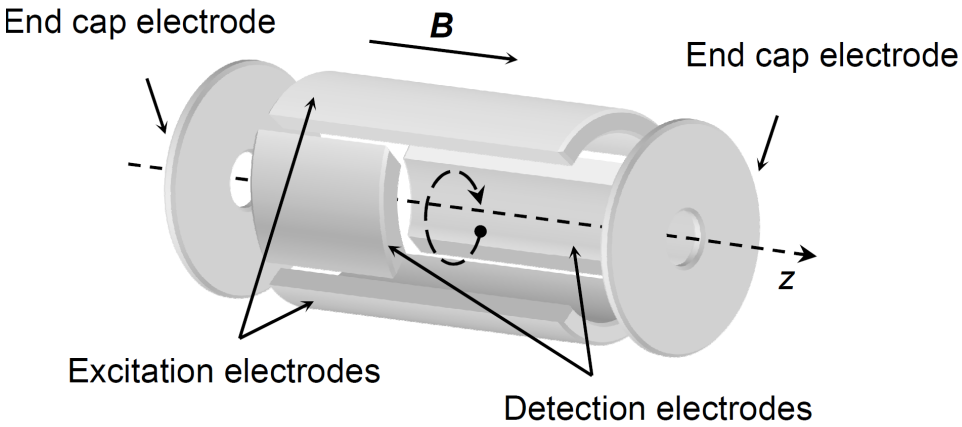

Figure 1.3 The schematic of a closed cylindrical ICR cell. Ions are trapped along the axis by the trapping potential applied to the trapping plates. Cyclotron motion of the ions is indicated, which is perpendicular to the magnetic field ***B***.

The magnet. Magnetic field is provided by an electromagnet, which is a main component of an FTICR mass analyzer. An electromagnet is made from a coil of wire that acts as a magnet when an electric current passes through it. Magnets used in FTICR-MS are primarily superconducting magnets made of superconducting wire. These magnets can produce greater magnetic fields than non-superconducting electromagnets. The magnetic field strength in an FTICR mass spectrometer typically ranges from 4 Tesla (T) to 18 T. An FTICR MS with a 21 T magnet is currently under development at the National High Magnetic Field Laboratory and PNNL.[28] An increase in the magnetic field strength improves the resolving power, signal-to-noise ratio, and mass accuracy of the mass spectrometer. However, the cost of the mass spectrometer also increases with the magnetic field strength, e.g. a 14.5 T FTICR magnet cost is approximately $2,000,000.

Ion transport. Ions can be generated inside or outside the ICR cell. Traditionally, EI and CI were used to generate ions inside the ICR cell. For analysis of large biomolecules such as proteins, however, soft ionization techniques, mostly ESI and MALDI, are usually used as external ionization sources. Once generated in the external ion source under atmospheric pressure or at relatively high pressure, ions need to be transferred to the ICR cell which operates in ultrahigh vacuum (UHV). Therefore, several differential pumping stages are usually needed to maintain the pressure difference of several orders of magnitude between the ion source and the mass analyzer. Ion transfers from the ionization source to the ICR cell can be achieved with implementation of various ion optics, such as ion funnels, RF-multipole ion guides, electrostatic lenses and various focusing lenses.

Ion motion. Inside the magnetic field, an ion with mass m, charge q, and velocity v experiences the Lorentz force (F_L) and circles an orbit of radius r in a plane perpendicular to the direction of the magnetic field B:

$$F_L = qE + q\,(\mathbf{v} \times \mathbf{B}) \qquad (1.8)$$

where E is the electric field. Ideally, in the center of the cell ion motion is unaffected by the electric field, thus:

$$F_L = q\,(\mathbf{v} \times \mathbf{B}) \qquad (1.9)$$

The ion trajectory with velocity v moving in the magnetic field B is stable if the centripetal force (the inward force) and the centrifugal force (the outward force) are equal:

$$(mv^2)/r = q\,(\mathbf{v} \times \mathbf{B}) \qquad (1.10)$$

The angular velocity

$$\omega = 2\pi r = v/r = (qB)/m \qquad (1.11)$$

Equation (1.11) is called the cyclotron equation and ω is the *cyclotron frequency*. The cyclotron frequency of an ion is inverselyproportional to its mass to charge ratio in a constant magnetic field and is independent of the ion velocity. This is the principle of mass analysis in FTICR MS, and ω is used to calculate the ion *m/z* ratio (where *z* is *q/e*, and *e* is the elemental charge).

Ion motion described in Equation (1.11) is called the cyclotron motion, which is confined to a plane perpendicular to the magnetic field direction. Ion trapping along the magnetic field lines is achieved by applying a small potential (usually in the order of ~1 V (V_{trap})) to the end cap electrodes of the same polarity as the ion charge. As a result, ions oscillate along the z-axis of the ICR cell. The potential applied to the end cap electrodes also creates a repulsive electric field in the xy-plane, which pushes ions towards the excitation and detection plates. The interplay between ions and the radial electric field and the axial magnetic field induces a third motion of ions, the magnetron motion, which causes the center of the ion cyclotron orbit to circle around the ICR cell axis.

The radial force F_{radial}, which ions experience due to the radial electric field induced by trapping potential V_{trap}, opposes the inward-directed Lorentz magnetic force F_L from the applied magnetic field and can be described as:

$$F_{radial} = qE(r) = (qV_{trap}\alpha\ r) / a^2 \qquad (1.12)$$

where *a* is the distance between the trapping plates, and α is a cell geometry factor. The Lorentz force equation (1.10) for the plane perpendicular to the magnetic field B_z can be reduced to:

$$m\omega^2 r = qB_z\omega r \qquad (1.13)$$

To obtain the equation for ion motion one needs to consider the total force combining equations (1.12) and (1.13):

$$m\omega^2 r = qB_z\omega r - (qV_{trap}\alpha\, r) / a^2$$

$$\text{or} \quad \omega^2 - (qB_z\omega)/m + (qV_{trap}\alpha) / a^2 m = 0 \qquad (1.14)$$

Equation (1.14) is a quadratic equation, with two solutions:

$$\omega_+ = \omega_c/2 + ((\omega_c/2)^2 - (\omega_z^2/2))^{1/2} \qquad (1.15)$$

$$\omega_- = \omega_c/2 - ((\omega_c/2)^2 - (\omega_z^2/2))^{1/2} \qquad (1.16)$$

where ω_+ and ω_- are the reduced cyclotron and magnetron frequencies, in which ω_c is the unperturbed cyclotron frequency, and ω_z is the trapping oscillation frequency of the ions moving in the *z*-direction, defined as (from (1.12)):

$$\omega_z = ((2qV_{trap}\alpha\, r) / ma^2)^{1/2} \qquad (1.17)$$

The magnetron motion causes radial diffusion of the ion and reduces its cyclotron frequency. The ω_z is proportional to the trapping potential, introducing a trade-off between efficient trapping of the ions and perturbing the cyclotron frequency. For this reason V_{trap} is usually kept low. Magnetron and axial frequencies are usually much less than the cyclotron frequency, and generally are not detected. An ion trajectory that shows all three motions experienced by the ion in an ICR cell is demonstrated in Figure 1.4.

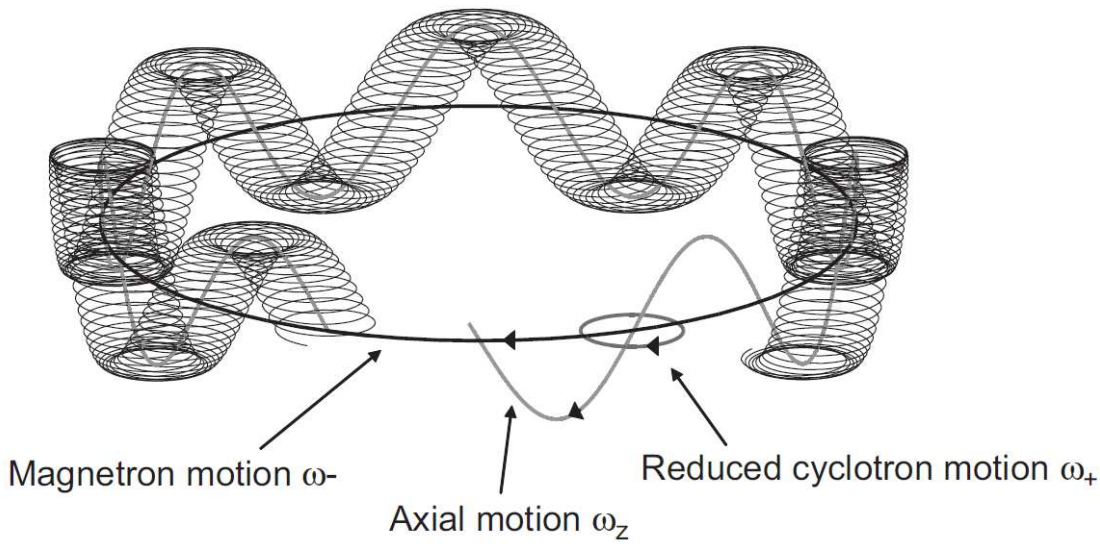

Figure 1.4 Ion motions in an ICR cell. The axis and the magnetic field face the paper. Reproduced from Kolhinen, V. S.; et al, Commissioning of the double Penning trap system MLLTRAP, *Nuclear Instruments & Methods in Physics Research Section a-Accelerators Spectrometers Detectors and Associated Equipment*, 2009, 600, 391-397, with permission.

Ion excitation and detection. Since the cyclotron frequency is constant for an ion of a given *m/z*, the radius of an ion's cyclotron orbit depends on its velocity or its kinetic energy. At room temperature, in a magnetic field of 9.4 T, the thermal cyclotron radius of a singly charged 1 kDa ion is rather small, ~0.08 mm.[27, 29] In order for ions to be detected, their cyclotron orbit radii need to be increased, so that ions circle at higher orbits close to the cell electrodes, which are typically ~5 cm away from the center. The coherent excitation of ions is achieved by differentially applying an RF voltage sweep containing a band of frequencies corresponding to the desired *m/z* range to excitation electrodes (called a chirp).[27] Each ion will respond only to its particular RF pulse corresponding to its cyclotron frequency. As the ion absorbs the RF energy, it is resonantly accelerated, increasing its cyclotron radius to that of a higher orbit (Figure

1.5). This process is called the *Ion Cyclotron Resonance* excitation, which gave rise to the name of the ICR cell. The radius of excited ions is dependent on the amplitude of the electric field E_0 and the duration of the resonant excitation T for a given magnetic field B, but is m/z independent, so all ions accelerate to the same orbit, provided that the excitation amplitude and duration are constant across the whole m/z range:[30]

$$r = (E_0 T)/2B \qquad (1.18)$$

When the ion packet moves to the proximity of a detection plate, it induces accumulation of charges with opposite signs to the ion packet at the plate (image charges). As ions rotate around the center of the ICR cell, image charges are induced alternately at opposite detection plates, creating an alternating image current between them. This image current is converted to an alternating voltage, which is amplified to generate a time domain signal (a transient). The acquired transient contains the cyclotron frequency information of all ion packets, which can be recovered via a mathematical operation called the Fourier transform. The frequency domain spectrum is then converted to the mass spectrum via the cyclotron equation.

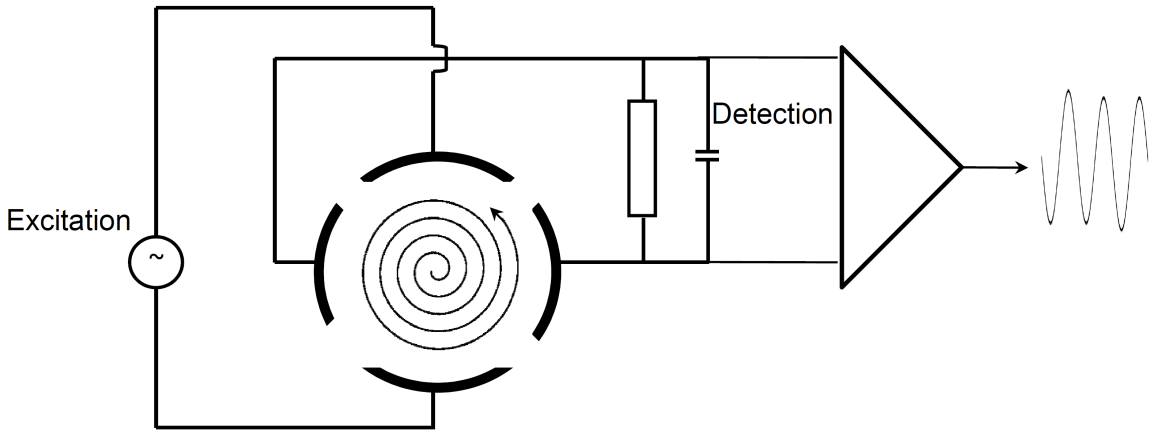

Figure 1.5 Excitation and detection of trapped ions in an ICR cell.

Ions excited to a lager orbit will eventually lose their energy and spiral back down to the center of the cell, so the signal on detection plates will drop over time. In addition, ion collisions with the background gas will cause the loss of coherence of the oscillating ion packet, dispersing it into a donut-shape. This in turn causes the loss of the differential signal and a fast decay of the transient. Thus, the pressure of the ICR cell should be kept below 10^{-8} torr (ideally10^{-9} torr or lower) to reduce collisions during the transient acquisition. The duration of the transient *T* is important as it directly influences the FTICR resolving power *R*:[31]

$$R = (f\,T)/2 \qquad (1.19)$$

FTICR MS performance. From the equation (1.19), it is apparent that the resolving power is also linearly dependent on the strength of the magnetic field. Thus, the magnet field strength and a good vacuum are essential for achieving the excellent performance of the FTICR MS, although its performance is also influenced by many other factors, such as the electric and magnetic field homogeneity, the cell geometry, ion transmission, and electronics, etc. The typical mass resolution achieved on a 12 T FTICR instrument is over 200,000 at *m/z* 400 in the analysis of proteins. Because ions can be trapped in the ICR cell for minutes or even hours, mass resolution greater than 1,000,000 can also be obtained. The typical mass accuracy is in the range of 1 ppm or better when internally calibrated, and in the low ppm range when externally calibrated for peptides of *m/z* ~1000-2000. The usual *m/z* range is 150-3,000, but can be extended up to 5,000 to detect ions of a mass of ~100 kDa. The low-mass cutoff is primarily limited by the sampling frequency to satisfy the Nyquist limit, but could also result from resonant excitation of ions by the multipole RF field as ions traverse the magnetic field gradient. For commercial FTICR instruments, the upper mass limit is primarily determined by the

ion transfer optics. The routinely achievable sensitivity of an FTICR MS is in the fmol range. The ICR dynamic range and the upper mass limit scale with the strength of the magnet field, and analysis/experiments which are difficult or impossible with a weak magnet can be routinely performed with a stronger magnet. When combined with high-resolution LC separations, the overall dynamic range of measurements can exceed 10^6.[32] The FTICR MS scan speed is compatible with the LC-MS time scale (in seconds); however, to achieve the best resolving power, longer transient acquisition is required for a given magnetic field strength. Use of a magnet with a higherfield strength can also improve the scan speed.

Applications. A unique FTICR MS feature is its ability to perform tandem MS inside the ICR cell. Multiple tandem MS methods can be implemented in an FTICR instrument. In particular, up to recently, electron capture dissociation (ECD)[33] was only available in FTICR MS. Other tandem MS methods suitable for FTICR MS include sustained off-resonance irradiation collision activated dissociation (SORI-CAD),[34] and infrared multiphoton dissociation (IRMPD)[35], etc.[29, 36] The versatile tandem MS capability afforded by an FTICR MS, in addition to its ultra high resolution and mass accuracy, and coupling to liquid chromatography led to its wide applications in both top-down and bottom-up analysis in proteomics, including protein sequencing, PTM characterizations, study of protein conformations, and analysis of protein complexes.[37] FTICR MS is used to analyze complex chemical mixtures such as crude oil, which can be made up of tens of thousands of different types of molecules. It is also used to determine the molecular structure of carbohydrates, nucleic acids and other biomolecules. In addition, FTICR MS can identify the chemical fingerprint of explosives and accelerants, thus, can be used for counterterrorism efforts. Overall, FTICR MS allows obtaining such information on the

sample as its elemental composition and its associated class, type, and carbon distribution information, amino acid composition, metal ion oxidation state, charge state distribution, identification of functional groups, isotopic distributions, and ultimately, isotopic fine structure.[38]

Orbitrap Mass Analyzer

The orbitrap is an electrostatic ion trap where ions are trapped by an electrostatic field.[39] The technology is based on the Kingdon ion trap.[40] The orbitrap mass spectrometer was recently introduced by Makarov and has been widely used in biological research since.[41, 42] The orbitrap operates by radially trapping ions about a central spindle electrode (Figure 1.6). Ions move in spirals around the central electrode. The axial component of the trapping field contains a quadratic term of the axial displacement, and the resulting restoring force is proportional to the axial displacement. Consequently, the ion axial motion takes the form of a harmonic oscillator, with its frequency inversely proportional to the square root of the ion *m/z* value. The outer electrode is split in the center by insulating ceramic ring and is used to detect the image current induced by the moving ions along the axis. The resultant transient is digitized and Fourier transformed to obtain the axial frequencies of ion oscillations, which are then converted into *m/z* values using the mass calibration equation to obtain the mass spectra.

Commercially available orbitrap instruments feature ESI, nanoESI, and APPI ionization sources. The ion source is connected to the orbitrap via a linear ion trap capable of generating MS and MS^n spectra itself, and a C-trap.[42] The C-trap is a bent quadrupole named after its C-shape. The C-trap allows ion accumulation, concentration into a small cloud, and radial injection into the orbitrap. The injection is accommodated

by focusing electrodes and a repeller at the orbitrap entrance. The central electrode voltage is lowered at the time of ion injection to allow ion entrance into the orbitrap.

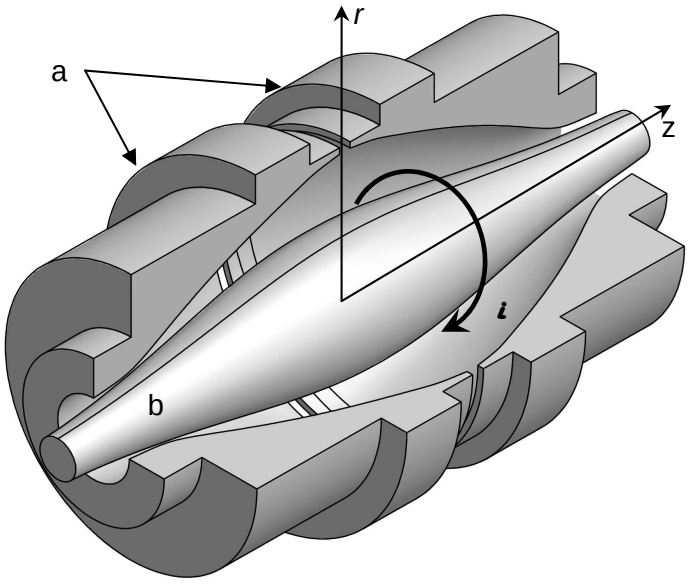

Figure 1.6 A schematic representation of the orbitrap mass analyzer. The outer electrodes form the shape of a barrel (a). Ions (*i*) move in spirals around the central spindle-shaped electrode (*b*) while oscillating back and forth along the *z* axis.

The orbitrap instrument performance is quite different from that of quadrupole ion traps. Compared with a Q-TOF instrument, the resolution is dramatically increased, and so is the dynamic range. The mass resolving power of the first-generation commercial orbitrap at *m/z* 400 with a 1 second transient is >60,000, with its maximal resolving power exceeding 100,000. At low *m/z* values, the orbitrap resolution is typically less than that obtainable on an FTICR instrument. However, the resolution of an orbitrap decreases not as rapidly as that of an FTICR when the *m/z* increases. The mass accuracy of an orbitrap is <5 ppm with external calibration, and <2 ppm with internal calibration. The instrument sensitivity is at the sub-fmol level with dynamic range greater than 10^3. The mass range is limited by the use of the linear ion trap and is either *m/z* 50-

2,000 or *m/z* 200-4,000. It is possible to detect 4 scans per second, acquiring 1 high resolution MS scan in the orbitrap and the rest in the LTQ as MS/MS scans. The latest improvements of the system with the implementation of the high-field orbitrap and advanced signal processing allowed further increase in its analytical performance.[43] An average mass resolution of 220,000 was achieved in the analysis of proteins.[44] Thus, the resolving power has become comparable with that obtained with 7 Tesla FTICR mass spectrometers. It is now possible to perform LC-MS/MS experiments on intact proteins of up to 50 kDa molecular weight.[45]

The orbitrap's ability to perform on the LC time scale has allowed its application to both small molecule analysis, such as metabolomics and metabolite analysis, drug metabolism, doping control and food contaminants, and proteomics.[46, 47] Implementation of the electron transfer dissociation (ETD) on the orbitrap further expanded its application in proteomics research.[48] Combining three different and complementary fragmentation techniques - CAD, high energy CAD (HCAD), and ETD, the orbitrap is capable of characterizing labile PTMs, such as phosphorylation and glycosylation. It has been used for the differentiation of phosphorylation and sulfation, glycan structure elucidation, PTM site determination, sequencing of peptides, top-down and middle-down analyses, and protein quantitation via stable isotope labeling.

1.2.3 Tandem Mass Spectrometry

Tandem mass spectrometry (MS/MS, MS^2 or MS^n) involves multiple stages of mass analysis with ion fragmentation happening between these stages. Tandem mass spectrometry is a three-step process: isolation of a precursor or parent ion of interest (first stage of mass analysis), fragmentation of the parent ion, and detection of the

resultant fragment ions (a.k.a. daughter or product ions) during the second stage of mass analysis. These mass analysis events might be happening in different mass analyzers or in the same mass analyzer. The former is typically referred to as “tandem mass spectrometry in space” due to the fact that mass analyses happen in distinct physical locations. Examples of mass spectrometers implementing tandem-in-space mass analysis are QqQ, QTOF, TOF/TOF, and others. The latter is known as “tandem mass spectrometry in time”, in which isolation of the parent ion, its fragmentation and the subsequent detection of the product ions are happening in the same mass analyzer, yet at different times. Examples of mass spectrometers capable of performing "tandem-in-time" mass analyses are 3D quadrupole and linear ion traps, and FTICR MS. As described above, tandem-in-time allows for MS^n analysis.

There are a number of different tandem mass spectrometry experiments or modes. These are:

Product ion scan – in this mode, the first mass analysis event selects the precursor ion of interest, which is fragmented followed by detection of all product ions in the second mass analysis event. This tandem mass analysis experiment can be performed on both in-space and in-time instruments.

Precursor ion scan – in this mode, the second mass analyzer detects a product ion of interest whereas the first mass analyzer scans for precursor ions that can produce this product ion. This mode can only be performed on in-space instruments.

Neutral loss scan – in this mode, both the first and the second analyzers scan across specified mass ranges simultaneously. The difference in the scanned masses for the analyzers matches the mass of the neutral loss of interest. Neutral loss scan can only be performed on in-space instruments.

Selected reaction monitoring (SRM) – the first and the second mass analyzers are set to detect specific precursor and product ion masses, respectively. Multiple reaction monitoring (MRM) is a mode in which multiple SRMs are cycled. SRM experiments are usually performed on in-space instruments.

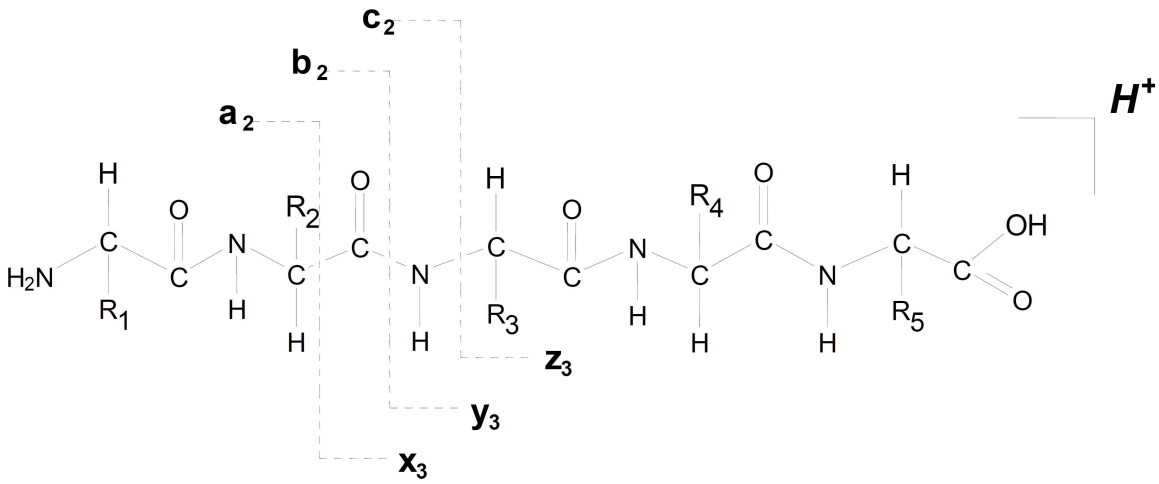

Figure 1.7 Peptide ion fragmentation nomenclature.

All these tandem mass spectrometry modes can be used to help deciphering the structure of or to quantitate various biomolecules. For protein and peptide mass analysis specifically, these modes are the necessary tools to deduce the structure or the sequence of the peptide/protein of interest. A common nomenclature describing peptide/protein product ions was proposed in 1984 by Roepstorff *et al*.[49] This ion fragmentation nomenclature is demonstrated in Figure 1.7. For a peptide containing *m* amino acid residues, fragmentation between the nth and the $(n+1)^{th}$ amino acids would provide N-terminal fragment ions a_n, b_n, and c_n, and C-terminal fragment ions x_{m-n}, y_{m-n}, z_{m-n}, depending on the bond cleaved. The identity of an amino acid residue can be deduced (with the exception of isomeric Leu/Ile residues) from the mass difference of fragment ions of the same series resulting from bond cleavages immediately N-terminal and C-terminal to this residue. It is possible to determine the complete peptide

sequence *de novo* from its tandem mass spectrum if at least one fragment ion between each adjacent residue pair is present, but a more common approach involves database searching.

Collisionally Activated Dissociation (CAD)

Collisionally activated dissociation, or CAD[50], (a.k.a. collision-induced dissociation (CID)), is a very powerful and most commonly utilized tandem mass spectrometry fragmentation technique. In CAD, a parent ion collides with neutral gas molecules resulting in subsequent generation of fragment ions. Helium, argon, or nitrogen gas is typically used as the collision gas.

There are two types of CAD: high- and low-energy CAD. In high-energy CAD, molecular ions of high kinetic energy (several thousands of electron volts (keVs)) collide with neutral gas molecules, inducing fragmentation usually upon a single collision. This fragmentation technique can be utilized on TOF-TOF instruments as well as on sector instruments. For peptide and protein analysis, high-energy CAD typically produces cleavage of the peptide bond to generate *y* and *b* ions but can also induce fragmentation of the side chains to produce *w* and *d* ions. The *w* and *d* ions can provide useful information such as to differentiate isomeric leucine and isoleucine amino acids;[51] however, they also introduce additional complexity to the mass spectrum and often complicate its interpretation.

Low-energy CAD is typically utilized in QqQ, ion traps, FTICR, and hybrid instruments. Low-energy CAD involves molecular parent ions of low kinetic energy (<1 - 100 eV). These ions, upon many low-energy collisions with gas molecules, become activated via translation-to-vibration energy transfer. The ion activation is not caused by electronic excitation but rather by vibrational excitation, and intramolecular

vibrational energy redistribution (IVR) often precedes ion fragmentation. Consequently, low-energy CAD usually results in the dissociation of a bond with the lowest dissociation energy. For peptide and protein analysis, low-energy CAD typically produces *y* and *b* ions. Additionally, other labile bonds, such as those formed during protein post-translational modifications (PTMs) (e.g. phosphorylation, glycosylation), often also dissociate during low-energy CAD. This tendency of CAD to produce abundant labile modification losses is one of its main limitations because localization of PTMs is a very important aspect of protein characterizations.

Nonetheless, low-energy CAD is a powerful protein and peptide tandem mass spectrometry technique because it can provide sequence information about the protein/peptide in question. Additionally, low-energy CAD performed on an ESI-triple quadrupole instrument is the preferred technique for identification and accurate quantitation of small biomolecules and biomarkers. This technique has led to a significant, multiplexed expansion of newborn screening for inborn errors of metabolism (IEM) testing in the early 1990's, enabling screening for various fatty acid and amino acid metabolic IEM disorders. Finally, positive and negative ESI and APCI QqQ instruments employing low-energy CAD have been recently utilized in various clinical *in vitro* diagnostics procedures.

Electron capture dissociation and related techniques

Electron capture dissociation (ECD) provides fragments (mostly *c* and *z* ions) complementary to those (mostly *b* and *y* ions) generated by other tandem MS methods such as CAD.[50] ECD was first introduced by Zubarev *et al.* in the late 1990s,[33] and has since been widely implemented for routine structural analysis of biological molecules.[52] The ECD fragmentation mechanism is believed to be fundamentally different from other

tandem MS methods. It is sometimes referred to as a 'non-ergodic' method,[33] *viz.* energy gained upon electron capture is used directly to cleave the N - C_α bond prior to IVR rather than being distributed among various degrees of freedoms within the molecule to break the weakest bond as in CAD,[50] an interpretation which is the subject of intense debate.[53-55] ECD is initiated by the capture of low-energy electrons by multiply charged gas phase molecular ions typically produced by ESI. ECD has been traditionally performed on an FTICR mass spectrometer because of its ability to confine low-energy electrons,[31, 36] and its implementation has recently been extended to a radio frequency ion trap.[56] The capture of the low energy electron (~0.2 eV) is believed to occur in proximity to the protonated site of the molecule, either at a protonated backbone carbonyl site according to the Cornell mechanism,[33, 57] or in the π orbital of an amide group in the presence of a remote charge according to the Utah-Washington mechanism,[58] producing a charge reduced cation radical, with the subsequent backbone N-C_α bond cleavage leading to the formation of *c* and $z^{\bullet}$ fragments. The radical on $z^{\bullet}$ can induce further rearrangements within the molecule, a free radical cascade,[53] producing additional backbone and side chain cleavages both in the proximity of and remote from the initial radical site.[59] The fragmentation pattern generated by ECD may vary dramatically depending on the number and location of certain amino acids, modifications, and charges.[60-64] A number of experimental and computational studies have been carried out since ECD was first introduced,[33, 65] yet its mechanisms remain under debate, probably because multiple competing pathways are involved.[54, 66-76] Nevertheless, the capability of ECD to produce unique fragment ions not obtainable by conventional methods has led to a rapid optimization of ECD and the development of other ion-electron reaction based tandem MS techniques such as electron transfer

dissociation (ETD),[77] electron ionization dissociation (EID),[78] electron detachment dissociation (EDD), collectively known as electron activated dissociation (ExD).

ETD was introduced as a substitute for ECD in instruments other than FTICR mass spectrometers, such as a 3D quadrupole or linear ion trap. In ETD, the electron is transferred to the molecular ion from a radical anion to produce fragmentation pattern similar to ECD. Radical anion (the ETD reagent) is produced by a negative CI (nCI) source and the electron transfer reaction occurs in a quadrupole or similar rf-field trapping module. The most commonly used ETD reagents include fluoranthene and azulene.

In *EID*, ions of interest are irradiated with energetic electrons (>30 eV) resulting in electron ejection and formation of excited radical ion species, which undergo rapid dissociation. EID has been successfully applied to analysis of both singly and multiply charged peptides and proteins. Additionally, EID was implemented in a radiofrequency linear ion trap instrument along with ECD and other fragmentation techniques for complementary analysis.[79] The ability of EID to produce ECD-like fragments from singly charged precoursor ions is unique among all ExD methods, because ECD and ETD are accompanied by charge reduction upon the electron capture or transfer and cannot be performed on singly charged ions as the products would be neutral and undetectable. This feature allows EID to be implemented in instruments with MALDI ionization sources.[80]

ExD has been broadly applied towards the structural analysis of various types of biomolecules, including proteins, oligosaccharides, oligonucleotides, and others.[52, 81-83] Further, ECD and ETD were found to be particularly useful for the characterization of

PTMs in proteins as they can cleave the backbone while preserving the labile groups and non-covalent interactions upon fragmentation.[84, 85]

In-source decay fragmentation

In-source decay (ISD) fragmentation during matrix assisted laser desorption ionization (MALDI) process is a pseudo tandem MS technique, which allows peptides and proteins to fragment in a single MS stage.[86] Fragmentation occurs as a result of the metastable decay of precursor ions during delayed extraction within the ion source.[87] In ISD, the polypeptide N-C_α bonds are cleaved to generate *c* and *z* product ions. These products are similar to those generated in ECD; however, the mechanism of their formation appears to be different. It is proposed that, in ISD, the intermolecular hydrogen abstraction occurs between the peptide and the MALDI matrix producing a hypervalent radical species that undergoes subsequent rapid cleavage of the N-C_α bond.[88] Therefore, ISD is induced by hydrogen atoms generated by a photochemical reaction of the matrix and not by electrons as in ECD.[89]

The cleavage of the N-C_α bond is normally observed when the following matrices are used: picolinic acid (PA), 1,5-diaminonaphtalene (1,5-DAN), and 2,5-dihydroxybenozoic (DHB).[90] These are hydrogen donating molecules with the hydrogen donating abilities the highest when PA and 1,5-DAN are used together. Different product ions can be observed in ISD with the use of another class of matrices – hydrogen accepting matrices. As was recently reported, with the use of such matrices, e.g. 5-formylsalicylic acid (5-FSA) and 5-nitrosalicylic acid (5-NSA),[91, 92] hydrogen abstraction from peptides results in the formation of oxidized peptides containing a radical site at the backbone amide nitrogen with subsequent radical-induced cleavage at the C_α-C bond, leading to the formation of *a*- and *x*-type fragments. Some matrices,

such as 2-aminobenzamide (2-AB), 2-aminobenzoic acid (2-AA) have mixed properties, i.e. they can both donate and accept hydrogen atoms generating various types of fragments.[93]

The two main limitations of the ISD method are the lack of precursor ion selection for fragmentation and interferences from matrix clusters. It is possible to mitigate these problems by applying HPLC separation prior to MALDI analysis and choosing matrices that produce relatively low amount of cluster ions, and by varying the experimental parameters and instrument setup. Nonetheless, ISD has become a valuable tool for the analysis of peptides and proteins. Importantly, PTMs are preserved during the ISD process. ISD has been applied to analyze peptides and proteins with phosphorylation and O-glycosylation, to differentiate the isobaric amino acid residues leucine and isoleucine, and to obtain information on disulfide-linkages.[94-96] Alternatively, disulfide bonds can be reduced allowing the analysis of Cysteine-containing peptides.[97] Further, it was shown that only limited hydrogen scrambling is observed during the ISD fragmentation process.[98] This is beneficial for the hydrogen/deuterium exchange studies of proteins to obtain information on their dynamic and structural properties. Finally, ISD has been implemented in MS imaging of tissue samples to simultaneously identify and localize proteins.[99]

1.2.4 ESI QqQ-FTICR mass spectrometer

One of the instruments used for the work described in this thesis is a custom-built hybrid electrospray triple quadrupole FTICR mass spectrometer (ESI qQq-FTICR MS).[100] The instrument scheme is demonstrated in Figure 1.8.

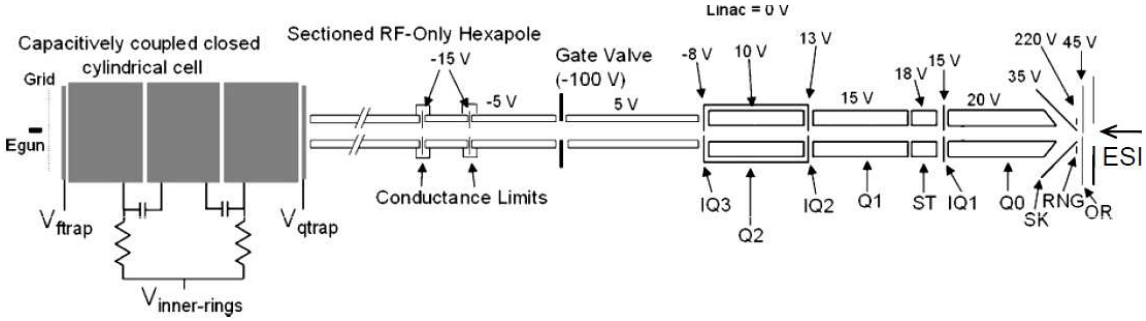

Figure 1.8 The ESI qQq-FTICR mass spectrometer. Reproduced (modified) from O'Connor, P. B. *et al*., Rapid Communications in Mass Spectrometry, *20*, 259-266, 2006, with permission.

In Figure 1.8, the direction of ions traveling through the instrument is from right to left. The ion source is a direct infusion nanoESI source. The in-house pulled glass capillary tips are used to generate a ~50 nmol/min flow and the nanoelectrospray by applying 1100-1300 V to a metal wire inserted into the tip. Ions are sucked into the vacuum interface region of the instrument at ~10^{-3} Torr by a combination of the electric field and the pressure gradient. Ion desolvation is accommodated by the curtain gas applied between the orifice and the curtain plate. Generated ions are focused by an RF-only quadrupole Q0, precursor ions are isolated in a mass analyzing quadrupole Q1, and accumulated and/or fragmented in a collision cell Q2 (modified from an AB/MDS Sciex API 365 instrument). IQ1, IQ2, and IQ3 are focusing lenses, and typical voltages applied to these lenses as well as the orifice (OR), ring electrode (RNG), and skimmer (SK) are denoted. A potential gradient is created by applying decreasing voltages across the instrument from the front to the end to efficiently transmit the ions and to decrease their initial kinetic energy. Stubbies (ST) is a set of short quadrupoles used to smoothen transition of ions from Q0 to Q1. Linac is a set of four rods used to create an axial electric field to push ions into a tighter packet towards IQ3 before ion extraction to

minimize the transfer efficiency reducing time-of-flight effect. After ion accumulation, the IQ3 is pulsed to a negative value to allow ion extraction into the next module – hexapole 1 (before the gate valve) and sectioned hexapole 2 (after the gate valve). These hexapoles are used for ion transfer to the ICR cell. Sectioned hexapoles allow for differential pumping with the use of conductance limits to maintain the UHV (~10^{-10} Torr) in the ICR cell region. The gate valve separates the instrument into two sections. When closed, it allows the front end of the instrument to be opened up for cleaning and other purposes without disturbing the UHV in the ICR cell region. The ICR cell is a capacitively coupled closed cylindrical cell with two end trapping plates positioned inside the homogeneous region of a 7 T magnetic field produced by an actively shielded magnet (Cryomagnetic Inc., Oak Ridge, TN). After ions enter the ICR cell, the front (hexapole) and back (filament) trapping plate voltages, V_{qtrap} and V_{ftrap}, respectively, are ramped to high positive value (~15 V) to trap the ions inside the cell. The trapping plate voltages are reduced to ~1 V before ion excitation to minimize the influence of ion magnetron motion. The inner trapping plates are also used to confine the ions in the homogeneous part of the magnetic field along the axis of the instrument by applying a small voltage of ~1 V ($V_{inner\text{ - }rings}$). All voltages above are listed for the analysis of positive ions, the polarity is inverted for the analysis of negative ions. The center plates are used for ion excitation and detection.

An indirectly heated dispenser cathode[101] (E_{gun}, Heatwave, CA, USA) and a grid (Grid) are used for ECD experiments. The cathode has a BaO surface which, when heated by passing a current (1.5-1.8 A) through a resistor, emits electrons. A pulsing negative voltage is applied to eject the electrons from the cathode surface, typically at -0.2 V to -1.5 V for generation of low-energy electrons. The grid is used to extract

electrons from the cathode for efficient transfer to the ICR cell by applying a constant positive voltage of ~10 V. The time period during which electrons are emitted from the cathode is called the electron irradiation time and is usually within a 5-100 ms range. At all other times, the cathode potential is set to 9.9 V to avoid introducing electrons into the ICR cell. The combination of magnetic and electric fields of an FTICR allows for simultaneous radial confinement of ions and electrons inside the cell and thus their reaction. Upon the electron beam passing through the center of the cell and the ions rotating in the center of the cell, the electron capture occurs to generate fragments as was explained previously. By varying the cathode potential it is possible to eject electrons of different energies for performing alternative ECD-like fragmentations, such as hotECD and EID. In addition, other fragmentation techniques can be performed on this instrument. These include CAD - either performed in the collision cell (Q-CAD), or inside the ICR cell (SORI-CAD),[34] and IRMPD.[35] This instrument was extensively used for the analysis of peptides, proteins, and their PTMs, as well as carbohydrates,[102] typically providing high mass resolving power of >100,000 and ~2 ppm mass accuracy with internal calibration.

1.2.5 Bruker Daltonics solariX FTICR MS

Another instrument used for the work presented in this thesis is a commercial hybrid Qh-FTICR mass spectrometer with a 12 T actively shielded magnet, named solariX^{TM} (Bruker Daltonics, Billerica, MA, USA). The instrument schematic is shown in Figure 1.9 (Bruker Daltonics) with the exception that only an ESI ionization source was available in the current configuration.

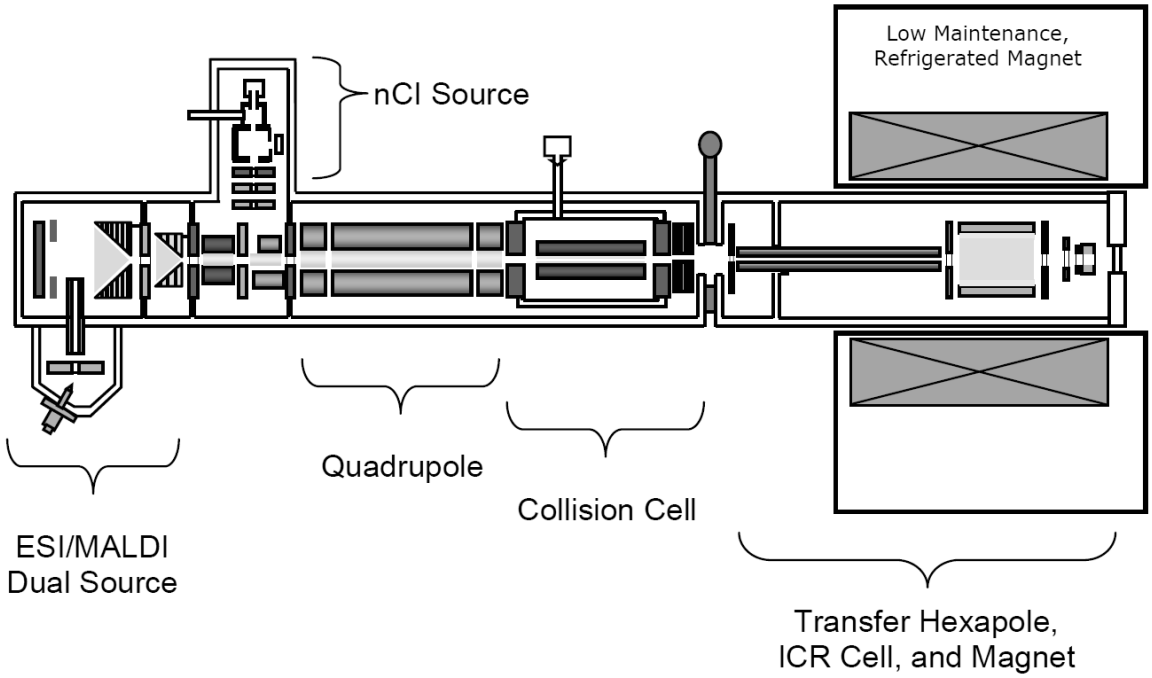

Figure 1.9 The solariX^{TM} FTICR mass spectrometer (Bruker Daltonics).

The atmospheric pressure nanoESI is implemented using either an in-house pulled glass capillary tips or a robotic Nanomate source (Advion, Ithaca, NY, USA). Ions, transmitted through a heated glass capillary positioned perpendicular to the axis of the instrument, are further guided by the electrostatic and RF multipole ion optics to the Quadrupole for isolation. Isolated precursor ions are then transferred to the Collision Cell (hexapole), which is used for ion fragmentation using either CAD or ETD, as well as for ion accumulation. The anion radical reagent is introduced to the collision cell from an external negative chemical ionization (nCI) source via a split octapole to induce ETD. Unfragmented precursor and fragment ions are transferred to the ICR cell via a Transfer Hexapole. The ICR cell is a closed cylindrical Penning trap. A hollow indirectly heated dispenser cathode is used to provide electrons for ExD experiments. A 25 W continuous wave (CW) CO_2 laser (10.6 µm, Synrad, Mukilteo, WA) is used for IRMPD experiments. The hollow cathode[103] allows for simultaneous irradiation of the ion cloud by electron and

photon beams to perform activated-ion ECD (AI-ECD). In addition, SORI-CAD can be performed inside the ICR cell. This instrument can be connected to an HPLC module for high throughput HPLC-FTICR MS proteomic analysis with a variety of fragmentation techniques available for protein identification and characterization of PTMs. The typical resolving power is ~200,000 at *m/z* 400, and the typical mass accuracy is <0.5 ppm with internal calibration, and <2 ppm with external calibration.

1.3 High Performance Liquid Chromatography (HPLC)

High Performance Liquid Chromatography (HPLC) is an analytical technique for analyte separation. An HPLC instrument contains four major components: a stationary phase packed into a column, HPLC pump(s), a mobile phase, and a detector. The separation of analytes in a mixture is based on the difference in interaction of analytes with the stationary phase and the mobile phase. Depending on the stationary phase and the mobile phase used, there are many different types of HPLC. The ones that are used for biomolecular sample preparation and sample separation are the size exclusion, ion exchange (either anion or cation), normal phase HPLC (NP-HPLC), and reversed phase HPLC (RP-HPLC).

Size exclusion chromatography (SEC), as its name implies, separates analytes based on their size. The basis for this technique is the physical, rather than chemical interaction of the analyte molecule with the stationary phase. As analytes move through the SEC stationary phase, smaller analytes can be temporarily trapped within the "pores" of the stationary phase whereas larger analytes cannot enter these pores and pass straight through; therefore larger analytes elute faster than smaller analytes. SEC

is often used for purification of large biological molecules such as proteins, DNA/RNA and carbohydrates.

Ion-exchange chromatography separation is based on the electrochemical interaction between the ions or the polar analytes with the stationary phase. The stationary phase for ion-exchange chromatography has ionic functional groups that interact with the oppositely charged analyte ions, thus providing the separation – the stronger the interaction, the longer the retention time. Counter ions are often added to the mobile phase (a.k.a. pH modifier) to affect the strength of interaction and the retention times. Ion-exchange chromatography is often used to separate and purify proteins and peptides, as well some classes of carbohydrates, such as glycosaminoglycans (GAGs).

Normal-phase HPLC separates analytes based on their interactions and adsorption to a polar stationary phase. NP-HPLC employs non-polar mobile phase and works well for analytes that can be dissolved in non-polar solvents. The more polar analytes interact more strongly with the polar stationary phase, which in turn results in longer retention time. The stereochemistry of the analytes also plays a role in retention and separation in NP-HPLC. The analyte retention and elution can be manipulated by increasing or decreasing the polarity of the mobile phase; however, when the mobile phase becomes too polar or aqueous, it will interact with the stationary phase and subsequently deactivate it. The NP-HPLC has not been used widely for biomolecular separation and analysis as most of the biomolecules are not soluble in highly non-polar solvents, and it eventually gave way to the reversed-phased HPLC for biomolecular separation and analysis (Section 1.3.1). However, recently a variation of NP-HPLC,

known as the hydrophilic interaction liquid chromatography (HILIC), has been used for biomolecular applications.[104]

HILIC stationary phase is polar and often based on such functional groups as amines, amides and zwitterionic groups. The HILIC mobile phase is non-polar in nature and often a mixture of acetonitrile and water. In HILIC, analyte retention and separation are based on two factors: the electrochemical interaction and liquid-liquid extraction/retention. The electrochemical interaction between the analytes and the HILIC stationary phase is a weak (e.g. hydrogen bonding) interaction facilitated by employing a polar mobile phase. The liquid-liquid extraction and retention is caused by formation of a water-rich layer at the surface of the stationary phase (without deactivating it as in the traditional NP-HPLC), and subsequently the analytes are dispensed between this layer and the mobile phase based on their hydrophilicity. The ability to utilize water as well as volatile organic solvent such as acetonitrile makes HILIC-HPLC a very attractive separation method for electrospray ionization mass spectrometry applications. HILIC-HPLC is often used for HPLC-ESI-MS (MS/MS) analysis of proteins, peptides and other biomolecules.[105]

1.3.1 Reversed Phase High Performance Liquid Chromatography (RP-HPLC)

Reversed-phase HPLC (RP-HPLC) was introduced as an analytical separation technique in the mid 1970's.[106] The name "reversed" comes from the fact that RP-HPLC adopts an inverted philosophy compared to the normal phase HPLC: whereas NP-HPLC utilizes polar stationary phase and non-polar mobile phase, RP-HPLC employs non-polar stationary phase and polar mobile phase. Since its introduction, the RP-HPLC has been used so extensively (including in biomolecular analysis), that often RP-HPLC and

RP-HPLC-MS applications are no longer denoted as reversed-phase and are assumed to be.

The most often used stationary phase in RP-HPLC is silica with bonded straight chain alkyl groups.[106] In RP-HPLC, samples are loaded onto the HPLC column using relatively polar solvents (i.e. with a higher water content). The analytes are retained on the column by hydrophobic interactions with the non-polar stationary phase. These hydrophobic non-covalent interactions occur between the hydrophobic parts of the molecules and the alkyl chains of the stationary phase; therefore, analytes with a larger hydrophobic patch interact more strongly with the stationary phase, and are retained on the column for a longer period of time. The analytes are eluted off the column by ramping up the organic (non-polar) content of the mobile phase. The basic process of elution is a result of the analyte/mobile phase hydrophobic interaction overcoming that between the analyte and the stationary phase. There are a number of factors affecting analyte retention and elution: stationary phase chemistry, stationary phase particle and pore size, column size and temperature, mobile phase composition and mobile phase gradient, mobile phase pH modifier (a.k.a. solvent additive) and the flow rate.

Silica with bonded straight alkyl chain of four, eight and eighteen carbons are the most commonly used RP-HPLC stationary phases, which are commonly referred to as C4, C8 and C18, respectively. These stationary phases interact differently with different analytes. C4 is most often used for protein separation and analysis. The reason for using a shorter alkyl chain for protein separation is that proteins contain large hydrophobic regions, which may interact with stationary phases employing longer alkyl chains too strongly to be efficiently eluted. On the other hand, C18 is often used for small molecule and peptide analysis. Unlike proteins, small molecules and peptides

have smaller hydrophobic molecular areas, thus necessitating longer alkyl chain stationary phase for better separation. C8 stationary phase is often considered as a universal RP-HPLC stationary phase and works well for peptide and small molecules separation and analysis.

Analyte retention and separation are also affected by the RP-HPLC column sizes (inner diameter (i.d.) and length). For LC-MS applications, relatively small analytical, and not larger preparative, HPLC columns are typically utilized. Typical RP-HPLC columns used for LC-MS analysis of biomolecules have either 2.1 mm or 4.6 mm i.d. and are 10 to 250 mm in length. Generally, as the column volume increases, the analyte retention time increases as well.

Additionally, column's stationary phase particle size and pore size play a role in analyte separation and retention. Typical RP-HPLC columns are packed with stationary phase beads or particles. These particles are spherical and porous in nature. The diameter of the particles is known as the particle size and the size of the pores is known as the pore size. The particle and pore sizes play off each other to determine the analyte retention and separation. Smaller particle size or pore size or both mean higher surface area of the stationary phase, thus more extensive interaction with analytes leading to longer retention. This also requires higher mobile phase column pressure. Typical LC-MS analysis of biomolecules utilizes RP-HPLC columns with particle size less than 10 microns and pore size between 100 and 300 angstroms (Å).

Both the column temperature and the mobile phase flow rate affect the HPLC performance. Because analytes interact with the stationary phase via hydrophobic interactions, changes in temperature will change the interaction strength, which in turn will affect analyte retention and separation. It is also desirable to control the column

temperature to achieve reproducibility and consistency in column performance and analyte separation. Flow rate also has an effect on analyte retention: generally higher flow rate leads to faster elution off the column, but this relationship is not linear.

Mobile phase composition and mobile phase gradient have a pronounced effect on analyte separation and elution in RP-HPLC. Typically, a sample is loaded onto the RP-HPLC column using an organic/water mixture which is relatively polar, i.e. high in water content. The organic solvent commonly used for LC-MS biomolecular analysis is either methanol or acetonitrile. Not only are these organic solvents optimal for reversed-phase chromatography, but they are also ideal for ESI and APCI ionization sources owing to their high evaporation efficiency. As the mobile phase is ramped up to higher organic/lower water content and becomes more non-polar, the hydrophobic interactions between the analytes and the stationary phase decrease resulting in eventual analyte elution. The organic solvent used and the water content, as well as the steepness of the gradient (% change in water content over time) all influence the analytical performance of RP-HPLC.

Another important factor determining the analyte retention and elution is the pH modifier. The pH modifiers are typically inorganic salts or weak acids that are added to water, or organic solvent, or both. The pH modifier increases the surface tension of the mobile phase which in turn tends to increase analyte retention and improve the separation. Some of the best pH modifiers that are often used for LC-MS applications are acetic acid (AA), formic acid (FA), triflouroacetic acid (TFA) and heptafluorobutyric acid (HFBA). These solvent additives not only improve the chromatographic separation and resolution, but also act as proton donors for analyte ionization. It is worth noting that

TFA tends to suppress ESI and APCI generated ions and should only be used at very low concentrations (0.01 – 0.05 %).[107]

1.3.2 On-line and off-line Liquid Chromatography Mass Spectrometry

Coupling HPLC to mass spectrometry results in hybrid analytical technique known as liquid chromatography-mass spectrometry (LC-MS). The ability of liquid chromatography to separate analytes in time and space provides additional specificity and selectivity to the mass analysis. Additionally, coupling LC to mass spectrometry analysis often improves sensitivity by sample complexity reduction, analyte concentration on column, and/or removal of impurities from the analytes of interest. In on-line LC-MS, the LC effluent off the column is directly connected to a mass spectrometer and the data acquisition happens in real-time. ESI, APCI, and atmospheric pressure photoionization (APPI) ionization sources are very amendable to on-line LC-MS, and specifically RP-HPLC-MS (or MS/MS). The reasons are appropriate flow rates coming off analytical HPLC column (~10 – 500 µl/min for ESI, and ~300 – 900 µl/min for APCI and APPI) and appropriate HPLC solvents (high organic content acetonitrile:water or methanol:water mixture). HPLC-ESI-quadrupole based LC-MS (or MS/MS) systems are widely used for biomolecular analysis due to the quadrupole scanning nature. For on-line HPLC-ESI-TOF systems, because of the pulsed nature of a TOF mass analyzer, ions need to be trapped (usually in a front end quadrupole), and then pulsed into the TOF analyzer, as employed in Q-o-TOF instruments. This happens on the millisecond scale and the HPLC performance or resolution is not affected.

In off-line LC-MS experiments, the LC effluent is not directed introduced into the mass spectrometer in real-time. In this case, the LC effluent is typically collected in

different fractions (as a function of time), which are later mass analyzed as a liquid (in ESI-MS) or deposited on the MALDI plate. There are a number of reasons to perform off-line LC-MS analysis. Primarily, some ion sources, especially those that operate under vacuum (e.g. EI, CI, and MALDI) are not amendable to LC-MS. Another reason to perform off-line LC-MS analysis is the incompatibility of LC effluent with liquid based ionization sources. For instance, the majority of normal-phase HPLC techniques utilize ESI or APCI unfriendly mobile phase (e.g. hexane). Therefore, in this case, the LC effluent needs to be collected as fractions and solvent exchanged to ESI/APCI amendable solvent type. Off-line HPLC MALDI-TOF technique is an extremely powerful technique for protein analysis, where a protein trypsin digest is subjected to HPLC separation and off-line fractionation, which are subsequently deposited onto a MALDI plate for MALDI-TOF analysis.

1.4 Introduction to deamidation and isomerization of peptides and proteins

1.4.1 Deamidation and isomerization of peptides and proteins

Deamidation of asparagine (Asn) and isomerization of aspartic acid (Asp) residues, are two of the most common PTMs found in all proteins. Under physiological conditions, deamidation of Asn proceeds through formation of a cyclic succinimide intermediate by the nucleophilic attack of the backbone nitrogen atom in the following peptide bond on the carbonyl group of the Asn side chain (Figure 1.10). Upon hydrolysis of the succinimide intermediate, two isomeric products, Asp and isoAsp are formed, typically in a 1:3 ratio in short unstructured peptides.[108, 109] In proteins, this ratio could be different from 1:3 and is influenced by higher-order structures.[110, 111] Asp can also be

directly isomerized into isoAsp through the same cyclic intermediate due to the dehydration process.[112] The succinimide formation from Asp is ~ 10 - 40 times slower than from Asn at neutral pH, yet the reaction rate may vary greatly depending on the adjacent residues, protein conformation, the proximity of the Asp/Asn residue to the protein surface and the molecular environment.[108, 112-114] For example, the first-order deamidation half-time of an Asn residue surrounded by Gly residues (at pH 7.4, 37.0°C, in 0.15 M Tris HCl) is 1 day; however, if the C-terminal residue is Pro, it would be ≥ 32 years.[115] It seems that the residue that follows the Asn residue is the most important factor on its deamidation rate, and the fastest times are for the following residues: Gly>His>Ser>Ala, etc.[115]

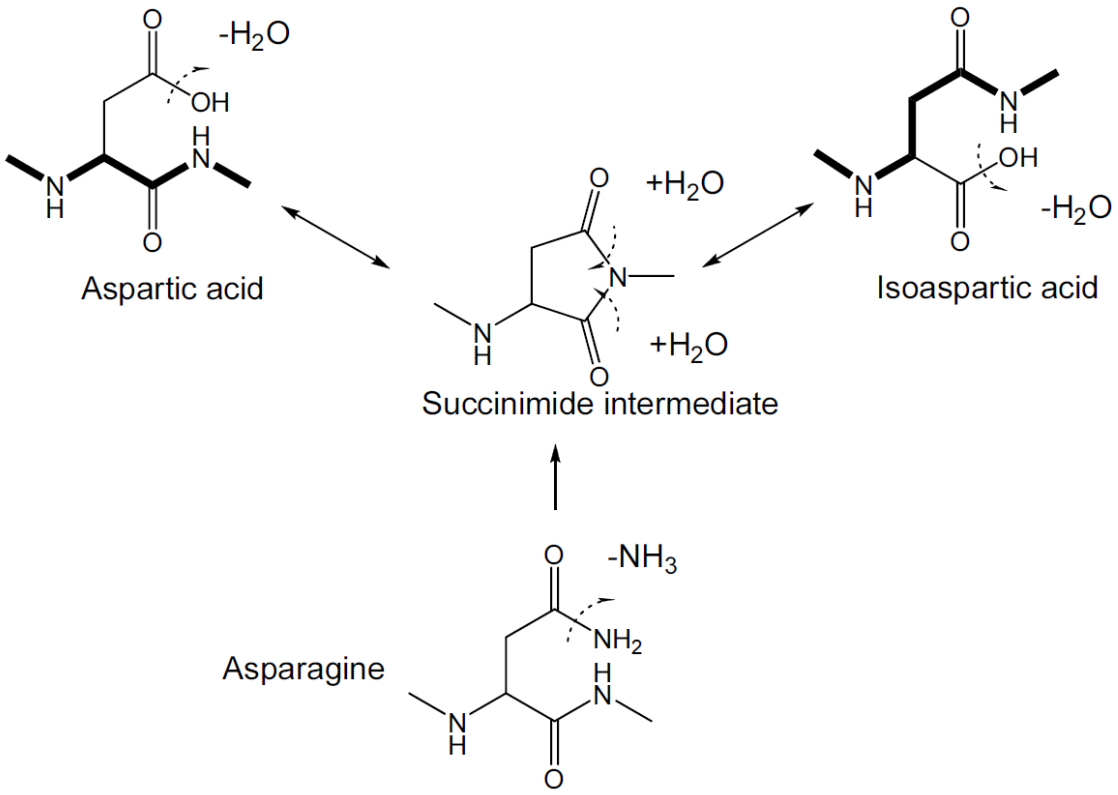

Figure 1.10 Isomerization of aspartic acid and deamidation of asparagine via a succinimide intermediate.

Under physiological conditions (at pH ≥7), both Asp isomerization and Asn deamidation are spontaneous nonenzymatic reactions, which proceed via a 5-membered ring succinimide intermediate.[108] At pH (4-7), deamidation proceeds by the initial formation of a tetrahedral intermediate that can be converted to succinimide. Deamidation rates reach the minimum at pH between 3 and 4. At low pH (<3), Asn deamidation occurs by direct acid-catalyzed hydrolysis to form the only product aspartate.[116] In addition, an increase in temperature leads to an increase in the reactivity of Asn and Asp residues in proteins leading to faster deamidation and isomerization rates.[117] These factors often lead to artifactual deamidation and isomerization during sample preparation and handling, thus, have to be considered when the protein characterization and PTMs analysis are performed.

1.4.2 Biological importance of deamidation and isomerization

Asn deamidation and Asp isomerization are common *in vivo*. They are particularly common in long-lived proteins and have been proposed as molecular timers of biological events.[112] These modifications are often associated with aging,[114] eye lens abnormalities,[118] amyloid diseases such as Alzheimer disease[119, 120] and Type 2 diabetes mellitus,[121] and apoptosis.[122]

Structural change. By introducing an additional methylene group into the polypeptide backbone (isoAsp) and a negative charge to the polypeptide (deamidation), these modifications may alter protein conformation, activity and stability, and trigger protein aggregation.[114, 119, 123] For example, the 3-dimensional crystal structure of Ribonuclease U2B revealed that formation of isoAsp32 led to a single turn unfolding of the α-helix to form a U-shape loop structure, affecting the hydrolytic activity of the

protein.[124] Single Asp isomerization was shown to deactivate the antigen-binding region of the immunoglobulin gamma (IgG)-2 antibody.[125] The presence of the isomerized Asp may also affect the proteolytic stability of the protein. For example, Lys-C proteolysis is hindered when the Lys residue is adjacent to an isoAsp in IgG-1 antibody;[126] isoAsp residues are also resistant to Asp-N proteolysis.[127-129] On the other hand, carboxypeptidase Y cleaves N-terminally to an isoAsp residue recognizing its α-carboxylic acid as if it is a carboxyl-terminal amino acid.[130]

Protein L-isoaspartyl O-methyltransferase. Although *in vivo* Asn deamidation is an irreversible reaction, the isoAsp accumulation can be minimized by protein L-isoaspartyl O-methyltransferase (PIMT), which catalyses isoAsp conversion to Asp (registry number: EC 2.1.1.77).[120, 131, 132] PIMT catalyzes the transfer of a methyl group from S-adenosy-L-methionine to the α-carboxyl group of L-isoAsp. As a result of the spontaneous hydrolysis of the methyl ester, the succinimide intermediate is formed, which again, upon hydrolysis, would generate a mixture of Asp and isoAsp. Multiple actions of PIMT enzyme can minimize isoAsp content with time. PIMT is highly conserved, ubiquitously expressed in many tissues, mostly as a cytosolic enzyme. Loss of PIMT has damaging consequences, especially in neuron cells. For example, in PIMT deficient mice, isoAsp accumulated in the cytosolic fraction of brain, heart, liver, and erythrocytes. The knockout mice showed significant growth retardation and fatal seizures at ~6 weeks after birth, suggesting that PIMT is essential for normal growth and central nervous system function.[133] Overall, formation of isoAsp residues and their subsequent correction by PIMT are widely believed to constitute an important pathway of protein damage and repair.[120, 132]

Potential biomarkers. The study of deamidation and isomerization processes has significant consequences for the identification of proteins and the search for potential biomarkers. For example, among several promising biomarkers for the risk of developing retinopathy of prematurity (ROP) disease, deamidation of globin chains may indicate underlying prenatal pathologic mechanisms in ROP developing.[134] In another example, the asparagine deamidation in peptides containing the Arg-Gly-Asn (RGN) sequence generates Arg-Gly-isoAsp (RGD) motif that is being exploited for ligand-directed targeted delivery of various drugs to angiogenic vessels and as a potential biomarker of related pathology.[135]

Pharmaceutical products. Finally, *In vitro* Asp isomerization and Asn deamidation can also occur during protein production and storage. IsoAsp buildup could be detrimental to the protein structural integrity and stability, which affects the shelf-life and potency of the therapeutic monoclonal antibodies (mAb) and other protein-based new drug entities in the pharmaceutical industry.[136] For example, spontaneous deamidation of Protective Antigen protein (PA), a key component in an anthrax vaccine, leads to its inactivation.[137]

1.5 Introduction to β-peptides

β-Amino acids. Similar to the isoAsp, a β-amino acid has an extra methylene group incorporated between its amino and carboxylate groups. There are two types of β-amino acids: β_2 and β_3, with the side chain attached to α and β carbon respectively (Figure 1.11). β-Amino acids do not normally occur in nature except for β-alanine (a component of pantothenic acid, of coenzyme A, and of carnosine in muscle tissue) and β-aspartate (isoAsp); neither do β-peptides, but those can be synthesized.[138, 139] It

should be noted, that naturally occurring β-alanine, and β-aspartic acid have the same total number of carbons as their α-analogues – one more in the backbone and one fewer on the side chain; however, β-amino acids normally used for β-peptide synthesis often have an extra carbon within the backbone, but contain the same side chain as those in α-amino acids, and thus are called β-homo-amino acids (in this thesis, all β-amino acids in synthetic peptides are β-homo-amino acids).

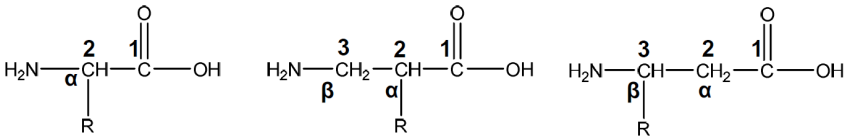

α-amino acid **β_2-amino acid** **β_3-amino acid**

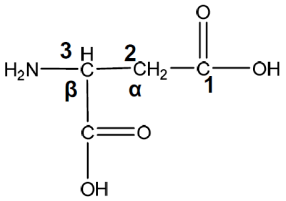

Isoaspartic acid

Figure 1.11 β-Peptide nomenclature.

β-Peptides. β-Peptides were first synthesized and examined in the mid-1990s by Seebach.[138] Since then, they have been intensively studied on their structural and biological properties, and on their interactions during peptide folding. Because the backbone of β-peptides is longer than that of α-peptides, they form different secondary structures, which appear to be more stable and have richer conformational energy surface compared with their α-analogues.[138, 140] They also fold into helices or hairpin-type structures, but with larger variety than α-peptide secondary structures. In contrast to α-peptides, β-peptides form such structures with shorter chain lengths starting at 4 residues. Furthermore, there are differences in similar structures, such as screw sense of the helix and the macrodipole direction; as opposed to α-peptidic parallel pleated

sheet, in that of β-peptides, all C=O bonds point in the same direction and all N-H bonds in the opposite one.[140]

Biological significance. The biologically important property of β-peptides is their stability against proteolytic degradation and other enzymes in human and various living organisms.[141-143] However, β-peptides can be designed in a way that they would resemble the epitopes of corresponding natural peptides to mimic their function and be used as agonists and antagonists in peptide-protein, protein-protein, and peptide-DNA/RNA interactions[144-146]. These features provide great potential for β-peptides in biomedical application as proteolytically stable therapeutics and antibiotics for antibiotic-resistant pathogens.

There are a number of examples of β-peptide application in mimicking the natural α-peptidic properties. A helical β_3-peptide was designed that recognizes a cleft on the surface of the human oncogene product double minute 2 (hDM2) mimicking an α-helix of the major tumor suppressor p53 protein in its activation domain.[145] When bound hDM2 inhibits p53, however, binding of the β_3-peptide to hDM2 inhibits the hDM2 and p53 interaction allowing p53 to proceed its function, which is important for cancer therapy. Another β-peptide with an amphiphilic helix was developed to mimic natural antibiotic of the magainin's class and was shown to be effective against bacterial species that are resistant to common antibiotics - the bacterium Enterococcus faecium A436 (vancomycin resistant) and Staphylococcus aureus 5332 (methicillin resistant). This peptide does not induce haemolysis (the erythrocyte rupture), which is essential for successful therapeutic application.[147]

Methods of analysis. Circular dichroism spectroscopy, X-ray crystal-structure analysis and nuclear magnetic resonance spectroscopy are primarily used to study the

structure of β-peptides.[138, 140, 142, 144] Radioactive labeling, HPLC and MALDI mass spectrometry have also been applied to monitor β-peptides in tissues.[141, 143] However, an improved, fast and accurate analytical method capable of distinguishing α from β, and β_2 from β_3 type amino acids would be of a great utility for structural confirmation and analysis of β-amino acid-containing peptides.

1.6 Thesis overview

This thesis focuses on the study of peptide and protein deamidation and isomerization by electron capture dissociation tandem mass spectrometry and liquid chromatography. IsoAsp is a β-type amino acid, thus other types of β-amino acids are also studied by ECD as well as ISD tandem MS. The deamidation and isomerization research includes: Chapter 2, isoAsp analysis in amyloid β fragments; Chapter 3, the analysis of isoAsp, Asp, and Asn containing peptide variants by LC; Chapter 4, the differentiation of the N-terminal Asp and isoAsp in peptides; Chapter 5, isoAsp in amyloid β fragments in CSF. β-Peptide studies include: Chapter 6, fragmentation of β-linked peptides by tandem MS using ECD and ETD; Chapter 7, in-source decay for β-peptide analysis. Chapter 8 is conclusion and future work. Overall in this thesis, new and improved methods are suggested for characterization and differentiation of β-amino acids.

Chapter 2

Identification of isoAsp in Amyloid β Peptides by Tandem ExD MS/MS

2.1 Introduction

2.1.1 Amyloid β in Alzheimer's disease.

Amyloid beta (Aβ) peptides are the major components of the vascular and plaque amyloid filaments in individuals with Alzheimer's disease (AD). Various forms of Aβ are proteolytically cleaved from the Aβ precursor protein, with Aβ1-40 and Aβ1-42 being the most abundant forms found in Amyloid deposits.[148] Ever since Aβ was first purified and characterized, it has been strongly associated with the pathology of AD,[149, 150] although it remains unclear what initiates the disease. According to the most widely accepted hypothesis, cerebral Aβ accumulation is the primary cause in AD. The rest of the disease process stems from imbalance between Aβ production and clearance.[151] Many attempts have been made to measure the concentration of Aβ peptides in biological fluids, but it is difficult to correlate Aβ levels with disease stage and, thus, to use it as an AD biomarker.[152] Further research and development of analytical methods is necessary for early AD diagnosis, disease progression, monitoring, and better understanding of the disease.

---

[1]This chapter has been partially reproduced with permission from Sargaeva, N. P.; Lin, C.; O'Connor, P. B., Identification of aspartic and isoaspartic acid residues in amyloid beta peptides, Including A beta 1-42, using electron-ion reactions, *Analytical Chemistry*, **2009**, *81*, 9778-9786. Copyright 2009, American Chemical Society.

2.1.2 Isoaspartic acid formation

Isomerization of aspartic acid (Asp) is one of the most common post translational modifications (PTMs) in all proteins that accumulate with age in long-lived proteins, especially in tooth, bone, cartilage, lens, and brain tissues.[114] The isomerization product is isoaspartic acid (isoAsp). It can also be formed from asparagine deamidation (Figure 1.10). At physiological pH both reactions proceed via an entropy driven[153] formation of the five-membered succinimide ring intermediate followed by a rapid hydrolysis. As a result, aspartic and isoaspartic acid residues are typically formed in a ratio of 1:3.[108, 109] Moreover, at pH ~7.4, IsoAsp formation is preferential because of the higher acidity of the isoAsp side chain.[153] Under physiological conditions, both Asp isomerization and Asn deamidation are spontaneous nonenzymatic reactions.[108, 109, 114, 120, 153, 154] The reaction rates depend mainly on the nature of the adjacent residues, the higher order structure of the protein, and the molecular environment.[108, 112, 114] Formation of isoAsp is speculated to change the protein structure as it introduces an additional methylene group into the polypeptide backbone. This can change protein function and activity, or trigger aggregation.[114, 119, 123] In addition, proteins containing isoAsp may not fully degrade as isoaspartate residue hinders proteolytic degradation.[155] Nonetheless, harmful isoAsp products can be partially repaired by the intracellular enzyme, protein isoaspartyl methyltransferase (PIMT), which selectively converts isoAsp residues back to the succinimide intermediate.[114, 120]

2.1.3 IsoAsp in Alzheimer's disease

Isomerization of aspartic acid is directly related to the pathology of Alzheimer's disease. Aβ peptides have 3 aspartic acids in the sequence at the 1st, 7th, and 23^{d}

residues and formation of isoaspartate is enhanced in Aβ peptides in AD. Roher *et al.* found that Asp1 and Asp7 were isomerized in the cerebral plaque samples of Alzheimer patients.[119] Recently, isoAsp7 and isoAsp23 were found in the core of senile plaques and Amyloid-bearing vessels as was shown with anti-isoasp7 and anti-isoasp23 antibodies.[120] Moreover, the Iowa (Asn23)[156] and Japanese-Tottori mutations (Asn7)[157] in familial AD have a potential to accelerate formation of isoAsp, presumably due to asparagine deamidation. Accordingly, isoAsp23-containing Aβ peptides were preferentially detected in vascular deposits in Iowa cerebral Amyloid angiopathy brain.[158] It was further suggested that spontaneous isomerization at position 23 induces the conformational change to form a β-turn of the polypeptide chain. This, in turn, plays a pathogenic role in the deposition of Aβ peptides in sporadic AD.[120] In vitro experiments showed increased fibrillogenesis and enhanced neurotoxicity of isoAsp23-containing Aβ peptides,[120, 159] however, other results suggested that Aβ aggregative ability and neurotoxicity were not enhanced by this modification.[160] Similar studies of Aβ with isoAsp7 revealed that it is primarily deposited in the core of senile plaques. IsoAsp7 accumulation was associated with the age of the plaque as the number of isoAsp positive plaques increased in parallel with the disease severity.[161]

There have been many studies of isomerization events in Aβ peptides, but its role in AD pathogenesis is still unclear. Formation of isoAsp in Aβ might be a reason for its impaired degradation leading to accumulation. This aggregation could be a way for biological systems to reduce the toxicity of the non-degradable Aβ peptides. Further research is needed to better understand the role of isoAsp formation.

2.1.4 IsoAsp detection methods

The detection of isomerization products is analytically challenging due to their similar chemical properties and identical molecular mass. Nevertheless, various methods have been applied to differentiate and quantify the isomers, including immunological methods based on detection by specific isoAsp antibodies,[120, 158, 161] liquid chromatography,[119, 154] PIMT enzyme utilizing assays,[119, 154] and tandem mass spectrometry (MS) analysis.[162-164] New methods addressing isoAsp detection are quickly emerging in the field to better understand the harmful effects isoAsp accumulation can generate in biological systems and pharmaceutical applications. These new methods often utilize a combination of existing methods, such as high-performance liquid chromatography (HPLC) separation followed by MS analysis.[165, 166] In addition, immunochemistry analysis, capillary electrophoresis, HPLC-MS, or tandem MS alone, can be applied to analyze *l*-Asp, *l*-isoAsp, *d*-Asp, and *d*-isoAsp isomerized/racemized peptides.[167-169] Upgraded HPLC, known as the ultra performance liquid chromatography (UPLC) system, could further separate isoAsp and Asp located directly at the *N*-terminus.[170]

Edman degradation is a chemical cleavage method useful for IsoAsp identification because it does not cleave the isopeptide bond. Similarly, enzymatic digestion with the endoproteinase Asp-N does not cleave N-terminal to the isoAsp acid.[110, 127-129, 171, 172] This was utilized in combination with ^{15}N isotope labeling and MS for the detection of IsoAsp.[127] The ^{18}O labeling coupled to MS can also be used for detection of Asn deamidation and Asp isomerization;[173, 174] however, this can only be applied to detection of in vitro modification sites in the protein, but not to identify modifications already existing in biological samples prior the analysis. In addition, Alfaro

et. al. recently introduced a new method for the affinity enrichment of isoaspartyl proteins, where chemo-enzymatic detection using the PIMT enzyme and hydrazine trapping were applied.[175]

Many of the methods for studying deamidation utilize mass spectrometry, which over several decades, has become one of the most powerful tools in biological sciences. Although a single stage of MS cannot normally distinguish isomers, because they have identical masses and are represented as a single peak in the mass spectrum, tandem MS has shown some successful results. For example, low-energy collisionally activated dissociation (CAD) has been applied for Asp/isoAsp differentiation based on the difference in the abundance of the immonium and *b* and *y* ions,[163, 164] as well as the *b* + H_2O and *y* - 46 ions that resulted from cleavages *N*-terminal to an isoAsp residue.[162] However, the abundance of all above-mentioned ions can be strongly influenced by the peptide sequence, and in some cases, diagnostic ions were not observed. Therefore, these methods require comparative analysis with standard peptides, which is not always possible for the analysis of biological systems.

An alternative tandem MS-based method was recently developed, where isoaspartic residues in peptides[176] and proteins[177] were unambiguously identified and quantified[178] by Electron Capture Dissociation (ECD). In ECD, electron capture results in the N-C_α bond cleavage producing *c* and $z^\bullet$ type fragments (Figure 2.1.a).[33] Furthermore, the radical created by electron capture can initiate additional backbone and/or side chain cleavages.[53, 179] ECD can also result in the cleavage of C_α-C_β, bond and formation of specific fragments in Asp- and isoAsp-containing peptides. For Asp residues, this leads to the loss of a $CH_2C(OH)_2$ molecule from the charge-reduced species and the formation of the $[M + nH - 60]^{(n-1)+\bullet}$ ion; for isoAsp residues, cleavage of

the C_α-C_β bond will result in a breakage of the polypeptide chain and formation of the c_m + 57 and $z^{\bullet}_{n-m}$ - 57 fragment ions will be generated (Figure 2.1.b).

2.2 Experimental section

2.2.1 Peptides and reagents

Standard Aβ1-40 was purchased from Sigma Aldrich (St. Louis, MO, USA). The isomerized form of Aβ17-28 (LVFFAEisoDVGSNK, custom synthesized), and Aβ1-42 with Tottori - Japanese Mutation at [Asn7] were obtained from AnaSpec (San Jose, CA, USA). Sequencing grade trypsin was purchased from Roche Diagnostics (Indianapolis, IN, USA).

2.2.2 Sample preparation

Aβ1-40 was digested with trypsin in 100mM Ammonium Bicarbonate buffer at an enzyme : substrate weight ratio of 1:50 in µg/µl concentration, overnight at 37℃ with prior incubation at 65℃ for 20 min. A β1-42 [Asn7] was deamidated overnight at 37℃ in 0.4 % aqueous Ammonium Hydroxide with pH >10.2 in µg/µl concentration. After digestion or deamidation, samples were dried in a SpeedVac system to stop the reaction and evaporate volatiles.

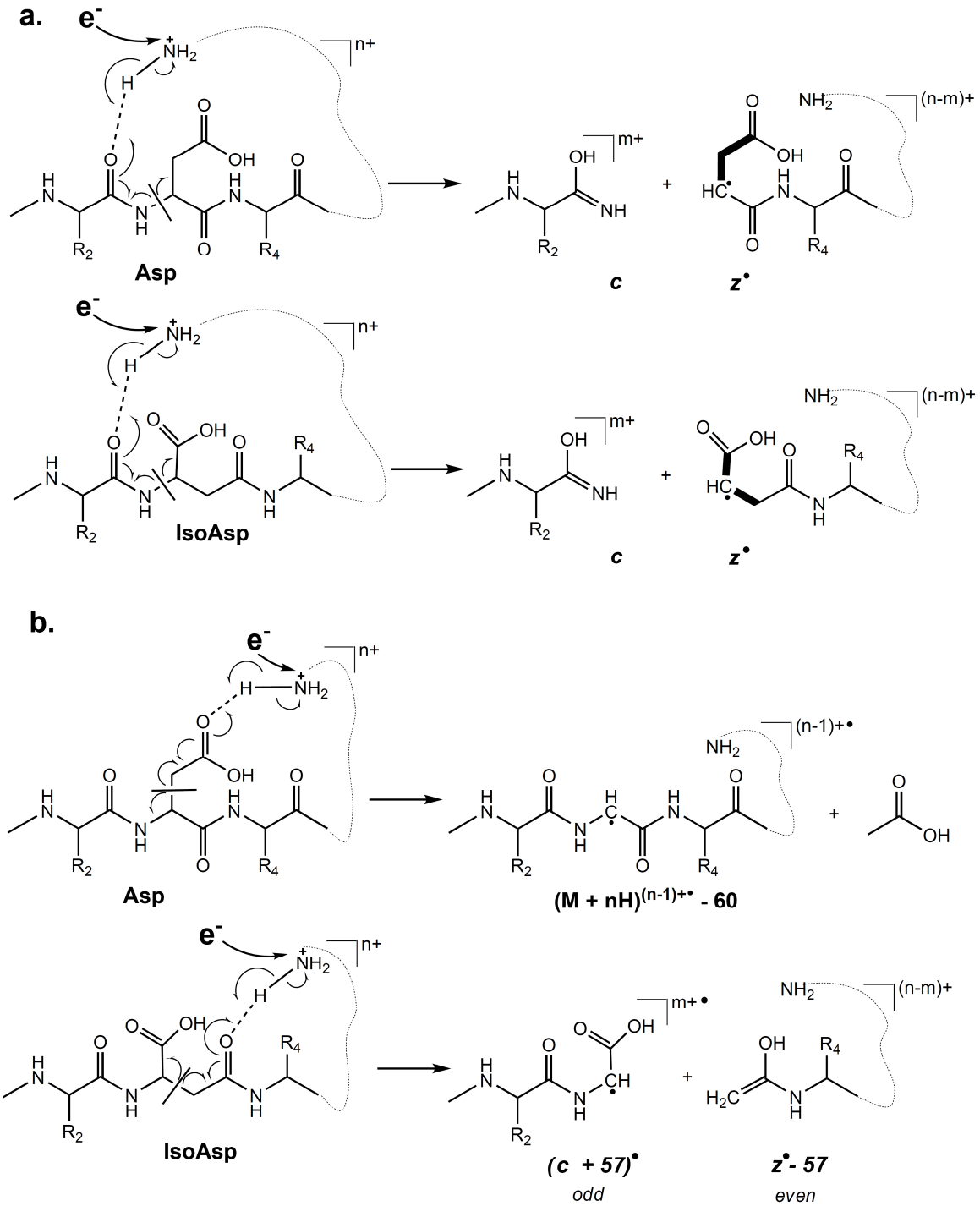

Figure 2.1 The ECD major pathway to produce *c* and *z* fragment ions (a); proposed ECD mechanism for formation of diagnostic fragment ions (b).

2.2.3 Mass Spectrometry

Mass spectra were acquired on a custom built qQq-FTICR MS with a nanospray source and a 7 T actively shielded magnet.[100, 102] Samples were electrosprayed at 1-5 µM concentration in 50:50 MeOH:H_2O with 1 % formic acid. Ions were isolated in the first quadrupole Q_1, accumulated in the second quadrupole Q_2, and transmitted into the ICR cell where they were irradiated with electrons emitted from an indirectly heated dispenser cathode (Heatwave, Watsonville, CA, USA) for ion fragmentation. The following ECD and EID parameters were employed: electron irradiation time between 35 and 100 ms, cathode potential at 0.2 - 1.2 V (ECD), or at 17 – 27 V (EID).

2.3 Results and Discussion

2.3.1 Distinguishing the isomers

ESI FTICR MS of the trypsin digested Aβ 1-40 (DAEFRHDSGYEVHHQKLVFFAEDVGSNKGAIIGLMVGGVV, hereafter abbreviated as Aβ40) revealed good ionization efficiency of the peptide 17-28 (Figure 2.2.a, LVFFAEDVGSNK, abbreviated as Aβ17-28). The doubly charged precursor ion of this peptide was isolated, accumulated, and irradiated with low energy electrons for the ECD event as described in the experimental section. ECD mass spectra of this peptide showed abundant fragmentation with 95 % sequence coverage (Figure 2.2.a). In addition, specific neutral losses from the reduced species of the doubly-charged tryptic peptide were observed, similar to those detected earlier:[180] the loss of ($C_3H_4O_2$+NH_3) from glutamic acid, (C_3H_7+NH_3) from leucine, CH_3NO from asparagine, and $C_2H_4O_2$ loss from aspartic acid, as well as NH_3 from the N-terminus.

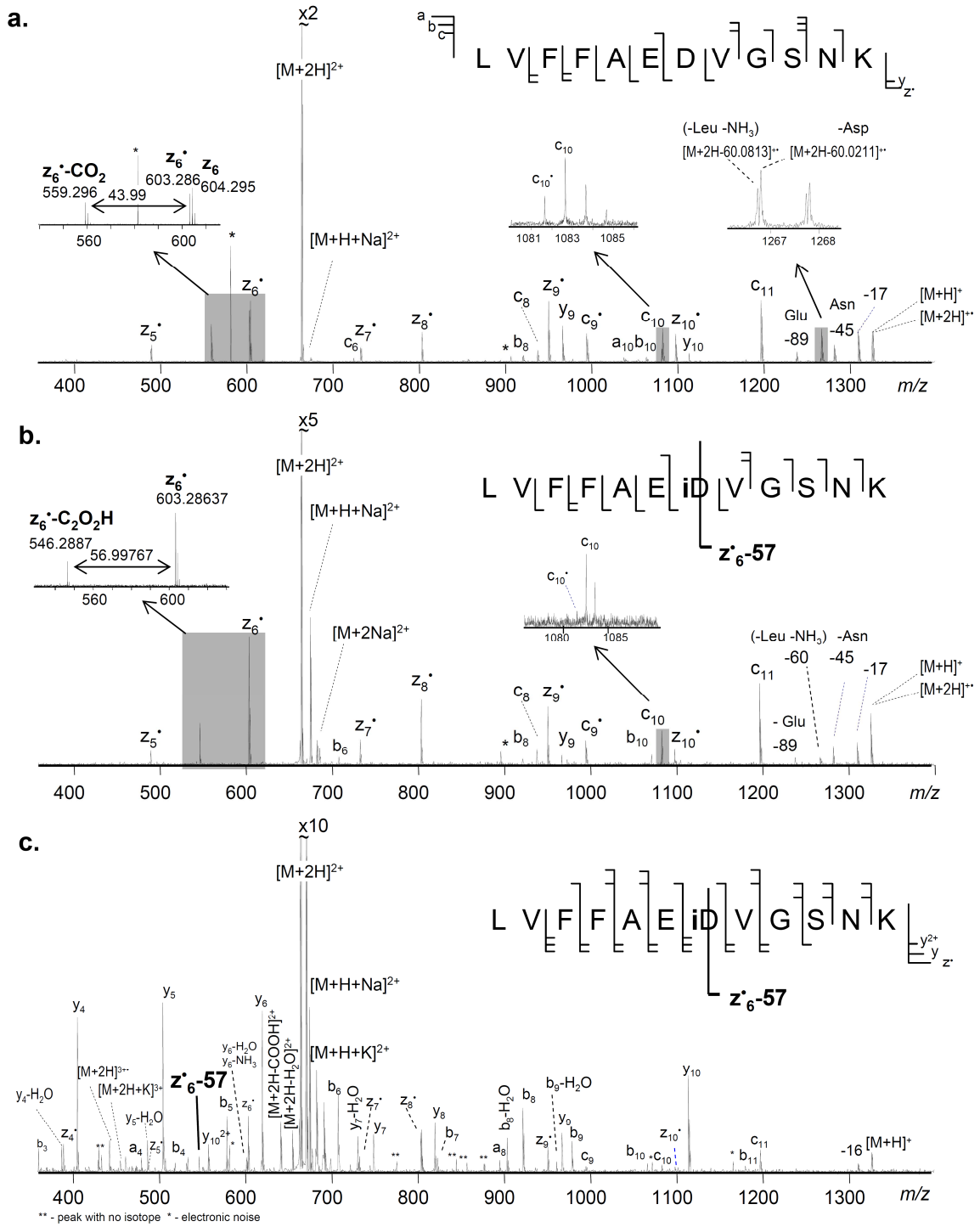

Figure 2.2 ECD of Aβ17-28 (a), ECD of isoAβ17-28 (b), and EID of isoAβ17-28 (c).

In order to perform a comparative analysis of peptide isomers, the same Aβ 17-28 peptide was custom-synthesized with isoaspartic acid at position *23* [isoD23] (Figure 2.2.b, LVFFAE**isoD**VGSNK, abbreviated as isoAβ17-28). ESI FTICR MS spectra of the isolated doubly charged Aβ17-28 and isoAβ17-28 precursor ions showed identical *m/z* (data not shown). ECD of isoAβ17-28 generated the $z_6^{\bullet}$-57 diagnostic fragment ion which was not found in the Aβ17-28 peptide ECD spectrum. In contrast, carbon dioxide (CO_2, *m/z* 43.9898) was lost from the same $z_6^{\bullet}$ fragment ion of Aβ17-28, but not from isoAβ17-28 (Figure 2.2.a, b insets), indicating that CO_2 loss is diagnostic for the presence of Asp, but not isoAsp at a particular residue. While the utility of CO_2 loss as a diagnostic ion has been previously shown,[178] it is not normally as reliable as the c_n+57/z_{m-n}-57 diagnostic peaks as isoAsp can also lose CO_2. However, loss of CO_2 from isoAsp appears to be a minor dissociation channel (as evident by the small peak in a 100 % isoAsp-containing peptide[178]). In the current study, loss of CO_2 from $z^{\bullet}_6$ is not observed (<1 % relative abundance) in isoAβ17-28 indicating that $z_6^{\bullet}$-*44* is another diagnostic fragment ion for Asp-containing Aβ peptides. A nominal loss of 60 was also detected from the charge reduced molecular ion species of the isomerized peptide, but its exact mass corresponds to the leucine side chain plus ammonium (60.0813, C_3H_7+NH_3), not the sidechain of aspartic acid (60.0211, $C_2H_4O_2$), indicating that aspartic acid was not present in the modified peptide. Interestingly, as shown in the inset of the $c_{10}^{\bullet}$ radical fragment, this ion was of a lower abundance in the isomerized version of the peptide. This could be explained by the fact that isoaspartic acid has a shorter side chain, which may affect hydrogen bond formation, and the hydrogen transfer within the complex of *c* and $z^{\bullet}$ fragments.[53, 69, 70, 181, 182] It could be assumed that a weaker

hydrogen bonded complex will have a shorter lifetime, leading to a lower degree of intracomplex hydrogen atom transfer ($c + z^{\bullet} / c^{\bullet} + z$), and fewer number of $c^{\bullet}$ radicals.

Furthermore, the fragmentation pattern of the isoAβ17-28 peptide produced by EID was also investigated to determine whether it could be used to establish the presence and location of an isoaspartic acid. EID spectrum of the isoAβ17-28 contained many *a, b* and *y*, as well as *c* and $z^{\bullet}$ type fragments (Figure 2.2.c). The $z^{\bullet}$-57 diagnostic fragment was also present in the spectrum (with an error of 1.2 ppm, indicating a confident assignment), although with lower abundance compared to the ECD spectra, correlating with a general reduction in abundance of all *c* and $z^{\bullet}$ type fragments as competing reaction channels were accessed. Nevertheless, this experiment demonstrated that EID can be applied in isoaspartomics research along with ECD. The EID technique will be particularly useful in the analysis of singly charged molecular ions, when small molecules are studied in ESI or when MALDI is used as the ionization technique.

Generally, the isomers were distinguished by means of ECD and EID using the diagnostic ions $[M+2H-60]^{\bullet+}$ and $z_6^{\bullet}$-*44* when aspartic acid and $z_6^{\bullet}$-57 when isoaspartic acid were present.

2.3.2 ECD of the full length Amyloid beta protein fragment 1-40

The analysis of Aβ40 is rather challenging due to its high hydrophobicity at its *C*-terminus and its tendency to aggregate. The ESI spectrum of its tryptic digest showed only one peptide Aβ17-28 with high abundance (data not shown). The other three tryptic peptides were either suppressed or had lower ionization efficiency, which made it difficult to isolate them for MS/MS analysis. In addition, top-down analysis of Aβ is

advantageous because digestion solutions are usually of elevated pH relative to physiological conditions, which can introduce undesired structural changes as well as additional deamidation and isomerization.[109, 116, 183] In biological fluids or tissues, Amyloid beta is present as a mixture of various length fragments from 13 to 42 amino acids long.[184] Digestion of this mixture will complicate the analysis and will create biases in the identification of the origins of the resulting digest peptides. Thus, it is important to create a top-down approach for the analysis of Aβ peptides. At this stage of the research, an entire Aβ40 peptide was electrosprayed into the mass spectrometer and analyzed by ECD. The 3^+ to 5^+ charged ions were observed in the spectra and the highest charge state $[M+5H]^{5+}$ ions were isolated for ECD analysis. The ECD spectrum of Aβ40 showed extensive fragmentation (Figure 2.3). Insets show the charge-reduced species $[M+5H]^{4+\bullet}$ and $[M+5H]^{3+\bullet\bullet}$, as well as their neutral losses. Importantly, the complementary fragment pairs $c_6/z_{34}^{\bullet}$, and $c_{22}/z_{18}^{\bullet}$ adjacent to aspartic acids at positions 6 and 23 respectively are present in the spectra. It is likely that these fragment ions would generate diagnostic fragments in isoAsp containing peptides, which could be used to determine the presence of isoaspartic acid.

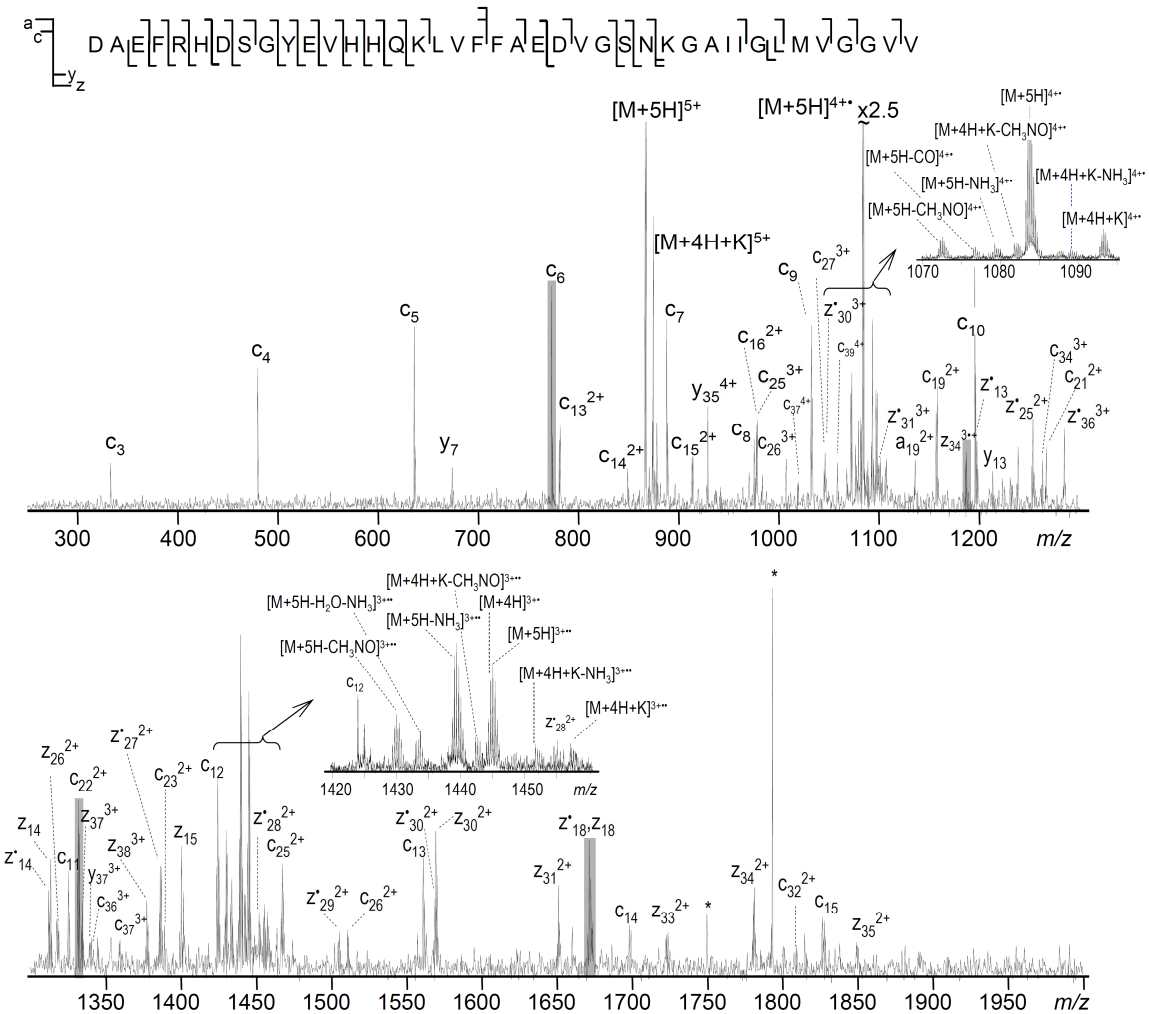

Figure 2.3 ECD of Aβ40.

2.3.3 Detecting isoAsp in Amyloid beta 1-42

The amyloid beta fragment 1-42, or Aβ42, which includes 2 more hydrophobic amino acids at the *C*-terminus compared to Aβ40 DAE…GAIIGLMVGGVVIA[42], is the most abundant in plaque deposits. Its level is greatly enhanced in AD brain, and it is believed to be the most toxic of all Aβ peptides.[185, 186] It is worthwhile, therefore, to develop a method for the analysis of this particular fragment, even though it is notoriously difficult to analyze due to its high hydrophobicity and tendency to aggregate.

In addition, longer peptides generally have higher probability for significant secondary structure in the gas phase and form numerous hydrogen bonds. Unless such ions are activated prior to ECD analysis to disrupt secondary structure, strong hydrogen bonds tend to keep *c/z*$^{\bullet}$ fragment pairs in a complex, reducing the net efficiency of ECD analysis. Nevertheless, successful analysis of Aβ42 would create a method suitable for different length Aβ peptides with the same or fewer number of amino acids.

Formation of isoaspartic acid in a standard Aβ42 was induced to create a relevant test-case for development of this method. Because the rate of aspartate isomerization is ~40 times slower than the rate of Asn deamidation,[109] the variant containing Japanese –Tottori mutation [Asn7] was chosen to accelerate formation of isoAsp by deamidating the asparagine residue. The sample was incubated in ammonium hydroxide at pH >10.2, overnight at 37℃ and analyzed in ESI FTICR MS using ECD. $[M+5H]^{5+}$ molecular ions were isolated, accumulated and irradiated with low-energy electrons. An ECD spectrum of the peptide is shown in Figure 2.4. The mass of the parent ion increased by one or two units (de-convoluted mass) indicating the presence of single and double deamidation correspondingly (see insets). Double deamidation was observed due to the presence of a second asparagine in the peptide sequence at position *27*. Partial deamidation of Asn27 was also observed, which is explained by the fact that the rate of HNS deamidation is faster than the rate of SNK deamidation. In particular, according to the experimental data acquired at near-physiological conditions, the first order deamidation half-life of G**HNS**G and G**SNK**G model pentapeptides are 15.7 and 55.5 days.[112] For the purpose of this experiment, however, deamidation of Asn27 was of a lesser interest, as was the completeness of the deamidation reaction in general. Deamidation of asparagine [Asn7] was performed to

induce the formation of isoaspartic acid at this particular residue because in Amyloid beta peptides found in the cerebral plaque samples of Alzheimer patients, aspartic acid is 75 % isomerized to isoAsp at the residue position *7*.[119] As a result of ECD analysis of the deamidated Aβ42 peptide (Figure 2.4 upper spectrum), the diagnostic fragment c_6+57 was observed (at 2.2 ppm mass accuracy), demonstrating the formation of isoaspartic acid at the 7th residue and the ability of the current method to detect and localize the modification. It should be noted that this model system experienced a highly non-physiological (pH >10) environment, so that the deamidation mechanism is unlikely to follow the *in vivo* mechanism as the pH would have been likely to unfold the peptide, thus perturbing the native deamidation rate. However, the results of this experiment provide a needed baseline for future studies. It was clearly demonstrated that ECD can be used to detect the isoAsp in a top-down experiment of the longest Aβ peptide.

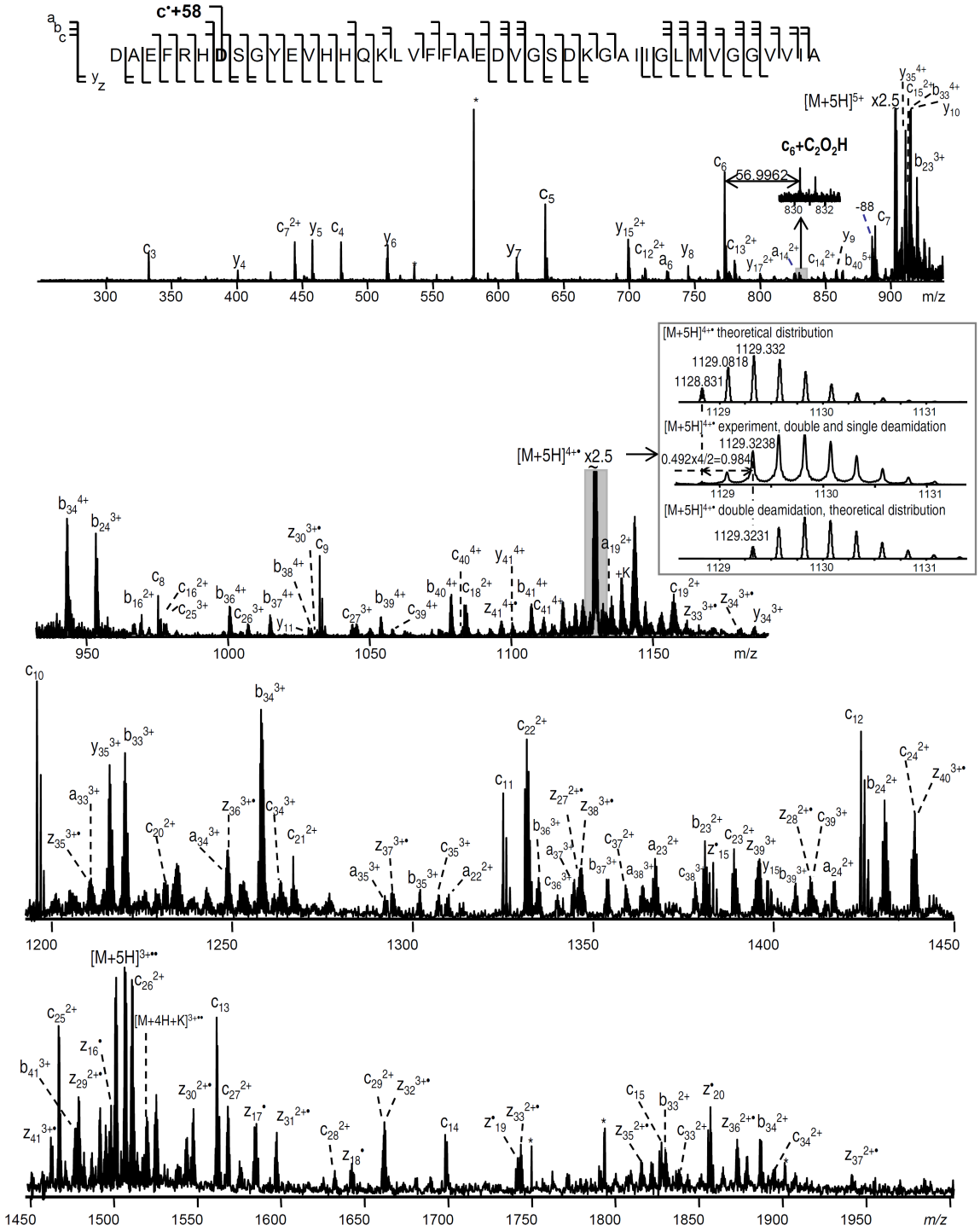

Figure 2.4 ECD of Aβ42 deamidated at Asn7 and Asn27.

Exploring these studies further in terms of quantitative analysis and combining this technique together with HPLC separation will present a powerful tool for the analysis of physiological fluids in Alzheimer's disease patients. Comparative studies of isoAsp containing Aβ peptides in normal and diseased samples of different stages might reveal a novel perspective on Alzheimer's disease initiation and progression.

2.4 Conclusion

The ECD diagnostic ions $[M+2H-60]^{\bullet+}$ and $z_6^{\bullet}$-57 were observed and successfully applied to differentiate the isomeric forms of the Amyloid β tryptic peptide 17-28. Differentiation of aspartic and isoaspartic acid residues is also possible using EID using the same diagnostic ion $z_6^{\bullet}$-57 as in ECD. Although the abundance of the diagnostic peak was relatively low compare to ECD, EID could be particularly useful in the analysis of singly charged precursor ions, where ECD is not applicable. Amyloid β 1-40 and 1-42 peptides can be analyzed by a top-down ECD approach without prior digestion and provide substantial sequence coverage. Isomerized Amyloid β 1-42 at the residue *7* can be differentiated by ECD using the c_6+57 diagnostic ion. Both ECD and EID can clearly define the presence and the position of isoaspartic acid residues in Amyloid β peptides; therefore, they could be applied to the samples of Alzheimer's patients or healthy individuals for better understanding of the disease.

Chapter 3

The analysis of isoAsp, Asp, and Asn containing peptide variants by Liquid Chromatography

3.1 Introduction

The great challenge of biological sample analysis is the complexity of the sample. Often, PTM-containing species represent the minority of the mixture and are easily neglected or lost. Thus, separation of the complex sample becomes crucial for its analysis. High performance liquid chromatography (HPLC) is a powerful technique for the separation of biological mixtures. It was shown in the previous chapter that isoAsp containing standard peptides and proteins can be unambiguously identified using ExD tandem MS methods. However, when isoAsp, Asp and Asn are present as a mixture, which is most often the case in a real biological sample, the abundance of diagnostic fragment is diluted in the spectrum and could be neglected or not observed during analysis. Thus, in many instances, it is important to perform sample separation for "enrichment" of the peptides containing the modification. Further, when ExD methods are not available to differentiate Asp and isoAsp residues in peptides, distinguishing between the two modifications is often based on the assumption that peptides with isoAsp residue normally elute earlier compared with their non-modified counterparts in RP-HPLC.[165, 187-189] However, this is not always the case and such assignment must be checked.[170, 171, 190, 191] Thus, in this chapter, HPLC separation is applied to study isoAsp,

---

[1]This chapter has been partially reproduced with permission from Sargaeva, N. P.; Goloborodko, A. A.; Moskovets, E.; Gorshkov, M. V.; O'Connor, P. B., Sequence-specific predictive chromatography to assist mass spectrometric analysis of asparagine deamidation and aspartate isomerization in peptides, *Electrophoresis*, **2011**, *32*, 1962-1969.

Asp, and Asn containing model peptides to better understand their elution behavior. These include several groups of peptides containing Asn deamidation and Asp isomerization sites at various positions within the peptide sequence. The change of the ion paring reagent in the mobile phase is tested on peptide elution as well. These data are compared to the results provided by other research groups in the summary table.

The second part of this chapter focuses on predictive chromatography. The retention time prediction is commonly used to predict the elution times of non-modified peptides to improve their identification.[192, 193] Recently, a novel model was introduced to describe separation of peptides under reversed phase (RP) high performance liquid chromatography (HPLC) conditions based on a concept of liquid chromatography at critical conditions (BioLCCC, Institute of Energy problems of Chemical Physics in Moscow, Russia).[194-196] The BioLCCC model considers the thermodynamic aspects of peptide separation in reversed-phases. Contrary to existing empirical models, it uses a limited number of free phenomenological parameters and is inherently sequence dependent.[197] The calibration of the BioLCCC model necessary to predict retention times (RT) in the RP-LC separation of unmodified peptides uses only 24 specially designed synthetic peptides. A new module accounting for presence of a phosphogroup[198] and isoAsp/Asp modifications[191] has been added very recently to the BioLCCC predictor. When extended to predict RTs in RP-LC separation of peptides with modified residues, the BioLCCC model, due to its inherent sequence dependence, is capable of predicting RTs of peptides differing only by location of modified amino acids. Therefore, based on the above results of the RP-HPLC separation of peptides with Asn, Asp, and isoAsp residues, the feasibility of using the BioLCCC model to accurately describe their retention times is tested.

3.2 Experimental section

3.2.1 Peptides and reagents

The following peptides were custom synthesized by Peptide 2.0 (Chantilly, VA, USA): yeast enolase peptide variants H-IGL**N**CASSEFFK-OH, H-IGL**iD**CASSEFFK-OH, H-IGL**D**CASSEFFK-OH, synthetic peptides Ac-**N**GVG**N**VGGVH-NH_2, Ac-**isoD**GVG**isoD**VGGVH-NH_2, Ac-**D**GVG**isoD**VGGVH-NH_2, and Ac-**D**GVG**D**VGGVH-NH_2. Angiotensin II (AngII) peptide variants H-**D**RVYIHPF-OH, H-**N**RVYIHPF-OH, and H-**isoD**RVYIHPF-OH were obtained from AnaSpec (San Jose, CA, USA). Trifluoroacetic Acid (TFA) and Formic Acid (FA) were purchased from Thermo Scientific (Rockford, IL, USA); HPLC grade Acetonitrile (ACN) and Methanol (MeOH) were purchased from Fisher Scientific (Fair Lawn, NJ, USA); deionized water was purified by a Millipore Milli-Q Gradient system (R=18.2 MΩ cm and TOC=9-12 ppb), (Billerica, MA, USA); Ammonium Hydroxide (20 %) was obtained from JT Baker (Phillipsburg, NJ, USA), and Ammonium Bicarbonate (ABC) from Sigma-Aldrich, (St. Louis, MO, USA).

3.2.2 Liquid Chromatography

Reversed-phase high performance liquid chromatography peptide separations were performed using an Agilent 1200 Series system (Agilent Technologies, Wilmington, DE, USA) and reversed-phase C18 columns Vydac 218TP54 C18 (250x4.6mm, 5µm particles, 300Å pore size) and Vydac 218TP5215 C18 (150x2.1mm, 3µm particles, 300Å pore size). 20 µl of 0.5-4 nmol peptide mixtures were injected directly onto the column and eluted with various gradients of acetonitrile with either 0.08 % TFA or 0.1 % FA at

0.5-1 ml/min flow rate and 35 ℃ unless indicated otherwise. These TFA and FA concentrations correspond to pH 2.0 and 2.6, respectively. A linear or step gradient was adjusted for each group of peptides. The chromatograms were measured using UV detection at 214 nm and the fractions were collected and dried in a SpeedVac (when eluted on TFA) or refrigerated at 4 ℃ (when eluted on FA) for further analysis.

3.2.3 Mass spectrometry

ECD-FTICR-MS. Electron capture dissociation Fourier transform ion cyclotron resonance mass spectrometry was performed on a 12 T SolariX FTICR MS instrument (Bruker Daltonics, Billerica, MA, USA). Peptides were nanosprayed at a typical concentration of 0.5-2 µM in ACN:H_2O (0.1 % FA) when mass analysis was conducted following HPLC separation with off-line fraction collection or in 50:50 MeOH: H_2O with (0.1 % FA) when infused directly. Doubly charged molecular ions were isolated and irradiated with low-energy (<1 eV) electrons for 0.05-0.08 ms to produce fragments. 100 scans were accumulated for each peptide and spectra were analyzed using Bruker's ESI Compass DataAnalysis 4.0 software.

3.2.4 RT prediction

Theoretical retention times for peptides were calculated using the BioLCCC model for sequence-dependent RT prediction. This software package was developed as an open source library and is available on-line at http://theorchromo.ru. It consists of a library written in both C++ and Python programming languages and allows setting the user-defined separation conditions including the choice of ion-pairing reagents, column parameters, and the gradient profile.

3.3 Results and Discussion

3.3.1 RP-HPLC separations of isoAsp-peptides

Yeast enolase model peptide variants containing Asp, isoAsp and Asn in the middle of the sequence are first separated using a mobile phase with FA as the ion paring reagent and then compared with that with TFA (Figure 3.1.a and 3.1.b respectively). The elution order in both scenarios is isoAsp <= Asn < Asp, although with FA, there is no baseline separation observed for isoAsp/Asn variants, and isoAsp tends to elute first. Nonetheless, the isoAsp elution prior to the Asp variant is consistent with the results reported earlier.[165, 187-189]

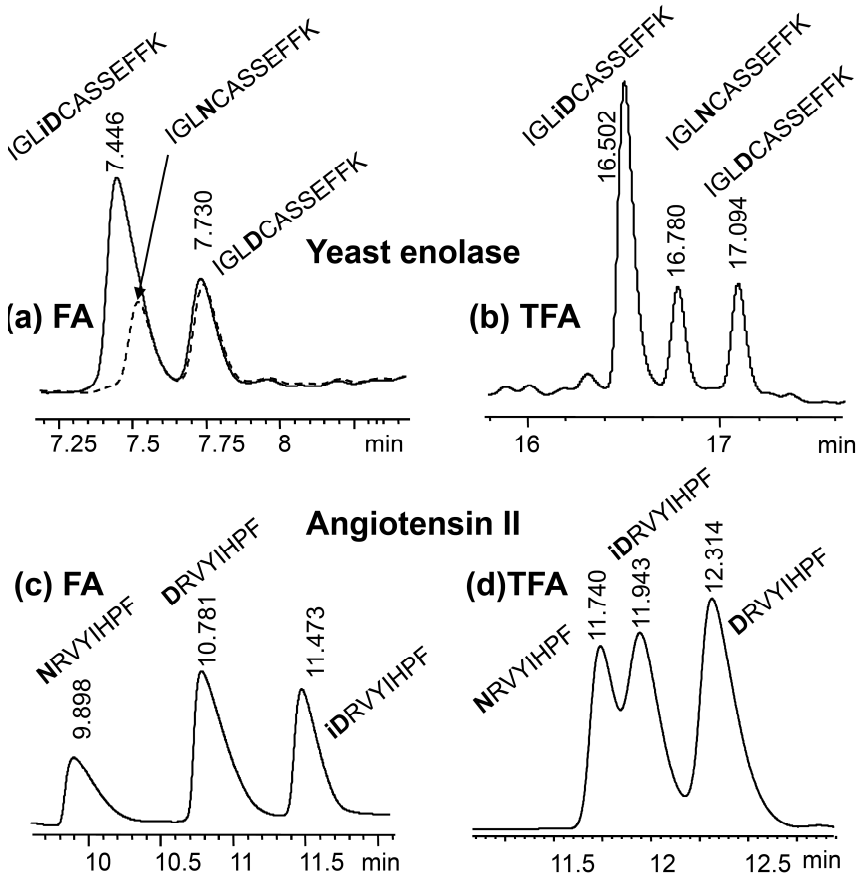

Figure 3.1 IsoAsp position affects the peptide elution order.

The next group of peptide variants of Ang II contains modification at the peptide N-terminal site. A sudden change is observed in the elution order of FA separated peptides: Asn < Asp < isoAsp, the isoAsp-peptide eluted last, however, Asn-, and Asp-peptides kept the order (Figure 3.1.c). The Ang II peptides are further separated with alternative ion paring reagent TFA and the isoAsp-peptide retention time is shifted again (Figure 3.1.d). The elution order is as follows: Asn < isoAsp < Asp. These results indicate that isoAsp position within the peptide sequence plays an important role in the hydrophobic interaction between the peptide and the column's stationary phase. The difference in the isoAsp-peptide elution order when different ion paring reagents applied

may be related to the difference in pH of the mobile phase: 2.6 (FA) and 2.0 (TFA). Although the difference is very small, the pKa value of an isoAsp residue (~3.3) is lower than that of an Asp residue (~4).[153] Therefore, at more acidic conditions such as in TFA, an isoAsp-peptide gets higher rate of deprotonation weakening the hydrophobic interaction, leading to a shorter retention time. Interestingly, this change is only observed when the isoAsp is positioned at the N-terminus, so it seems that for small peptides the charge of the N-terminus plays a very important role in peptide partitioning between the mobile phase and the RP column.

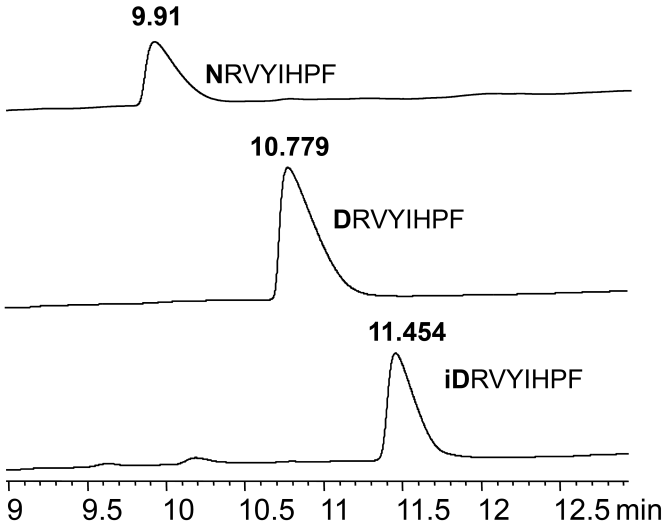

Figure 3.2 Chromatograms of Ang II peptide variants.

It must be noted that chromatogram assignment is based on multiple separations (>2) for each peptide group and at first each model peptide was loaded onto the column by itself to obtain the reference retention time information. An example is shown for Ang II peptide in Figure 3.2. In addition, fractions were collected for each group of peptides when loaded as a mixture onto the column and sequence information was confirmed by ECD (data will be presented in the following chapter).

To further test the importance of the isoAsp position within the peptide, the next group of synthetic peptides is analyzed. In this case, the N-terminal isoAsp is capped with an acetyl group. There is also an additional modification site present in the middle of the sequence. Peptides were separated at the same conditions with either an FA or a TFA pH modifier. Corresponding chromatograms and sequences of peptides are presented in Figure 3.3.a and Figure 3.3.b. This time, the elution order has not changed with the change of the ion paring reagent. Overall, the elution behavior of this group of peptides resembled that of the yeast enolase peptide variants (Figure 3.1.a, b). Therefore, it seems that acetylation of the N-terminal isoAsp preserves the elution order of peptide variants.

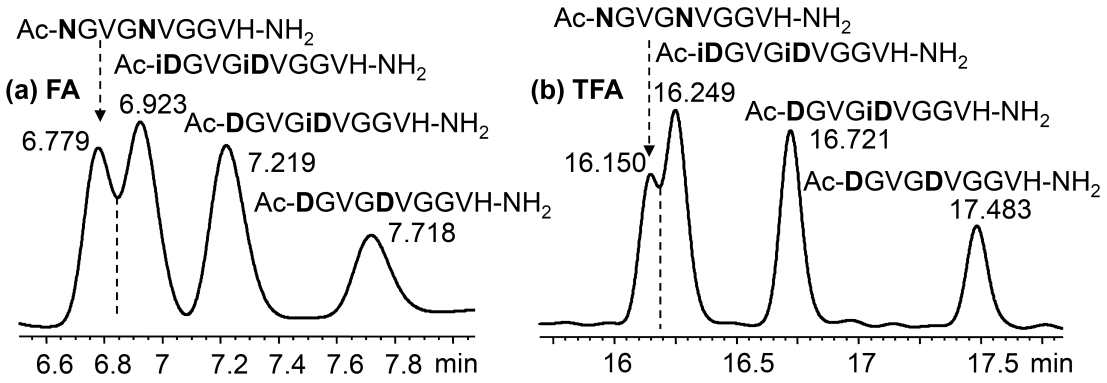

Figure 3.3 N-terminal acetylation preserves the elution order of isoAsp modified peptides.

Isoform sequences	Stationary phase	Pore size, Å	T, ℃	reagent	Elution order	Ref.#
Ac-NGVGNVGGVH-NH2 Ac-isoDGVGisoDVGGVH-NH2 Ac-DGVGisoDVGGVH-NH2 Ac-DGVGDVGGVH-NH2	Vydac218 TP54 C18	300	35	FA	NN< isoDisoD < DisoD <DD	this work
Ac-NGVGNVGGVH-NH2 Ac-isoDGVGisoDVGGVH-NH2 Ac-DGVGisoDVGGVH-NH2 Ac-DGVGDVGGVH-NH2	Vydac218 TP54 C18	300	35	TFA	NN< isoDisoD < DisoD <DD	this work
H-IGLisoDCASSEFFK-OH H-IGLNCASSEFFK-OH H-IGLDCASSEFFK-OH	Vydac218 TP54 C18	300	35	FA	isoD~N<D	this work
H-IGLisoDCASSEFFK-OH H-IGLNCASSEFFK-OH H-IGLDCASSEFFK-OH	Vydac218 TP5215 C18	300	35	TFA	isoD<N<D	this work
H-NRVYIHPF-OH H-DRVYIHPF-OH H-isoDRVYIHPF-OH	Vydac218 TP54 C18	300	35	FA	N<D<isoD	this work
H-NRVYIHPF-OH H-isoDRVYIHPF-OH H-DRVYIHPF-OH	Vydac218 TP5215 C18	300	35	TFA	N<isoD<D	this work
H-ILPGNGNINYNEK-OH H-ILPGisoDGNINYNEK-OH H-ILPGDGNINYNEK-OH	Zorbax SB300 C18	300	ambient	FA	N<isoD<D	Huang, L, et al.
H-SLisoDGEWR-OH H-SLNGEWR-OH H-SLDGEWR-OH	Vydac218 TP C18 C18 PepMap 100 C18	300 300 100		FA FA FA	isoD~N<D isoD~N<D N<isoD<D	Krokhin, O.V., et al.
H-SLisoDGEWR-OH H-SLNGEWR-OH H-SLDGEWR-OH	Vydac218 TP C18 C18 PepMap 100 C18	300 300 100		TFA TFA TFA	isoD<N<D isoD<N<D isoD~N<D	Krokhin, O.V., et al.
H-IGLisoDCASSEFFK-OH H-IGLDCASSEFFK-OH	BEH C18	130	35	FA	isoD<D	Winter, D., et al.
H-DQPIASTK-OH H-isoDQPIASTK-OH	BEH C18	130	35	FA	D<isoD	Winter, D., et al.
H-GFSYTDANKNKGITW-OH H-GFSYTisoDANKNKGITW-OH	Vydac C18	300		FA	D<isoD	Ni, W., et al.
H-GFSYTDANKNKGITW-OH H-GFSYTisoDANKNKGITW-OH	Vydac C18	300		TFA	isoD<D	
H-DAEFRHDSGYEVHHQK-OH H-DAEFRHisoDSGYEVHHQK-OH	Vydac C18	300		FA	D<isoD	Ni, W., et al.
H-DAEFRHDSGYEVHHQK-OH H-DAEFRHisoDSGYEVHHQK-OH	Vydac C18	300		TFA	isoD<D	

Table 3.1 The elution order results for peptides containing Asn, Asp, and isoAsp residues.

Table 3.1 summarizes the obtained results and results reported on similar peptides in earlier works.[170, 171, 187, 190] In general, the use of TFA results in isoAsp-

containing peptides eluting before the Asp-containing ones. The same is applicable to peptides with isoAsp located in the middle of the peptide sequence and separated using FA; however, this is not always the case as was shown for Cytochrome-C and Aβ 1-16 peptides studied by Ni, W., et al.[171] Additionally, based on the results of Ang II peptides (Figure 3.1), when isoAsp is located at the non-acetylated N-terminus (i.e. the one with normal composition), the observed retention time is increased, and the elution order is reversed: Asp < isoAsp. This was also demonstrated earlier on the DQPIASTK peptide variants by Winter et al. (Table 3.1).[170] The reversed order of the N-terminal isoAsp containing peptides may be attributed to the presence of the charged N-terminal group, which may be overcome by acetylation of the N-terminus as shown in Figure 3.2.

In conclusion of this section, it seems clear that when dealing with peptides with deamidation and isomerization modifications, the LC separation results alone may lead to erroneous assignment, because the elution order depends on the peptide sequence as well as on conditions of separation. Additional methods such as ExD tandem MS is a necessary complementary technique to validate the assignment.

3.3.2 Predictive chromatography

When ExD tandem MS is not available, other means of complementary analysis would be desired for correct identification of the isoAsp-peptides. One such tool is predictive chromatography. The retention time prediction is offered as an additional step of the analysis in the standard proteomic approach of peptide sequence identification (Figure 3.4). Information from the database search and the HPLC parameters could be used to predict the retention time of the eluted peptides. Thus, for instance, the results may be corrected to reduce the false positive identifications from the database outcome.

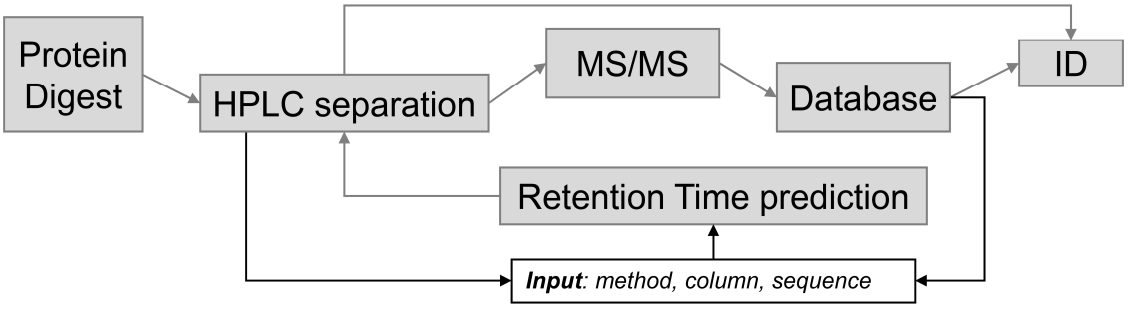

Figure 3.4 Improved sequence identification (ID)

One analytical model of retention time prediction is the BioLCCC model developed at the Institute of Energy problems of Chemical Physics in Moscow, Russia for non-modified peptides.[194] This model takes into account column dimensions (length, i.d.), packing material (pore size), mobile phase components, gradient details, flow rate, and peptide sequence. It is possible to extend this model toward modified peptides[196]; the model was recently extended to take into account the separation of peptides containing isoAsp residues. As a result of a collaborative project, this model is tested on modified peptide separations presented above. Ang II peptide variants separation in FA (Figure 3.5.a) provided perfect correlation between the predicted theoretical and the experimental data. RT was also calculated for a group of peptides separated in TFA as demonstrated for synthetic peptides (Figure 3.5.c, d). Correlation between the theoretical RT and the experimental RT is also near 100 %. Notably, when predicting peptide elution orders in FA vs. TFA, the model had to be recalibrated to address separation selectivity change.

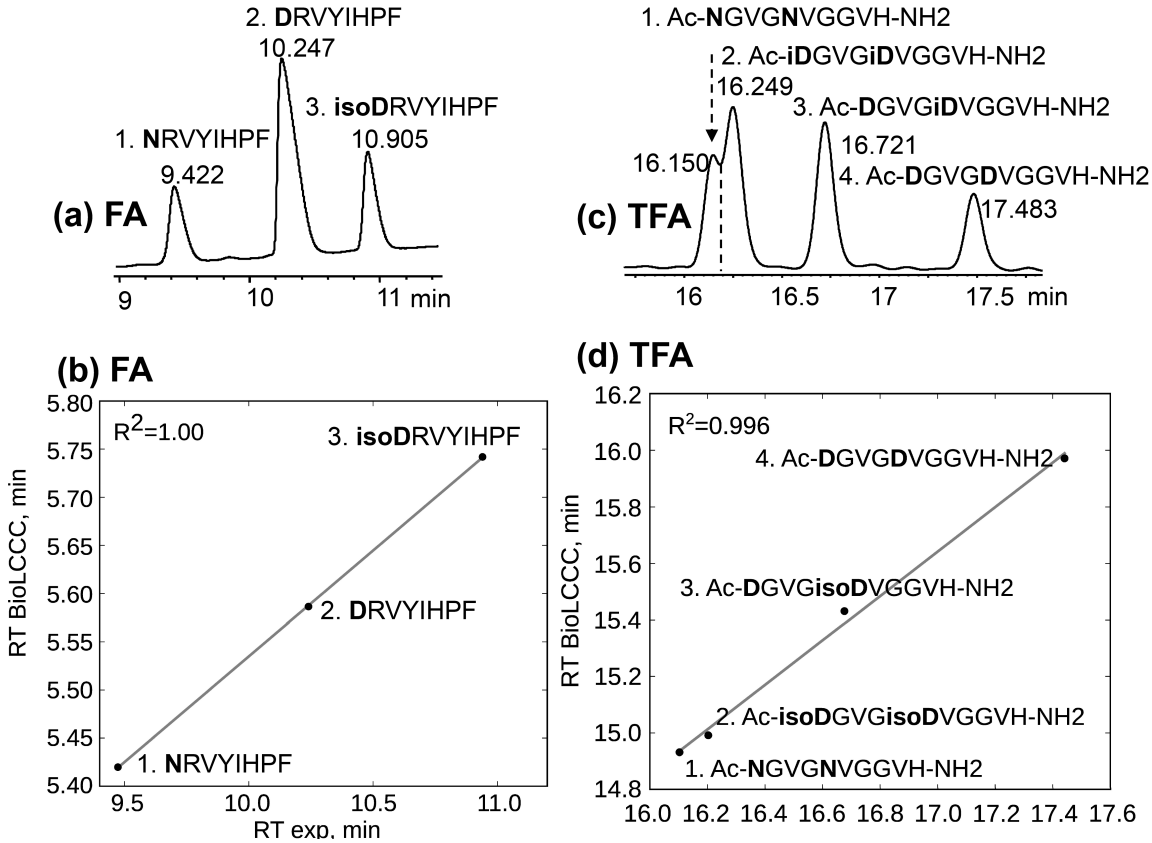

Figure 3.5 Correlation between the predicted and the experimental retention time: Ang II variants separated in FA (a) experiment and (b) correlation; synthetic variants separated in TFA (c) experiment and (d) correlation.

The results shown in Figure 3.5 demonstrate that the BioLCCC model describing the separation of peptides in reversed-phase gradient HPLC can be used to predict elution times and elution order for peptides containing Asn, Asp and isoAsp residues. In the course of protein analysis that requires identification of localization of the modified residues and characterization of the level of protein deamidation or isomerization, the sequence specific prediction of retention times for such peptide variants will provide an additional set of sequence data complementary to MS/MS results as suggested in Figure 3.6. The use of retention time prediction specific to amino acid sequence, may assist in

characterization of proteins with isomeric amino acid residues in a variety of applications. These applications may include selected reaction monitoring (SRM) or multiple reaction monitoring (MRM) analysis in targeted proteomics, which are increasingly used in biomarker discovery. The match between observed and predicted retention times can serve as an independent validation of identifications of peptides with PTM in large-scale proteomic projects.

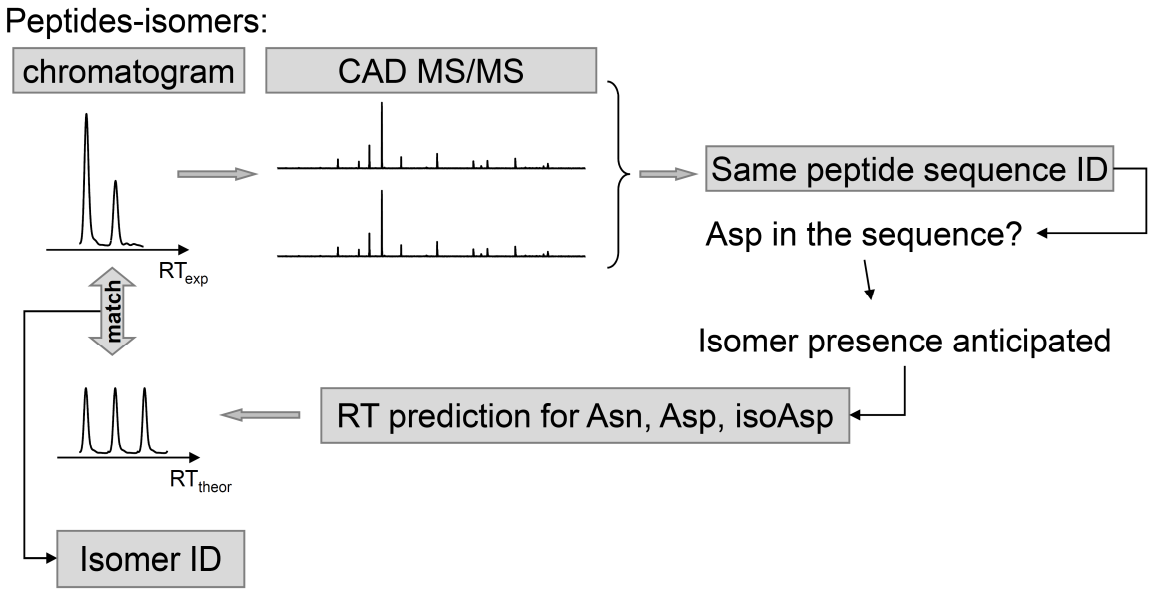

Figure 3.6 Improved identification of modified peptides.

3.4 Conclusion

In this chapter, it is demonstrated that chromatographic results alone may be biased especially when N-terminal isoAsp is present. The ExD methods would be required to validate or correct isomer assignment. When ExD methods are not available, the use of other complementary techniques is needed. Predictive chromatography was suggested as one such tool. Indeed, it was shown that sequence specific retention time predicting model, the BioLCCC, is capable of providing correct

elution orders for isoAsp-containing peptides. Matching of the predicted and experimental retention times allows additional validation of peptide identifications obtained from MS/MS spectra and filtering out possible false positives due to sequence specificity of chromatographic data. It is worth noting, that any predictor model, such as the one described above, needs to be established and validated by employing a vast variety of experimental data. While mathematical predictor models can significantly aid in experimental design and outcome, it is desirable to validate the data and the data assumption by obtaining empirical data.

Chapter 4

Differentiating N-terminal Asp and isoAsp residues in peptides

4.1 Introduction

Formation of isoaspartic acid (isoAsp) is a common modification of aspartic acid (Asp) or asparagine (Asn) residue in proteins. Differentiation of isoAsp and Asp residues is a challenging task owing to their similar properties and identical molecular mass. A number of techniques have been developed to detect isoAsp, and they are often used in conjunction. These include the Edman degradation reaction,[199] PIMT-utilizing assays,[154] affinity enrichment of isoAsp-containing proteins,[175] use of isoAsp-specific antibodies,[120, 158] endoproteinase Asp-N-based approaches,[125, 127, 171] isotopic ^{18}O labeling,[111, 173, 183] and various liquid chromatography (LC)-based techniques: hydrophobic interaction chromatography,[200] size-exclusion high performance liquid chromatography (HPLC),[125] cation exchange HPLC,[200] Reversed-Phase (RP) HPLC,[168, 190] and Ultra HPLC (UPLC).[170] Asp/isoAsp differentiation has been demonstrated by tandem mass spectrometric approaches including collisionally activated dissociation (CAD),[162, 164] fast atom bombardment,[163] and post-source decay fragmentation.[201] Recently, isoAsp identification and quantitation by tandem MS methods employing ion-electron or ion-ion interactions (ExD) have been developed[176, 178, 202-204] and successfully applied,[171, 205, 206] based on the diagnostic fragment ions $c + 57$ and $z^{\bullet} - 57$ that result from the C_{α} - C_{β} bond cleavage unique to isoAsp residues. All the above-mentioned MS

---

[1]This chapter has been partially reproduced with permission from Sargaeva, N. P.; Lin, C.; O'Connor, P. B., Differentiating N-terminal aspartic and isoaspartic acid residues in peptides, *Analytical Chemistry*, **2011**, *83*, 6675-6682.

methods were accomplished in the positive ion mode; however, in the negative ion mode, the isoAsp-containing peptides were not differentiated.[207]

In spite of a large number of existing approaches, isoAsp identification remains a challenging task. In HPLC, the elution order of Asp/isoAsp-containing peptides depends on conditions of separation (column type, mobile phase, temperature, etc.), materials, and the instrument used.[171, 190] In particular, as was shown in the previous chapter, the elution order can be inverted when isoAsp is located at the N-terminus, leading to erroneous assignment.[170, 208] Thus, unless a standard mixture of the same peptide pair separated at the same condition is available, a further analysis would be required for correct isomer assignment. ExD-based tandem MS seems to be a fast and accurate approach well suited for this task. However, to the best of author knowledge, a detailed ExD study of peptides with N-terminally located isoAsp residues has not been performed and the N-terminal isoAsp-specific fragments have not yet been demonstrated. In this chapter, the potential of ExD for N-terminal isoAsp residue identification is investigated, either by performing the ExD analysis alone or following RP-HPLC separation. The role of N-terminal acetylation and the effect of ion activation in isomer differentiation are also examined.

4.2 Experimental section

4.2.1 Peptides and reagents

Angiotensin II (Ang II) peptide variant i**D**RVYIHPF (hereinafter iD represents isoAsp in peptide sequences), synthetic peptides Ac-**D**GVG**D**VGGVH-NH_2 and Ac-**iD**GVG**iD**VGGVH-NH_2, and Amyloid beta 1-10 peptide variant **N**AEFRH**N**SGY with

Asn residues at position 1 and 7 (hereafter A_{β}1-10 (N1N7)) were custom synthesized by Peptide 2.0 (Chantilly, VA, USA). Ang II (**D**RVYIHPF) and $A_{\beta}1^{-}10$ (**D**AEFRH**D**SGY) were ordered from AnaSpec (San Jose, CA, USA). Formic Acid (FA) was purchased from Thermo Scientific (Rockford, IL, USA). HPLC grade Acetonitrile (ACN) and Methanol (MeOH) were obtained from Fisher Scientific (Fair Lawn, NJ, USA). Deionized water was purified by a Millipore Milli-Q Gradient system (R=18.2 MΩ cm and TOC = 9 – 12 ppb) (Billerica, MA, USA). Ammonium Bicarbonate (ABC) was ordered from Sigma-Aldrich (St. Louis, MO, USA).

4.2.2 Deamidation

The A_{β}1-10 peptide variant (NAEFRHNSGY) was incubated at 0.44 mM concentration in 0.1 mM ABC, at pH ~7.7 and 37 ℃ for 4 days. The resulting peptide mixture was separated on reversed-phase C_{18} column prior to MS/MS analysis.

4.2.3 Chromatography

RP-HPLC peptide separations were performed on an Agilent 1200 Series system (Agilent Technologies, Wilmington, DE, USA) using a reversed-phase C18 column Vydac 218TP5215 (150 x 2.1 mm, 3 µm particles, 300 Å pore size). 4 nmol of peptide mixture (in 20 µl) was injected directly into the column and eluted using a linear gradient of acetonitrile with 0.1 % FA (0 min - 1 % B, 20 min - 11 % B) at 0.7 ml/min flow rate at 60 ℃. The chromatograms were measured using UV detection at 214 nm. Fractions were collected and refrigerated at 4 ℃ prior to MS/MS analysis.

4.2.4 Mass Spectrometry

ExD analyses were performed on:

1) a solariX FTICR instrument (Bruker Daltonics, Billerica, MA, USA) with a 12 T actively shielded magnet: electron capture dissociation (ECD), hotECD, and electron transfer dissociation (ETD). Peptides were nanosprayed with 0.5 - 2 µM concentration in 50:50 ACN:H_2O with 0.1 % FA following HPLC separation with off-line fraction collection or in 50:50 MeOH:H_2O with 0.1 % FA when infused directly. Doubly-charged molecular ions were isolated and irradiated with low- (cathode bias 0.4-0.8 V) or high- (cathode bias 4.5 V (hotECD)) energy electrons for 0.05 - 0.5 ms to produce fragments. Each ExD spectrum was the result of 100 scans.

2) an LTQ-Orbitrap XL with ETD capability (Thermo Scientific, San Jose, CA, USA): ETD with or without supplemental activation (SA). Peptides were nanosprayed in solutions as stated above at ~ 0.5 µM using a robotic Nanomate source (Advion, Ithaca, NY, USA). Activation energy parameter “En” of 5 or 15 was applied when SA was on (typical En values range from 0 - 20).

and 3) an amaZon Ion Trap instrument (Bruker Daltonics, Billerica, MA, USA): ETD with or without smart decomposition (SD). Peptides were electrosprayed (2 µl/min, glass capillary temperature 220 ℃) at 1 µM concentration in 50:50 MeOH:H2O with 0.1-1 % formic acid using an Apollo II ion source.

Fluoranthene was used as the anion radical reagent in all ETD experiments with 150 - 250 ms reagent accumulation, and 50 - 150 ms reaction time was used to produce fragments. Data acquired on solariX and amaZon were analyzed using Bruker’s ESI Compass DataAnalysis 4.0 software. The Orbitrap data were analyzed using Thermo's Xcalibur 2.0.7 software.

4.3 Results and Discussion

4.3.1 Diagnostic fragments for the N-terminal Asp/isoAsp

As originally proposed, ECD of peptides with isoAsp located at the nth position may generate a unique complementary ion pair c_{n-1} + 57 and $z_{m-n+1}^{\bullet}$ - 57 as a result of the C_α - C_β bond cleavage, where *m* is the total number of amino acid residues and 57, or more accurately, 56.9976 corresponds to the mass of a $C_2HO_2^{\bullet}$ group. For an isoAsp residue located at the N-terminus, *n* = 1, and the diagnostic fragments become c_0 + 57 and $z_m^{\bullet}$ - 57. The c_0 fragment is essentially an ammonia molecule which is neither informative nor observed in ECD spectra, and the $z_m^{\bullet}$ ion contains no sequence information, and is usually assigned as a loss of ammonia from the charge-reduced species $[M + 2H - NH_3]^{+\bullet}$. Thus, when an N-terminal isoAsp residue is present, the C-terminal diagnostic fragment would be $[M + 2H - (NH_3 + C_2HO_2^{\bullet})]^{+\bullet}$ or $[M + 2H -74.0242]^{+\bullet}$ (hereinafter indicated as $[M + 2H - 74]^{+\bullet}$), and the N-terminal diagnostic fragment would be $C_2H_5NO_2^{+\bullet}$ (*m/z* = 75.032). Although the *m/z* = 75 peak is usually below the low mass cut-off, it is still possible to look for the corresponding neutral loss $[M + 2H - 74]^{+\bullet}$.

In order to see if the isoAsp can be differentiated from the Asp when located at the N-terminus, ECD spectra of the two synthetic isomers of Ang II were directly compared (Figure 4.1). The two spectra were very similar with only a few exceptions. Careful examination revealed the presence of the specific fragment "$z_8^{\bullet}$" - 57 or $[M + 2H - 74]^{+\bullet}$ only in the ECD spectrum of the isoAsp-containing Ang II peptide. In contrast, the loss of 60.0211 ($C_2H_4O_2$) and a double CO_2 loss were observed only for the

Asp peptide. Indeed, the loss of 60 is characteristic of the Asp side chain[180] and cannot be formed from the isoAsp. The loss of two CO_2 molecules can be generated by a combined loss from the C-terminus and from the Asp side chain. Although the CO_2 loss can also come from an isoAsp residue, it is normally of a much lower abundance[178, 205] or undetectable.[202] For example, the $a_6^{\bullet}$ - NH_2 - CO_2 peak was very abundant in the ECD spectrum of the Ang II peptide, but was not detected in that of its isoAsp variant. Thus, in Figure 4.1a, the CO_2 loss from the charge-reduced species was probably generated from the C-terminus.

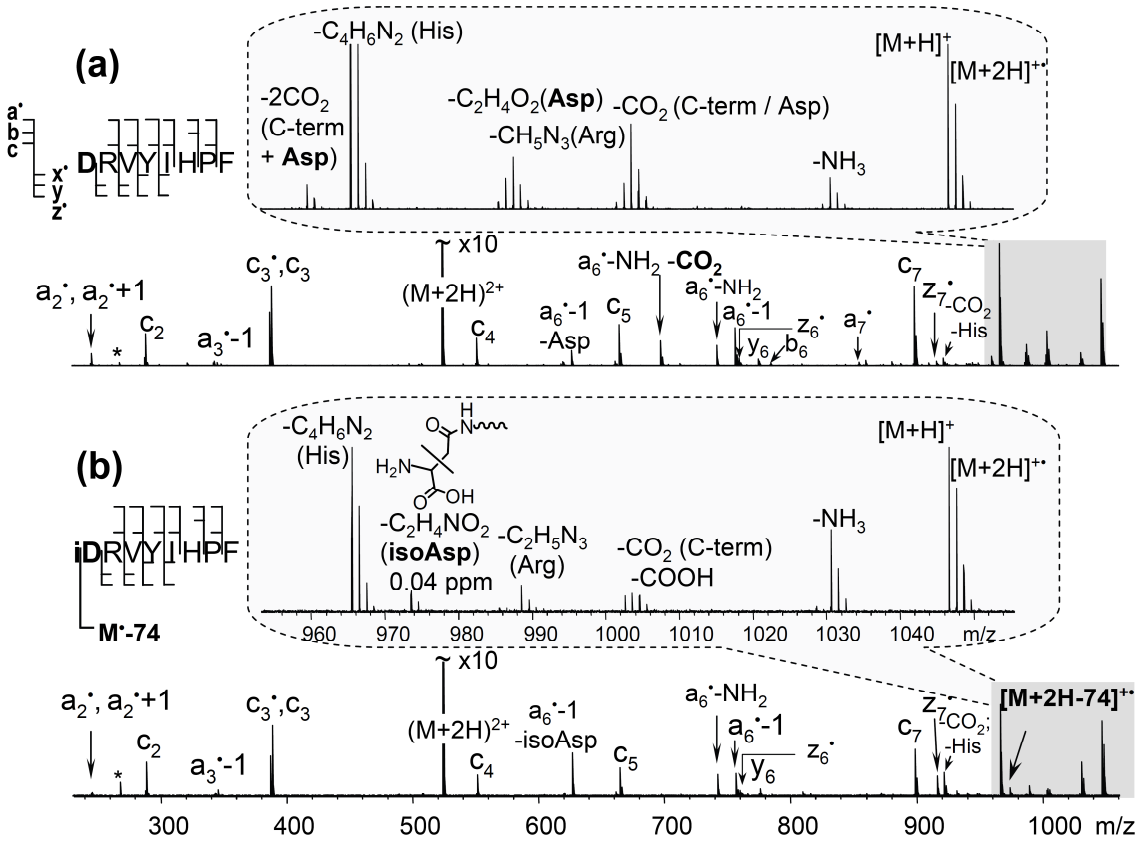

Figure 4.1 ECD spectra of the Angiotensin II (a) and its modified variant with isoAsp at the N-terminus (b). Insets show side-chain losses from the charge-reduced species $[M + 2H]^{+\bullet}$. IsoAsp specific fragment $[M + 2H - 74]^{+\bullet}$, produced as a result of the C_α - C_β bond cleavage within the N-terminal isoAsp residue, is present in the modified variant only, (b) inset.

4.3.2 Analysis of the deamidation products of Aβ1-10 (N1N7) by off-line RP-HPLC followed by ECD

An Aβ1-10 peptide variant with Asn residues at position 1 and 7 was deamidated to artificially introduce isoAsp residues into the sequence. The resulting mixture of peptides was separated on a C_{18} reversed-phase column. 11 peaks were detected in

the chromatogram (Figure 4.2, top panel), collected into fractions, and further analyzed using ECD. It was possible to differentiate and to define the elution order of the isomeric peptides containing isoAsp residues based on the diagnostic fragments observed, i.e. $[M + 2H - 74]^{+\bullet}$ for the isoAsp1 and $c_6 + 57$ for the isoAsp7, as shown in Figure 4.2. Non-deamidated Asn residues were distinguished based on the 0.984 mass difference of the precursor ions and their fragments containing Asn, as shown in the example of $z_6^{\bullet}$ fragments (Figure 4.3. fractions I and V). Fraction VI contained both peptides **D**AEFRH**N**SGY and **N**AEFRH**iD**SGY, which are isomers and thus indistinguishable at the MS level yet could be easily identified by ECD because some fragment ions exhibited two components, separated by 0.984 Da (Figure 4.3. fraction VI, inset). The **D**AEFRH**N**SGY peptide comprises only a small fraction of fraction VI, based on the relative abundance of the two components within the $z_6^{\bullet}$ isotopic cluster. This is consistent with the fact that the **D**AEFRH**N**SGY peptide has a lower probability of formation comparing to the **N**AEFRH**iD**SGY peptide (from original peptide **N**AEFRH**N**SGY) because the Asn in the NA sequence has a slower deamidation rate than Asn in the NS sequence.[115, 209] Spectra for fractions II and III are not shown as they consist of unrelated peptides originated from synthesis impurity. Although the separation of this closely related mixture of peptides was challenging and for some peaks there was no base line separation, all peptides were successfully identified by ECD, highlighting the utility of ECD in isoAspartomic research.

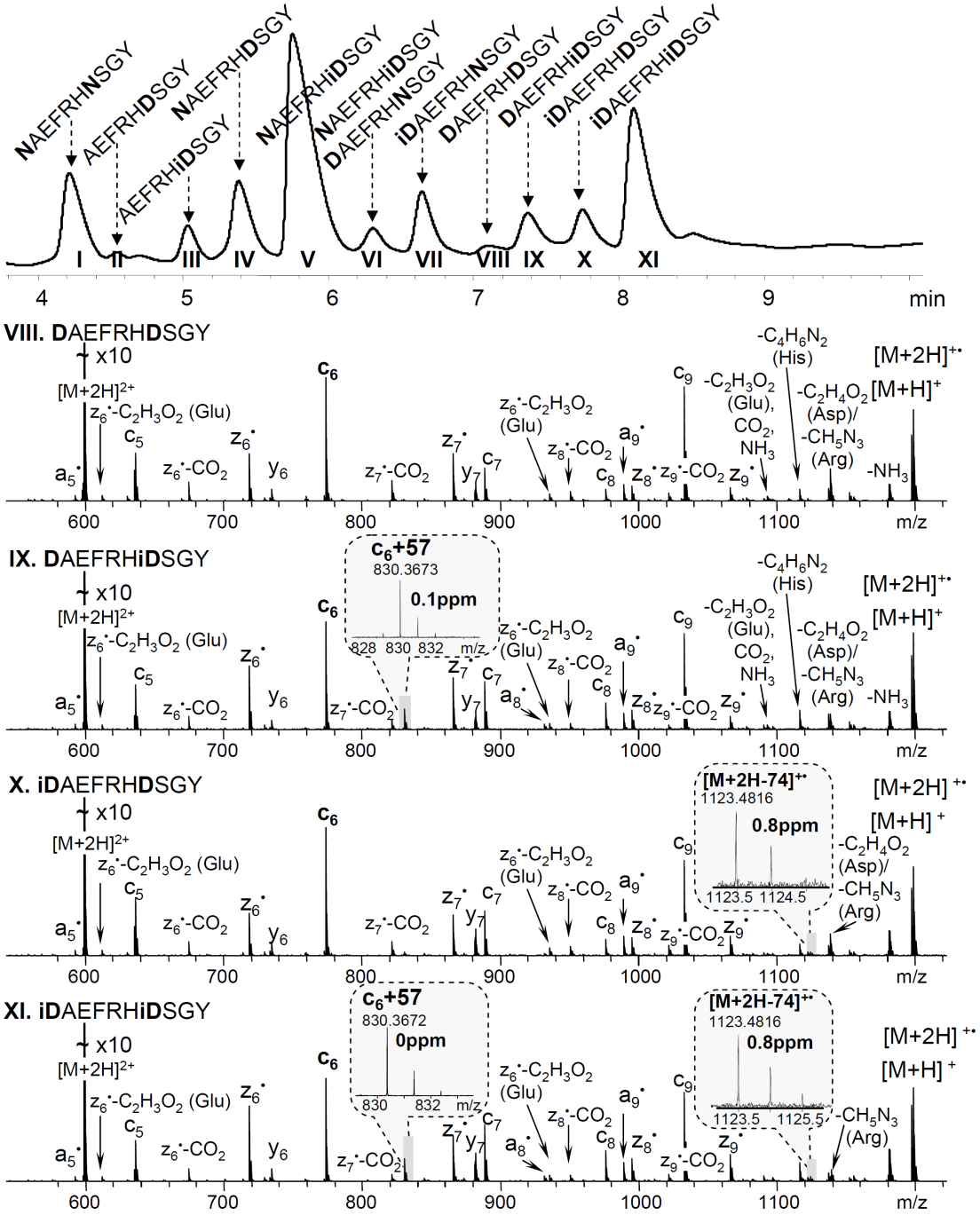

Figure 4.2 Chromatogram of the peptide mixture, generated by partial deamidation of the Aβ1-10 (N1N7) peptide (top panel). Each chromatographic peak labeled based on ECD results. ECD spectra shown correspond to the VIII-XI fractions with the isoAsp specific fragments indicated in the insets.

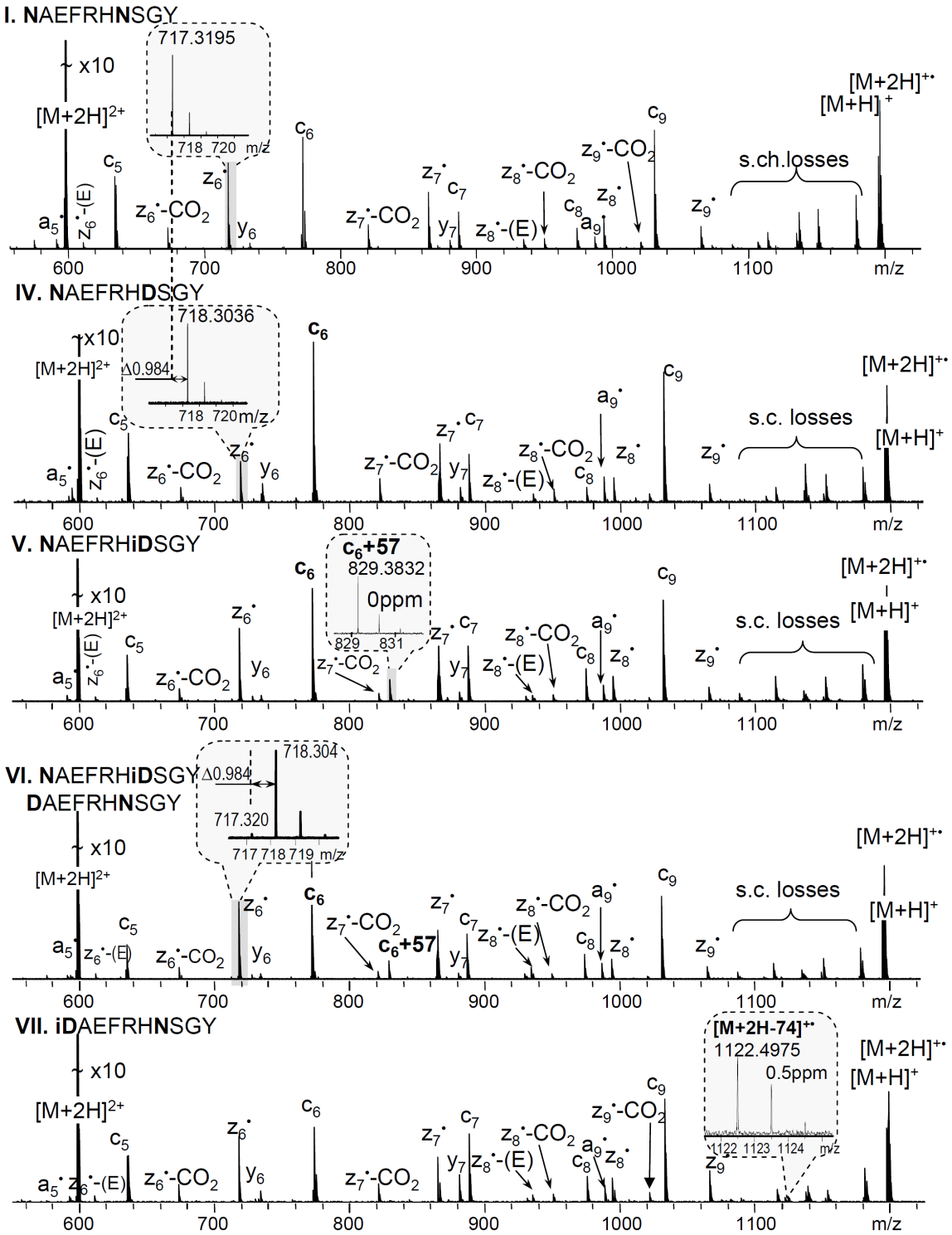

Figure 4.3. ECD spectra of chromatographic peaks I, IV-VII from the partially deamidated Aβ1-10 (N1N7) peptide mixture.

4.3.3 Peak interference

Caution should be taken if the peptide of interest contains methionine (Met) or isoleucine (Ile) residues because they may produce side-chain loss fragment ions with *m/z* close to that of the diagnostic fragment ion: the Met side-chain loss (C_3H_6S) results in a peak at $[M + 2H - 74.01902]^{+\bullet}$, and the Ile side-chain loss with an additional ammonia loss ($C_4H_8 + NH_3$) at $[M + 2H - 73.0891]^{+\bullet}$. Although these interfering peaks could lead to erroneous identification of N-terminal isoAsp, they do not usually pose a problem if the analysis is performed on an instrument with sufficient resolving power. For example, differentiating the singly-charged N-terminal isoAsp signature fragment ion at *m/z* = 1000 from the interfering Met side-chain loss ion would require a mass resolving power of > 190,000, which is easily achievable on an FTICR mass spectrometer such as the one used here.

4.3.4 N-terminal acetylation

For experiments conducted on instruments with limited mass resolving power, such as ETD analysis done on an ion trap instrument, the peak interference problem could be circumvented by shifting the diagnostic peak out of the small molecule and side-chain loss region. This can be done by, for example, N-terminal acetylation. In this case, the C-terminal diagnostic fragment would be $[M + 2H - (C_2H_5NO + C_2HO_2^{\bullet})]^{+\bullet} = [M + 2H - 116.0348]^{+\bullet}$ (hereinafter indicated as $[M + 2H - 116]^{+\bullet}$), and the N-terminal diagnostic fragment would be $C_4H_7NO_3^{+\bullet}$ with *m/z* of 117.042. The effect of N-terminal acetylation was examined on the synthetic peptide Ac-DGVGDVGGVH-NH_2 and its isoAsp-variant Ac-iDGVGiDVGGVH-NH_2 using ECD. Specific diagnostic fragment peaks were observed for both isomers (Figure 4.4,

insets): $[M + 2H - 116]^{+\bullet}$ was present exclusively in the isoAsp-peptide spectrum, and the neutral loss of 60 ($C_2H_4O_2$ = 60.0211) was only observed from the charge-reduced species of the Asp-peptide variant, indicated as $[M + 2H - 60]^{+\bullet}$. The peak at *m/z* = 894.4195 in the isoAsp-peptide spectrum (Figure 4.4, lower panel inset) is not related and corresponds to the neutral loss of 59 (C_2H_5NO = 59.0371) from the acetylated N-terminus. In addition, many of the fragments containing the Asp residue of the Asp-peptide also exhibit an accompanying loss of CO_2 (Figure 4.4, upper panel); however, there are no such losses observed in the isoAsp-peptide ECD spectrum, except for the $z_6^{\bullet}$ - CO_2. This ion was produced as a result of a secondary reaction following the $z_6^{\bullet}$ fragment ion formation via hydrogen rearrangement that only occurs when the C_α radical formed is adjacent to the isoAsp side chain. Similarly, a peak at *m/z* = 832 also has the CO_2 loss, which could have been formed as a result of a secondary reaction upon the loss of an acetamide (C_2H_5NO).

It should be noted that, if the N-terminally acetylated peptide contains a tryptophan (Trp) residue, the Trp side-chain loss of $C_8H_6N^{\bullet}$ (116.05002) would interfere with the isoAsp diagnostic fragment peak $[M + 2H - 116.0348]^{+\bullet}$ (to correctly identify such fragments at *m/z* ~ 1000, the minimum required resolving power is 65,000). In addition, no N-terminal isoAsp diagnostic fragment ion was observed in the N-terminally acetylated peptide, likely because of its small size and lack of a charge carrier. Therefore, other types of N-terminal elongation could be used for a more confident identification of the N-terminal isoAsp. Presumably, the use of larger tags may help to avoid undesired interference from the side-chain losses and for the detection of the N-terminal diagnostic ion.

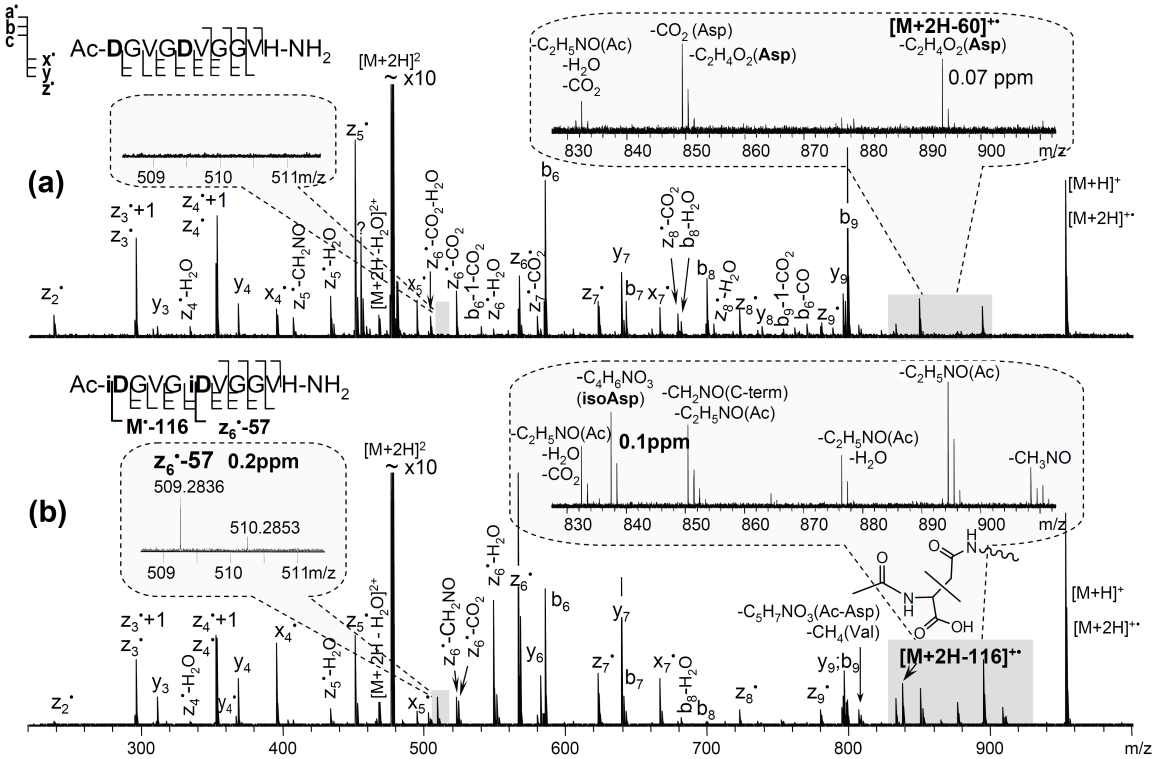

Figure 4.4 ECD spectra of the synthetic peptide variants with Asp (a) and isoAsp residues (b) amidated at the C-terminus and acetylated at the N-terminus. IsoAsp1 and isoAsp5 specific fragments, $[M + 2H - 116]^{+\bullet}$ and $z_6^{\bullet} - 57$, are observed only for the isoAsp-peptide variant. Asp side-chain losses are also indicated, (a) inset.

4.3.5 Analysis of the N-terminal isoAsp by ETD

Peptides with N-terminal isoAsp were also analyzed using ETD. The N-terminal isoAsp diagnostic fragment peak $[M + 2H - 74]^{+\bullet}$ was observed for all peptides, although in some cases, diagnostic peak detection was challenging as it exhibited low intensity. In particular, in ETD (LTQ-Orbitrap) of isoAsp-containing Aβ1-10 peptide, the peak corresponding to the diagnostic fragment ion was barely observable above the noise threshold level even with the supplemental activation (Figure 4.5a, inset). In addition,

some low-abundance peaks were barely detectable or absent in the ETD spectrum, e.g. $a_5^{\bullet}$, and $z_7^{\bullet}$ - CO_2. ECD provided 4.5 times larger S/N ratio for the diagnostic fragment peak (Figure 4.5b, inset), possibly owing to the higher energy available in the ECD process than in the ETD process. Thus, the effect of additional energy input on diagnostic ion generation was further explored by means of supplemental activation.

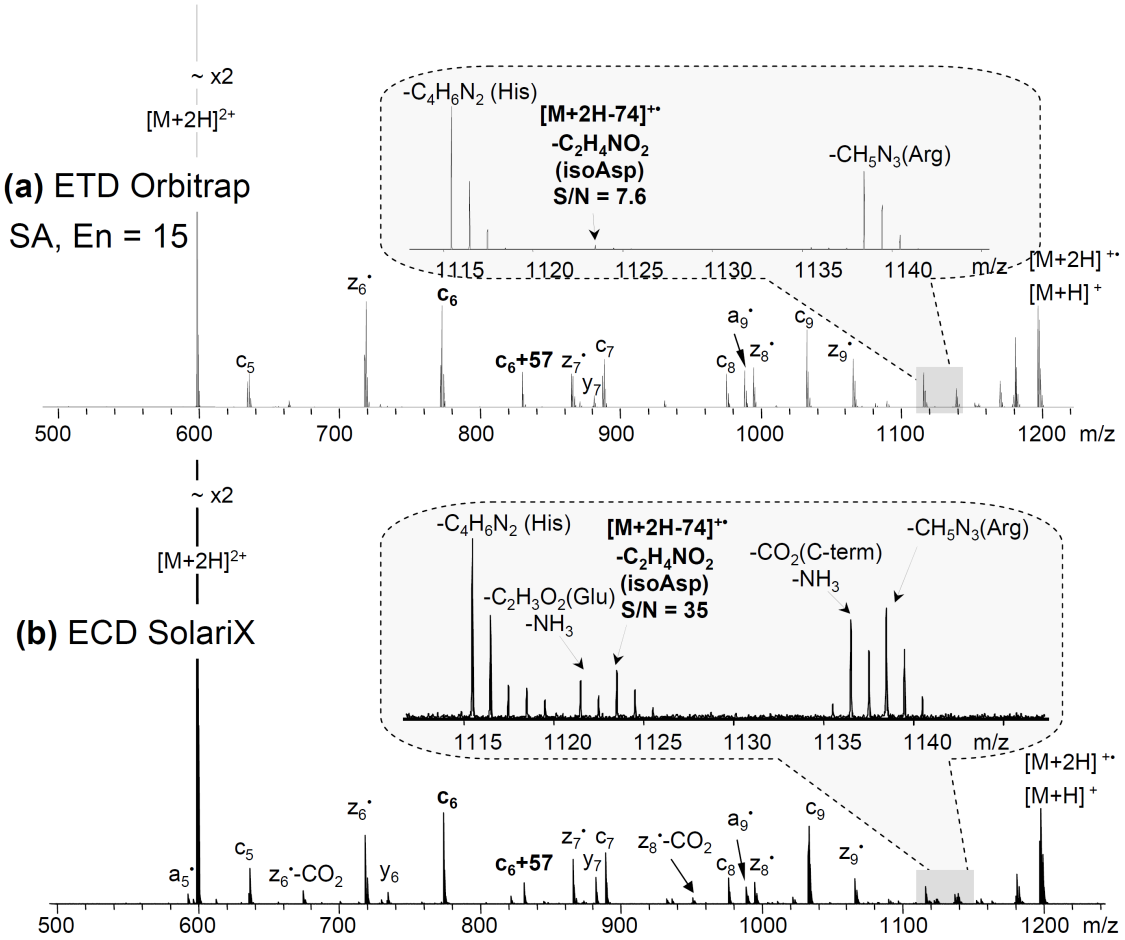

Figure 4.5 N-terminal isoAsp residue diagnostic fragment peak $[M + 2H - 74]^{+\bullet}$ detection for the Aβ1-10 peptide variant (**iD**AEFRH**iD**SGY, fraction XI in the Figure 4.4, top panel) by: (a) ETD on LTQ-Orbitrap, with supplemental activation energy parameter 15; and (b) ECD on SolariX. Insets show diagnostic peaks and their S/N ratios.

4.3.6 The effect of ion activation

Supplemental activation can improve fragment detection.[203, 210, 211] Thus, the effect of supplemental ion activation (via SA, hotECD, and SD) on the diagnostic fragment peak intensity was investigated for all isoAsp-peptides studied. The S/N ratios and the relative intensities (Rel. Int.) of the diagnostic ion peaks are presented in Table 4.1. At first, the Rel. Int. was calculated, but it did not reflect the true picture for some peptides, because the absolute intensity of all fragments could change significantly with ion activation. Absolute S/N ratio seemed to be a better indicator than relative intensity, for example, with the Ang II ETD spectrum acquired on the amaZon instrument, application of SD resulted in a five-fold increase in the S/N ratio of the diagnostic fragment peak, while the Rel. Int. value did not change much (Table 4.1).

Peptide	Angiotensin II (**iD**RVYIHPF)		Amyloid β (**iD**AEFRH**iD**SGY)		Synthetic (Ac-**iD**GVG**iD**VGGVH-NH_2)	
Signature ion	**$[M+2H-74]^{+\bullet}$**		**$[M+2H-74]^{+\bullet}$**		**$[M+2H-116]^{+\bullet}$**	
m/z	973.5259		1123.4807		837.4218	
Method	**S/N**	**Rel. Int.**	**S/N**	**Rel. Int.**	**S/N**	**Rel. Int.**
ETD Orbitrap no SA	8.2	0.04	6.6	0.0022	316.3	0.0793
ETD Orbitrap SA, En=5	40.5	0.053	6.4	0.0022	313.6	0.0803
ETD Orbitrap SA, En=15	21.3	0.032	7.6	0.0014	293.9	0.0706
ECD solariX	104.6	0.029	35.0	0.0095	120.5	0.0549
hotECD solariX 4.5V	128.9	0.025	28.0	0.0096	291.3	0.0524
ETD solariX	145.8	0.059	4.0	0.0044	98.4	0.0828
ETD amaZon no SD	17.7	0.057	8.2	0.007	160.7	0.0786
ETD amaZon SD	92.2	0.052	17.3	0.0036	162.3	0.0818

Table 4.1 The effect of additional energy input on the diagnostic fragment formation. Relative intensity (Rel. Int.) was calculated as the absolute intensity of the diagnostic fragment divided by the sum of the absolute intensities of all *c* and *z* fragments.

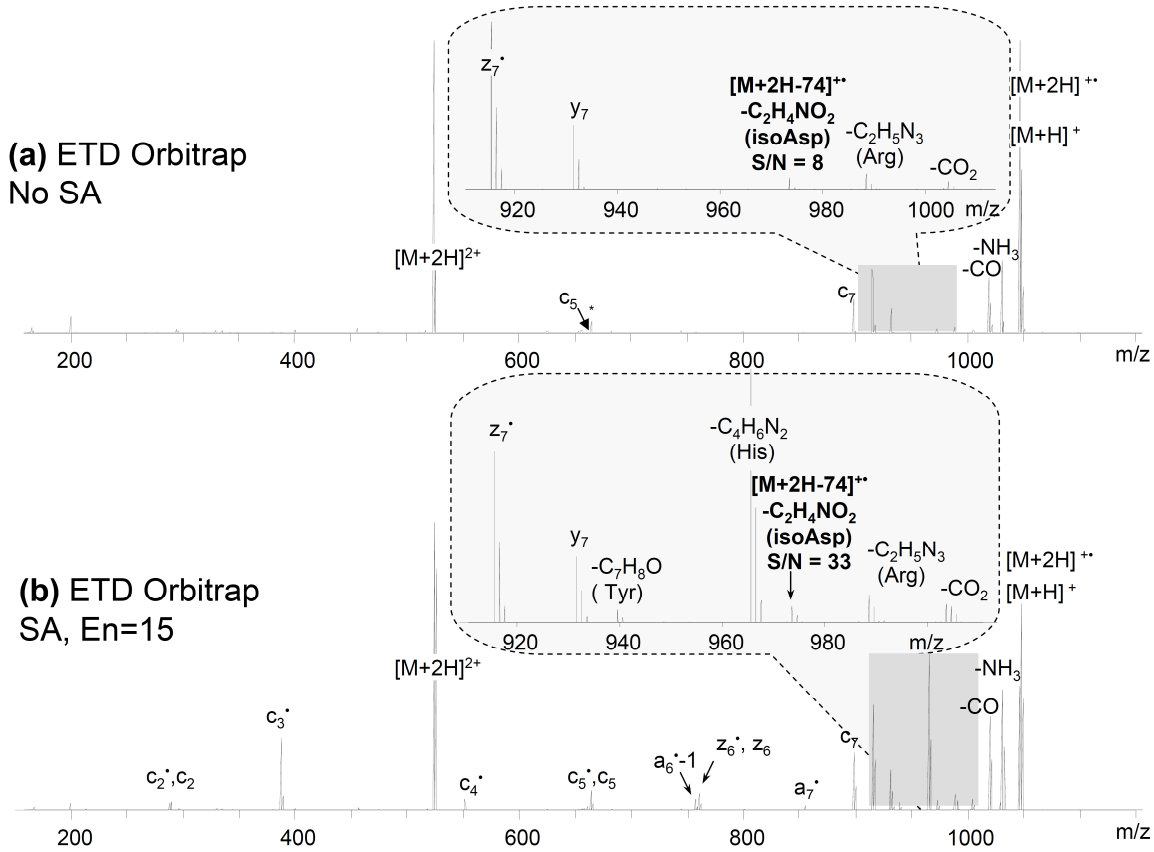

Figure 4.6 N-terminal isoAsp residue diagnostic fragment peak $[M + 2H - 74]^{+\bullet}$ detection using ETD without (a) or with SA (b) for the modified Ang II peptide variant (**iD**RVYIHPF). Both spectra were acquired on Orbitrap. Insets show the S/N ratio of the $[M + 2H - 74]^{+\bullet}$ peak and the appearance of additional side-chain losses upon SA (His and Tyr).

A direct comparison of the results acquired on different instruments is not possible because of the difference in multiple operating parameters, energetics of the reactions and the mass analyzers. When comparing spectra obtained using the same instrument, the results suggest that supplemental activation generally leads to higher S/N ratios for diagnostic ions. The effect of additional energy input on fragmentation

depends on the peptide sequence, particularly, on the presence of basic residues and side-chain interactions. An example is shown on the ETD data acquired on an Orbitrap instrument with or without SA for the modified Ang II peptide (Figure 4.6). Similar to the ETD results acquired on an amaZon instrument mentioned earlier, the S/N ratio of the diagnostic ion became 4 times greater when SA was applied (Figure 4.6b).

4.4 Conclusions

The N-terminal isoAsp residue was differentiated from Asp using ECD, hotECD, and ETD. Based on the detection of the specific fragment $[M + 2H - 74]^{+\bullet}$ (isoAsp1), $c_6 + 57$ (isoAsp7), and $[M + 2H - 60]^{+\bullet}$ (Asp1, Asp7) it was possible to differentiate a mixture of 9 peptides containing isoAsp, Asp, and Asn residues, produced upon partial deamidation of the Aβ1-10 (N1N7) peptide and separated by a RP-HPLC system. This result illustrates that HPLC separation followed by ExD analysis can be a powerful method for isoAsp-containing peptide mixture differentiation. Although the detection of the N-terminal diagnostic fragment peak can be challenging, it is possible to substantially improve its detection by application of supplemental ion activation. In some cases, the S/N ratio of the signature fragment ion peak was increased by up to 6 times. Several interfering peaks may further complicate the analysis when Met or Ile amino acids are present. This can be overcome by the N-terminal elongation, with, for example, acetylation, which introduces a mass shift of the diagnostic peak to the smaller *m/z* region where fewer side-chain losses are available. However, if a Trp residue is present in the sequence, other types of elongation would be preferred. In addition, with a larger tag attached to the N-terminus, an N-terminal diagnostic peak may become detectable.

Chapter 5

Detection of IsoAsp in Amyloid β Peptides From CSF

5.1 Introduction

Alzheimer's disease (AD) is a neurodegenerative disorder of the central nervous system with the loss of brain function leading to impaired memory, cognitive dysfunction, and altered behavior. AD is characterized by abnormal accumulation of intraneuronal neurofibrillary tangles of hyperphosphorylated tau protein[212] and extracellular accumulation of amyloid plaques.[213] The major components of the amyloid plaques are the β-Amyloid peptides of 40 and 42 amino acids long (Aβ40 and Aβ42) derived from the amyloid precursor protein. Recently, independent of the clinical diagnosis, the biomarkers of AD were proposed – the elevated level of the 181-phosphorylated Tau protein and the decreased level of Aβ42 in cerebrospinal fluid (CSF).[214, 215] CSF occupies the space around and inside the brain and spinal cord, providing basic mechanical and immunological protection to the brain. It is absorbed into the bloodstream, rinsing the metabolic waste of the central nervous system and can be used to diagnose nervous system disorders and infections. The amount of CSF at each time in the brain is 150 ml and it is produced at a rate of 500 ml/day. CSF contains 15 - 40 mg/dL of protein, which is only 0.3 % of plasma proteins.

In addition to Aβ42, a number of Aβ peptides were detected in CSF: Aβ13, Aβ14, Aβ15, Aβ16, Aβ17, Aβ19, Aβ20, Aβ30, Aβ33, Aβ34, Aβ37, Aβ38, and Aβ40.[184] This data along with the fact that isoAsp was detected in Aβ peptides of amyloid plaques[119] suggests screening for the isoAsp in peptides present in CSF as another

potential biomarker of the disease. HPLC-ECD and ETD MS seems to be a promising method for fast and accurate analysis of isoAsp formation in Aβ peptides of CSF. This chapter will describe the preliminary results, challenges of the proposed approach, and future directions.

5.2 Experimental section

5.2.1 Standard peptides

Standard peptides Aβ40 and Aβ42 of 90 % and 95 % purity, respectively, were purchased from Sigma Aldrich (St. Louis, MO, USA). The isomerized form of Aβ17-28 (LVFFAEisoDVGSNK) was custom synthesized by AnaSpec (San Jose, CA, USA). Peptides were dissolved in water, aliquoted into vials, dried, and kept at -20 ˚C for immediate use.

5.2.2 Immunoprecipitation of Amyloid β peptides from human CSF

CSF immunoprecipitation (IP) was performed in a collaborator laboratory, at the Institute of Neuroscience and Physiology, University of Gothenburg, Sweden as previously described.[184] CSF was pooled from people with memory disorders, without a clear AD or non-AD biomarker signature. The IP was performed using three different Aβ-specific antibodies: 6E10, 4G8, and 11A50-B10 (Signet Laboratories, Dedham, Mass., USA), which target epitopes 4-9, 18-22, and C-terminal amino acids of the Aβ40 respectively; 5 ml of CSF was used for each sample. Antibodies were cross-linked to 250 µl magnetic Dynabeads (sheep anti-mouse, IgG) and added to the CSF, followed by 50 µl 2.5 % Tween-20 (Bio-Rad, Hercules, Calif., USA). After washing and purification

using the KingFisher magnetic particle processor, Aβ peptides were eluted using 0.5 % FA. The collected eluents were speedvac-dried, freezed, shipped in dry ice to Boston University, and kept at -80 ^{o}C until use.

5.2.3 On-line nanoLC - ETD MS

Dried peptides were dissolved in a solvent containing various amounts of ACN (1 - 50 %), H_2O (99 - 50 %), and FA (0.1 - 8 %), vortexed for 2 - 60 min, and injected with or without further dilution.

Direct infusion MS along with on-line nanoLC – ETD – MS analyses were performed on an LTQ-Orbitrap XL spectrometer with ETD capability (Thermo Scientific, San Jose, CA, USA) coupled to a Waters NanoAquity (Milford, MA) and a TriVersa NanoMate system (Advion Biosciences, Ithaca, NY) for nanoESI. For online LC-MS analysis, samples were first passed through a C18 trapping column for clean up and desalting (Symmetry C18: 180 µm x 20mm, with 5 µm particle size), followed by separation on an analytical reversed-phase column (BEH130 C18: 150 µm x 100mm, with 1.7 µm particle size, Waters Corporation, Milford, MA). Mobile phases were 1 % ACN, 99 % H2O, 0.1 % FA (A), and 99 % ACN, 1 % H2O, 0.1 % FA (B). The separation was performed using various gradients starting at 5 - 45 % phase B and increasing up to 60 - 80 % phase B in 45, 52, and 90 min at 0.5 µl/min flow rate. Peptide standards were injected in solutions at 5 – 45 % B composition in accordance with the starting conditions of the separation in the amount of 200 fMol – 1 pMol, at 0.5 - 5µl injection volumes. For direct infusion nanoESI analysis, peptides were dissolved in 50:50:0.1 ACN:H_2O:FA.

A typical MS/MS scan cycle consisted of one full FTMS scan (300-2000 *m/z*) acquired at a resolution of 60,000 at *m/z* 400 followed by MS/MS of the three most abundant ions in the full MS scan acquired at a resolution of 30,000 with the low mass limit set to 100 *m/z*. MS/MS was performed using ETD with supplemental activation enabled (En = 15). ETD reagent (fluoranthene) accumulation time was set to 250 ms, and ETD reaction time to 90 ms. The MS/MS isolation width was set to 5.0 *m/z* and the normalized collision energy to 30. Singly charged ions were excluded. The results were analyzed by the Xcalibur 2.0.7 software.

5.3 Results and Discussion

5.3.1 NanoESI of Aβ standards

In order to successfully develop a method for analysis of biological samples, it is always a good idea to start with the standards due to the limited amount of sample available to the researcher. Synthetic amyloid peptides are readily available because of the great interest in AD, and the extensive endeavour to understand the disease and to find its cure. Aβ peptides are known to be very hard to work with due to its amyloidogenic properties: high hydrophobicity along with the “stickiness” of the longest peptides, such as Aβ40 and Aβ42, makes method development challenging. Nonetheless, it was shown in the past that Aβ peptides could be analyzed by ECD, ETD, and related techniques, and the isoAsp can be differentiated.[202, 216, 217]

At first, Aβ40 standard peptide was nanosprayed on the LTQ-orbitrap in direct infusion mode (Figure 5.1) to check the sample integrity. The signal of Aβ40 sprayed at 500 fM concentration was very strong (the absolute intensity was ~10^7), and molecular

ions in 4+, 5+, and 6+ charge states were observed. In addition, the spectrum contained a small fraction of doubly charged Aβ26-40 peptide, which most probably originated from the impurity in synthetic peptide standards. The sequence of Aβ26-40 was confirmed by ETD. The ETD parameters were adjusted for the method and a mock LC-MS method was run during direct infusion of the standard to further test it.

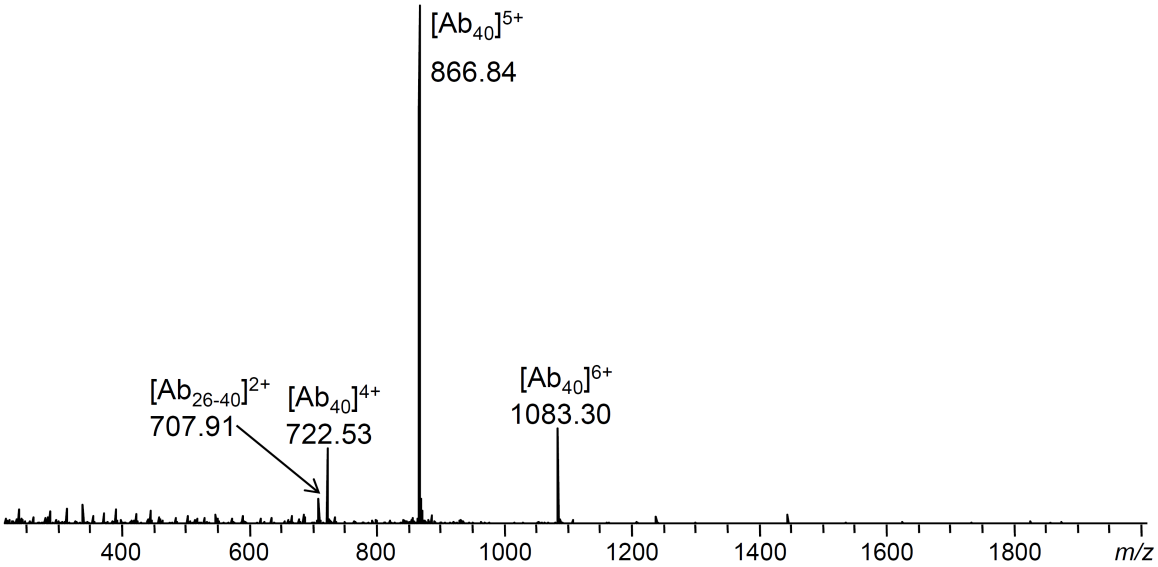

Figure 5.1 NanoESI mass spectrum of the Aβ40 standard peptide. Note the presence of the Aβ26-40.

5.3.2 On-line nanoLC - ETD MS analysis of the standards

After passing through the column, Aβ40 standard was no longer detected. This could possibly result from the poor solubility of this large Aβ peptide in solvent with low organic content, which prevented it from entering the column. To address this issue, various starting conditions of separation were applied, with increasing ACN and FA contents. After multiple attempts of changing experimental parameters, such as solvent, gradient, trapping conditions, etc., Aβ40 was still not detected in the LC-MS mode. It was found, however, that injecting at ≤ 20 % ACN may be problematic for sample

introduction, as the peptide standard prepared in solvents containing 20 % ACN also gave very weak Aβ40 signal in the direct infusion mode. Increasing the ACN concentration of the same sample by simply adding ACN to the autosampling vial improved the signal regardless of the sample dilution. Nonetheless, even injecting Aβ40 onto the column in 50 % ACN did not improve its detection in the LC-MS mode.

It must be noted that the smaller peptide Aβ26-40, which was present in the direct infusion mode, was also detected in LC-MS runs (Figure 5.2). The elution peak width of Aβ26-40 was fairly broad, which may be due to its strong interaction with the surface of the C18 column. Indeed, this peptide contains the most hydrophobic part of the Aβ40 as shown on the hydrophobicity chart of the Aβ40 (Figure 5.3). Similarly, Aβ40 interaction with the stationary phase may be so strong that it could precipitate on the surface without ever being released. It is also possible that Aβ40 peptide degrades on the column into smaller peptides, such as Aβ26-40; however, this is very unlikely and, to the best of our knowledge, has not been reported in the literature.

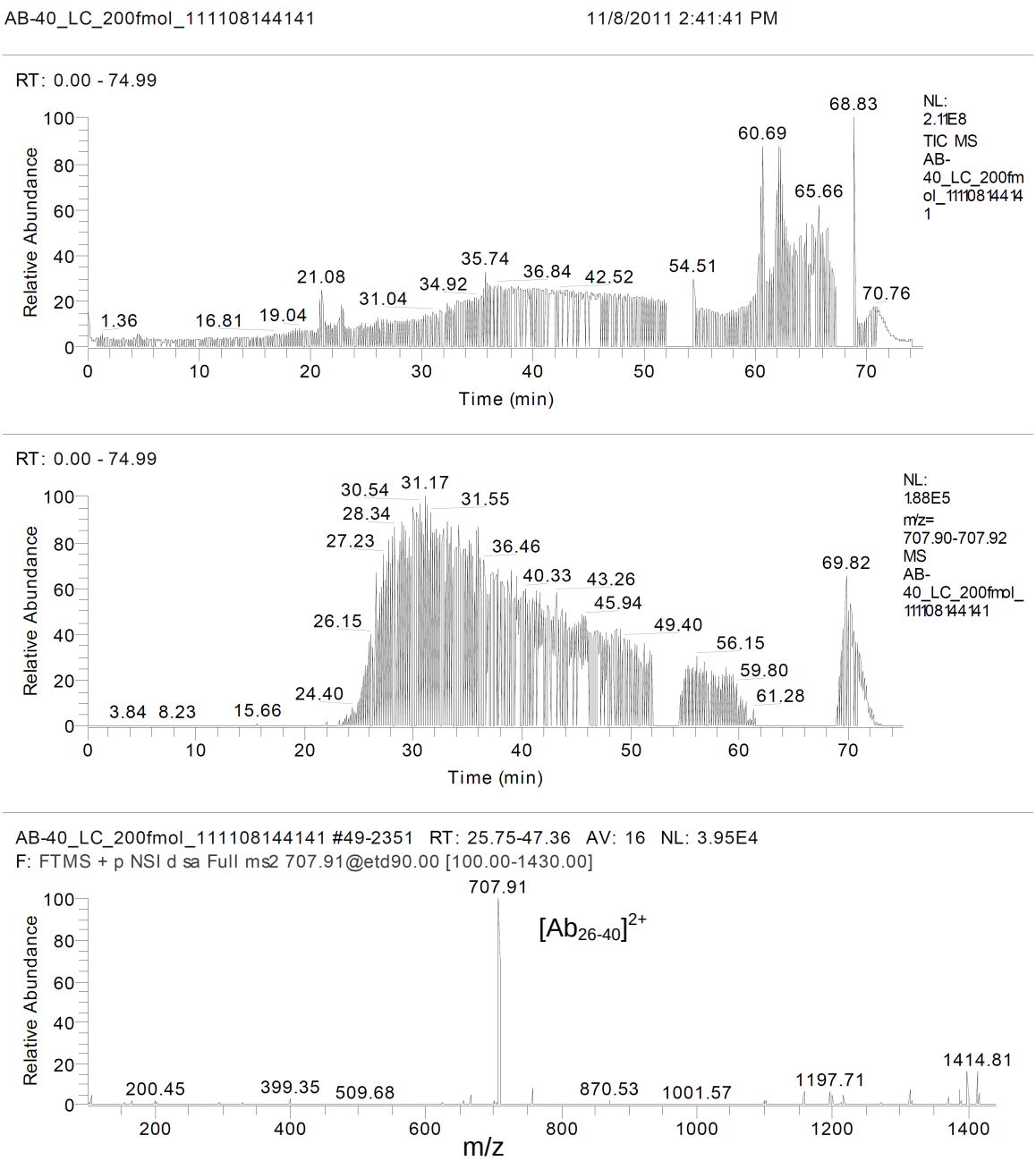

Figure 5.2 LC-MS run of Aβ40, 200 fMol injected. On top is the total ion chromatogram (TIC). In the middle is the base peak chromatogram for the 707.90-707.92 *m/z* region, corresponding to the doubly charged ions of Aβ26-40 peptide as confirmed by ETD, which is shown on the bottom.

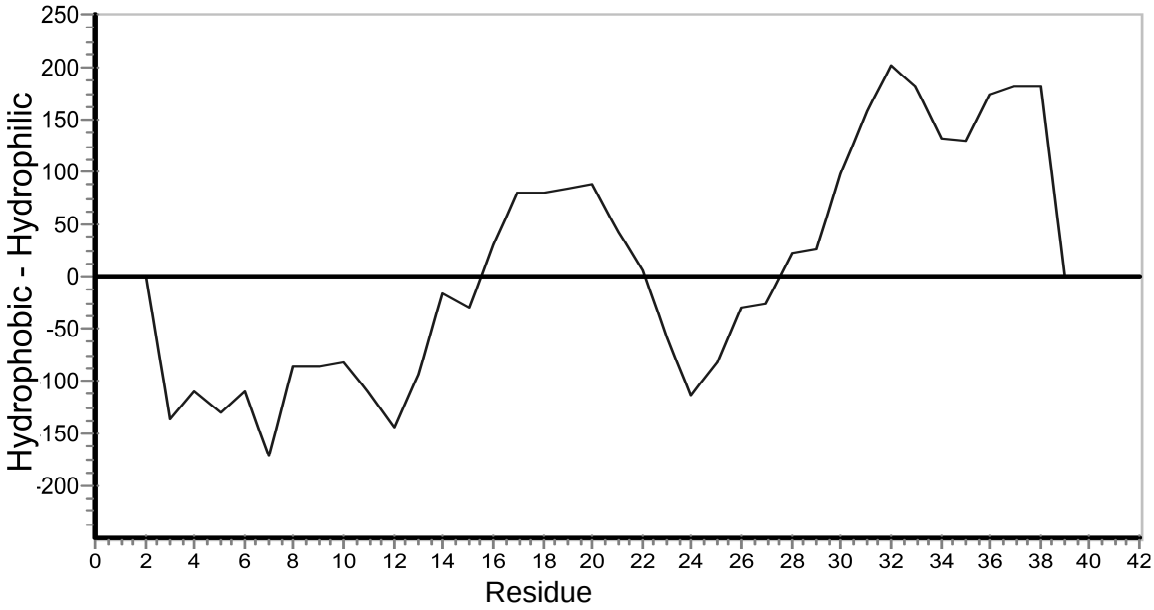

Figure 5.3 Hydrophobicity index of the Aβ40 peptide, generated by GPMAW 5.02.

5.4 Future concepts

LC-MS analysis of the CSF samples has been postponed until successful analysis of the Aβ standards is demonstrated. It is well known that Aβ peptides are difficult to work with; however, they have been successfully analyzed by LC-MS before by various groups. The poor Aβ peptide recovery may be caused by the slight difference in the system used in the current experiment, which needs to be addressed before proceeding further. In particular, switching to a less hydrophobic column that uses shorter chain stationary phase packing material, such as C8, or C4, would be suggested, although this may worsen the separation of peptide mixtures. Further, starting with slightly shorter Aβ peptides (less hydrophobic) for testing might help.

Chapter 6

β-Peptide analysis by ExD tandem MS

6.1 Introduction

Isoaspartic acid (isoAsp) is a β-type amino acid that has one extra CH_2 group in the polypeptide backbone, and one fewer on the side chain compared to Asp. As discussed previously electron activation dissociation (ExD) of isoAsp containing peptides generates signature fragment ions (*c*+57 and $z^{\bullet}$-57) at the positions of the isomerized residues, allowing differentiation from the non-modified residues. These ions are formed by the C_{α}-C_{β} backbone bond cleavage. In peptides consisting solely of α-amino acid residues, there is no such bond within the backbone. Fragments produced upon C_{α}-C_{β} bond rupture are unique to β-amino acid residues and could be used to locate the position of the β-amino acid if observed. The result from the isoAsp experiment suggested a possible extension of the method to characterize peptides containing other β-type amino acids.[216, 218, 219]

Circular dichroism spectroscopy, X-ray crystal-structure analysis and nuclear magnetic resonance spectroscopy are primarily used to study the structure of β-peptides.[138, 140, 142, 144] Radioactive labeling, high performance liquid chromatography (HPLC) and matrix assisted laser desorption and ionization (MALDI) mass spectrometry (MS) have also been applied to monitor β-peptides in tissues.[141, 143] However, a fast and accurate MS based method capable of distinguishing α from β and β_2 and β_3 type amino

---

[1]This chapter has been partially reproduced with permission from Sargaeva, N. P.; Lin, C.; O'Connor, P. B., Unusual fragmentation of beta-linked peptides by ExD tandem mass spectrometry, *Journal of the American Society for Mass Spectrometry*, **2011**, *22*, 480-491.

acids would be of a great utility for characterization of β-peptides. In this chapter the potential of the ExD based tandem MS methods to differentiate β-amino acid containing peptides from their alpha analogues, as well as β_2 from β_3-type amino acids are addressed. In general, the results are in good agreement with the findings of recent electron capture dissociation (ECD) and electron transfer dissociation (ETD) studies of small β-peptides[220] and ε-peptides.[221] In the present study, in addition to simple model peptides such as Q_{06} and substance P, a more complicated system of Puma BH_3 peptide analogues of 26 amino residues is investigated. Furthermore, charge state dependence of the fragment appearance is considered. An alternative mechanism of ion-electron reaction induced dissociation of peptides within β-amino acid residues is discussed.

6.2 Experimental section

6.2.1 Peptides and reagents

The Q_{06} β-peptide ($\beta_2V\beta_2A\beta_2L\beta_3V\beta_3A\beta_3L$) was kindly provided by Prof. D. Seebach, and Dr J. Gardiner, ETH Zurich, Switzerland. C-terminally amidated Substance P with two amino acids modified to β_3-type amino acids (RPKPβQQFFGβLM) was custom synthesized by AnaSpec (San Jose, CA, USA). Puma BH_3 pro-apoptotic protein analogue I (βEEQβWAREβIGAβQLRRβMADβDLNAβQYEβRR) and analogue II (βEEQWβAREβIGAQβLRRβMADDβLNAβQYERβR) were kindly provided by the group of Prof. S. Gellman at the University of Wisconsin (Madison, WI, USA), where β indicates β_3-type amino acids. Other reagents: non-modified substance P, (2-Aminoethyl)-trimethylammonium chloride hydrochloride (cholamine), triethylamine

(TEA), and dimethyl sulfoxide (DMSO) were purchased from Sigma-Aldrich (St. Louis, MO, USA); 2-(1H-Benzotriazole-1-yl)-1,1,3,3-tetramethylaminium hexafluorophosphate (HBTU) from Novabiochem (La Jolla, CA, USA); and 1-Hydroxybenzotriazole (HOBt) from AK Scientific, Inc. (Palo Alto, CA, USA).

6.2.2 Sample preparation

Cholamine reaction. Covalent attachment of cholamine to the Q_{06} β-peptide was performed as previously described.[222] Briefly, 0.1 μmol of Q_{06} β-peptide was treated sequentially with 10 μl of 200 mM HOBt in DMSO, 200 μl of 100 mM cholamine in DMSO containing 200 mM TEA, and 10 μl of 200 mM HBTU in DMSO. The sample was left to react overnight at room temperature, and purified using a ZipTip C_{18} solid phase micropipette extraction column before MS analysis.

6.2.3 Mass Spectrometry

Most ECD experiments were performed on a custom built triple quadrupole Fourier transform ion cyclotron resonance mass spectrometer (qQq-FTICR MS) with a nanospray source and a 7 T actively shielded magnet.[100, 102] Samples were nanoelectrosprayed (nanoESI) (50 nl/min, room temperature) at 5 μM concentration in 50:50 MeOH:H_2O with 1 % formic acid. Ions were isolated in the first quadrupole Q_1, accumulated in the second quadrupole Q_2, and transmitted into the ICR cell where they were irradiated with electrons emitted from an indirectly heated dispenser cathode (Heatwave, Watsonville, CA, USA) for ion fragmentation. The following ECD and electron ionization dissociation (EID) parameters were employed: electron irradiation time 35-100 ms, cathode potential -0.2 - 1.2 V (ECD), - 18 V (EID). Acquired spectra

were zerofilled twice, internally calibrated, and analyzed manually using BUDA (Boston University Data Analysis, Version 1.4, © 2000 by Peter B. O'Connor). ECD experiments of triply charged Substance P ions were performed on solariX FTICR instrument (Bruker Daltonics, Billerica, MA, USA) with 12 T actively shielded magnet. Electrospray was applied for enhanced production of triply charged ions.

ETD spectra with supplemental activation were acquired on an amaZon Ion Trap instrument (Bruker Daltonics, Billerica, MA, USA) using fluoranthene as the ETD reagent. Peptides were electrosprayed (2 µl/min, glass capillary temperature 220 ˚C) at 1 µM concentration in 50:50 MeOH:H_2O with 1 % formic acid using an Apollo II ion source. Data acquired on solariX and amaZon were analyzed using Bruker's ESI Compass DataAnalysis 4.0 software.

6.3 Results and Discussion

6.3.1 Q_{06} beta peptide $_{\beta 2}V_{\beta 2}A_{\beta 2}L_{\beta 3}V_{\beta 3}A_{\beta 3}L$.

Although the Q_{06} β-peptide only contains six β-amino acid residues, it can form helical secondary structures.[140, 144] This small and relatively simple peptide contains both β_2 and β_3 type amino acids, making it potentially an ideal system to study for the differentiation of β_2 and β_3 amino acids. However, only singly charged ions $[M+H]^+$ were detected in all ESI/ECD experiments, either with the nanospray or with the electrospray ionization sources (Figure 6.1.a), which is likely due to the lack of basic amino acid residues within the peptide sequence. Since ECD and ETD are accompanied by charge neutralization upon the electron capture or transfer, they cannot be performed on singly charged ions as the products would be neutral and undetectable. In this case, other

fragmentation techniques could be applied that do produce fragments from singly charged ions such as collisionally activated dissociation (CAD)[50] or infrared multiphoton dissociation (IRMPD).[35] Expectedly, IRMPD of the Q_{06} beta peptide resulted in *b* and *y* fragments with no information on the position of the modifications (Figure 6.1.b).[218] Additionally, Electron Ionization/Impact Dissociation (EID) can generate ECD type fragments from singly charged molecular ions,[78] as well as C_α-C_β cleavage for isoaspartic acid.[202] However, only *b* and *y* fragments were detected in EID mass spectra of the Q_{06} β-peptide (Figure 6.1.c).[216] The lack of *c* and $z^{\bullet}$ fragments could be due to the low fragmentation efficiency of EID in this particular experiment. Thus, the well established ECD method would seem to be a better approach, but it requires an increase in the number of charges on the peptide.

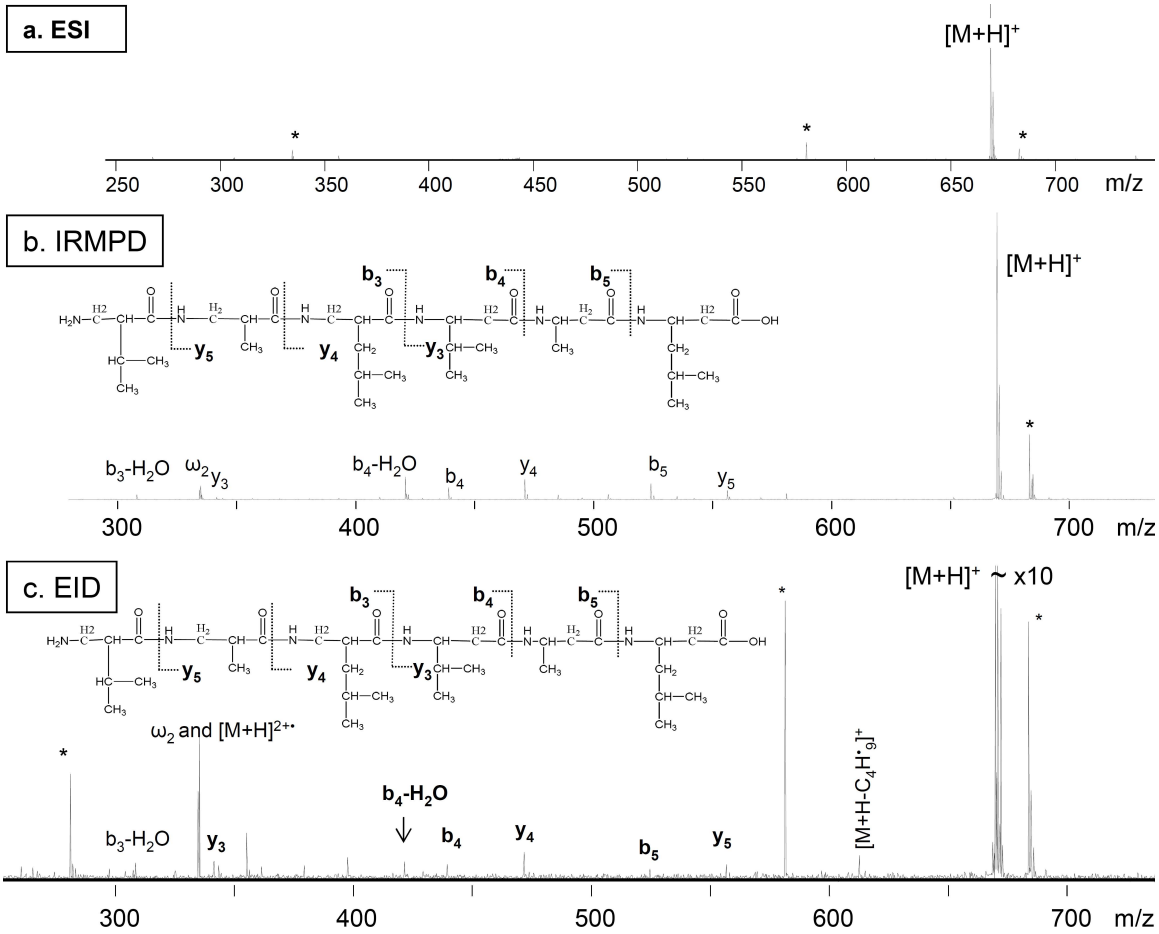

Figure 6.1 Q_{06} beta peptide $_{\beta 2}V_{\beta 2}A_{\beta 2}L_{\beta 3}V_{\beta 3}A_{\beta 3}L$: a) ESI, b) IRMPD, c) EID. Asterisk indicates noise peaks.

6.3.2 Charge increase

Three different approaches were applied in order to enhance the formation of higher charged molecular ions. These include the addition of nitrobenzyl alcohol or calcium salt into the ESI solution, and the covalent attachment of the cholamine tag to the peptide.[218, 222-225] Although doubly charged ions were observed in all three cases, only the cholamine reaction produced sufficient ions for ECD analysis. Inefficiency of

other methods could be due to the lack of a preferred calcium ion binding site and potentially low charge stabilization in the peptide. Cholamine reacts with the carboxylic acid and was attached to the peptide at its C-terminus. The second charge could be provided by the protonation of the N-terminal amine. Doubly charged species $[M{\bullet}Ch^{+}+H]^{2+}$ were readily observed in the ESI MS, isolated, and further subjected to ECD (Figure 6.2).

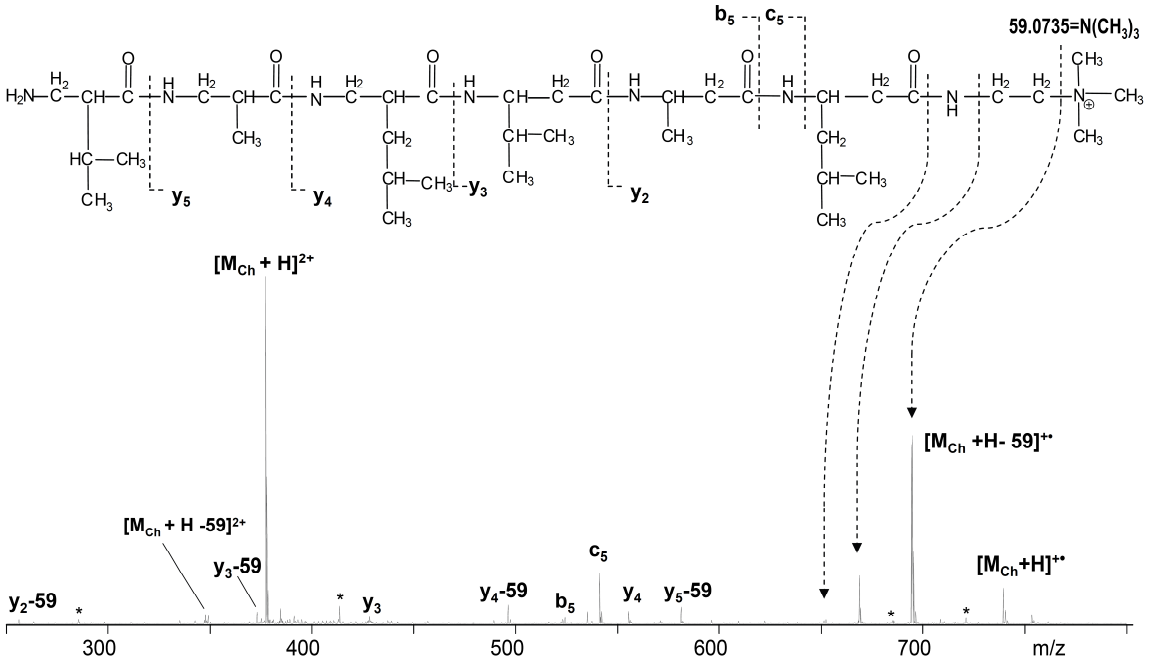

Figure 6.2 ECD of Q_{06}•cholamine.

Similar experiments of C-terminal charge tag attachment to α-peptides were done by Hunt's group.[226] Their result demonstrated increased formation of *z* ions. In the current study, no *z* fragments and only one ECD-type fragment, c_5, was observed for the Q_{06} β-peptide. The electron capture at the quaternary ammonium provides an abundant loss of the neutral trimethylamine 59.0735 = $N(CH_3)_3$, leaving the radical on the C-terminal methylene group (Figure 6.2). This is expected to further induce radical initiated reactions and cleavages, such as the loss of ethylene. Although charge neutralization

on the quaternary ammonium may not lead to backbone cleavages,[227] electron capture at the protonated N-terminal amine of the doubly charged Q_{06} peptide should result in backbone fragmentations. Further, the recombination energy of the protonated N-terminal amino group is higher than that of the quaternary ammonium as calculated for the singly charged model cations by Jensen et al. (4.3 eV ($MeNH_3^+$) vs. 3.1 eV (NMe_4^+)),[228] making it the preferred electron capture site. However, ECD type fragments were lacking in the ECD spectrum of the tagged Q_{06} peptide, which was dominated by b_5 and *y* fragments which could be merely the result of the residual vibrational excitation.[57] Alternatively, the formation of *y* fragments could be facilitated by the backbone nitrogen protonation or a rearrangement that transfers a hydrogen atom to the backbone nitrogen.[61, 84, 221] Upon charge neutralization at the tag site and the subsequent tag loss, the excessive vibrational energy could induce the formation of the b_5 ion, similar to that suggested by Cooper et al. in their study of *b*-ion formation in ECD.[60] Nevertheless, it is hard to make definitive conclusions why this unusual fragmentation pattern was observed as two variables were introduced at the same time in the studied system: a cholamine tag and the incorporation of β-amino acids.

6.3.3 ETD of Q_{06} beta peptide

Electron transfer dissociation was further used to analyze the Q_{06} beta peptide. As opposed to the first ESI experiment, a small peak corresponding to the doubly charged molecular ions, $[M_{Q06}+2H]^{2+}$, was observed, which could be due to the difference in the ionization sources between two instruments. In particular, the glass capillary in the electrospray source used in the ETD study was heated to 220˚C which

could possibly increase the desolvation efficiency and production of higher charged ions compared to the unheated source used in the previous ECD experiment.

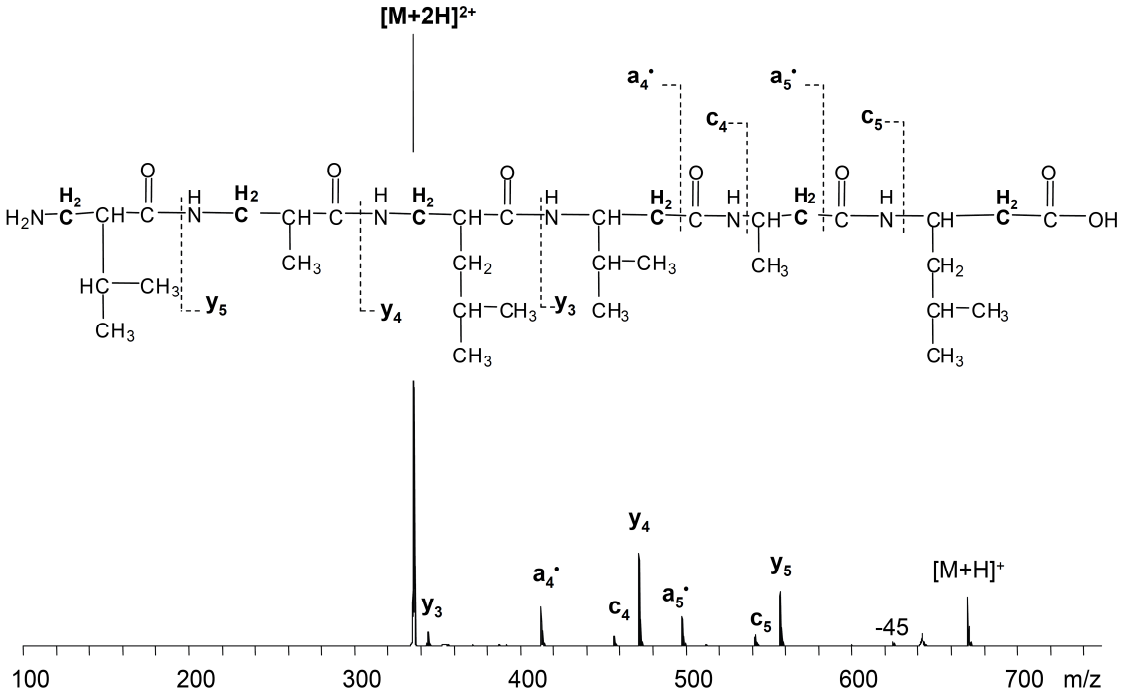

Figure 6.3 ETD of Q_{06} β_2/β_3-peptide.

ETD of the Q_{06} beta peptide produced an unusual fragmentation pattern with abundant *y* and a• fragments, and only two *c* fragments in low abundance (Figure 6.3).

The assignment of $a^{\bullet}_5$ ion was ambiguous due to the interference from x_4 ion [x_4 (*m/z*=497.33), and $a^{\bullet}_5$ (*m/z*=497.39)], which could not be resolved using the ion trap. The assignment is probably correct, because *x* ions are not commonly observed in ECD and ETD, and they were not detected for this peptide in ECD experiments. It is not clear how such abundant *y* fragments could be formed without a C-terminal charge carrier. It might be due to the backbone nitrogen protonation, similar to the cholamine attached Q_{06} β-peptide ECD results. Likewise, the alternative dissociation pathway seems to be enhanced. Meanwhile, low vibrational energy applied to the charge reduced species to

increase dissociation efficiency upon electron transfer (smart decomposition) may also be a reason for enhanced *y* fragment formation. However, this cannot explain the formation of $a^{\bullet}$ fragment ions as those are radicals species and more likely to be a product of ion-electron reaction. In general, the observed fragmentation pattern for this peptide is not following the usual ETD behavior. ExD of this very simple β-peptide demonstrates a big difference for fragment formation in β-peptides compared to their α-analogues.

6.3.4 Modified Substance P

In order to better understand the unusual ExD behavior of β-peptides, ECD experiments were carried out on a well studied system, the substance P peptide, and its variant which was modified at two positions: glutamine 5 and leucine 10 to β_3-homo amino acids. Q_5 and L_{10} were specifically selected for modification as they normally provide abundant c_4 and c_9 fragments (Figure 6.4.a.), and the expected fragments resulted from the C_α-C_β bond cleavage (discussed below) would not interfere with other peaks in the spectrum. The introduction of the two extra methylene groups in the backbone increased the molecular mass of the peptide by 28 Da. Fragment ion mass shift at 14 Da per additional methylene group was also observed correspondingly. As was discussed in the introduction, the extra methylene group present in isoAsp leads to a C_α-C_β backbone bond cleavage and the formation of signature diagnostic fragments. Similar cleavages were expected for the current modifications which would result in formation of c_4+85 and c_9+70 fragment ions. However, not only were these ions absent, the c_4 and c_9 fragments also disappeared from the ECD spectrum entirely (Figure 6.4).

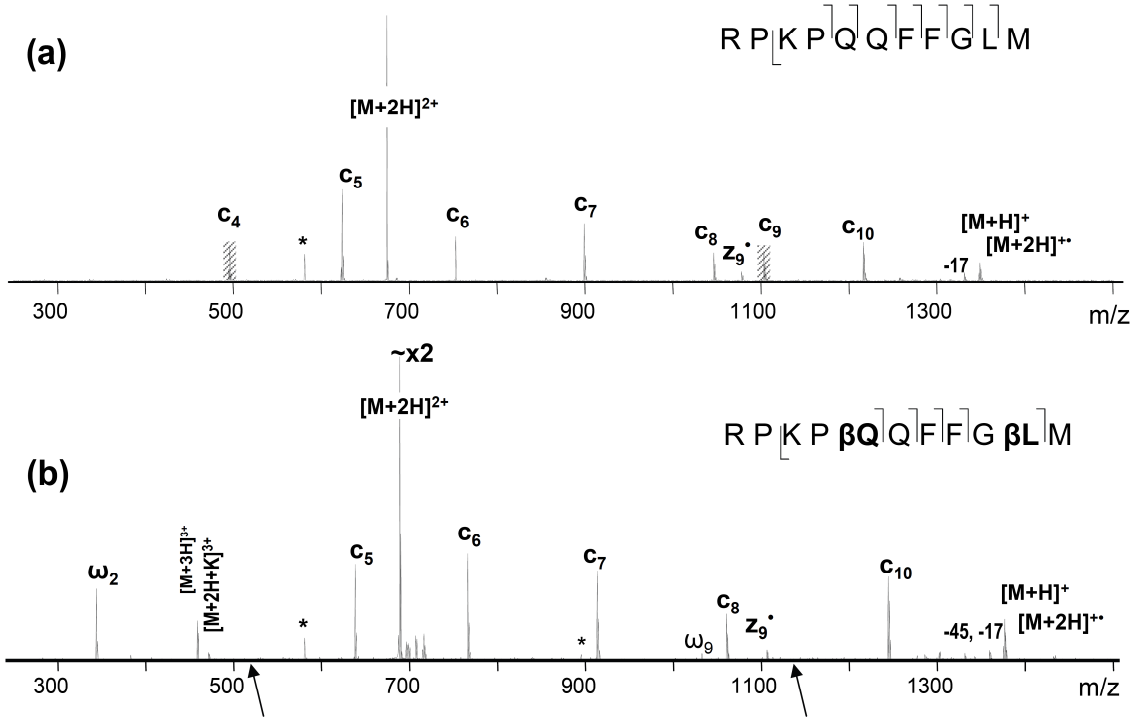

Figure 6.4 ECD of Substance P: a) unmodified, b) modified at Q_5 and L_{10} to β_3-type amino acids.

One may speculate that introduction of the CH_2 group could lead to such a conformational change that would hinder the formation of c_4 and c_9 fragments; or they may still be formed, but not separated due to the new, possibly tighter hydrogen bonding, although the incorporation of only one extra methylene group is unlikely to create such a big difference in intramolecular hydrogen bonds. As proposed previously,[216, 219] it is more likely that the absence of C_α-C_β bond cleavages resulted from the lack of radical stabilization effect by a sidechain carbonyl group as in isoAsp containing peptides. Further, in α-amino acid residues, the α-carbon radical formed by N-C_β bond cleavage can be resonantly stabilized by the neighboring carbonyl (Figure 6.5); in β-amino acid residues, the carbonyl is located further away providing no such

stabilization, making the N-C_β bond cleavage not energetically favorable. Within the isoAsp, however, a carboxylic acid on a side chain is located at the close proximity to the backbone β-carbon atom, which can play a stabilization role for the β-carbon radical and thus ensure both the C_α-C_β and N-C_β bond cleavages. In agreement with this explanation, in a previous ECD study of γ-glutamic acid containing peptides, N-C_γ, C_α-C_β, and C_β-C_γ bond cleavages were all observed.[229] Similar stabilizing effect can be provided by the aromatic structure as well, such as that observed in the β-phenylalanine containing peptides, which was recently reported by Hamidane *et al.*[57] supporting the radical stability hypothesis.

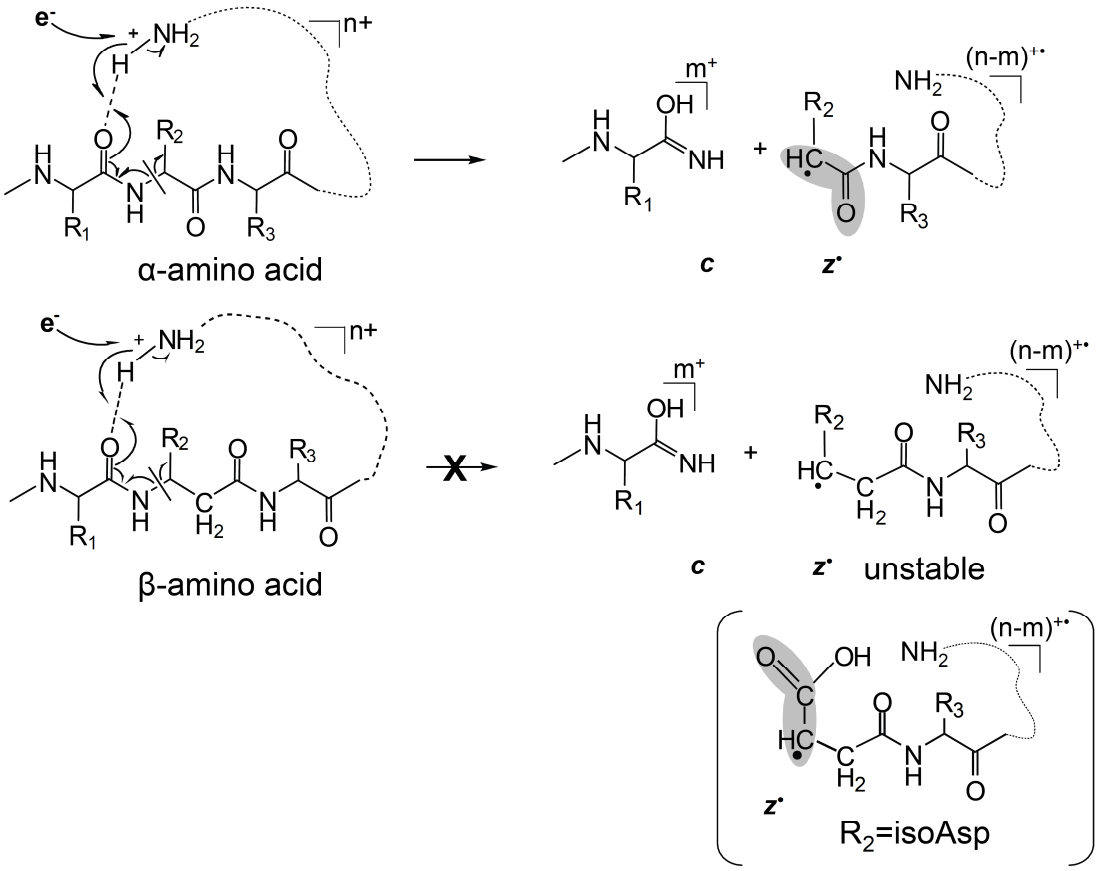

Figure 6.5 ECD mechanism within α- vs. β-amino acid residues.

6.3.5 Puma BH_3 protein analogues

Further ECD analysis was performed on a set of bigger peptides, originally designed to mimic foldamer ligands for the BH_3 recognition cleft of the protein Bcl-x_L.[230] The primary sequence of the two 26-residue α/β-peptide analogues corresponds to a Puma BH_3 domain (EEQWAREIGAQLRRMADDLNAQYERR). Both peptide analogues have amino acid residues modified to β_3-homo amino acids after each 2nd or 3rd residue, but not all at the same positions. Such a backbone repeat ααβαααβ allows formation of an α-helix like conformation that helps mimic the original binding behavior of an α-helical domain. For the purpose of the current study, the two peptide analogues provide an excellent system for the direct comparison of fragmentation within α- and β-type amino acids. The ECD spectrum of the 3.3 kDa Puma BH_3 protein analogue I (**βE**EQ**βW**ARE**βI**GA**βQ**LRR**βM**AD**βD**LNA**βQ**YE**βR**R) is shown in Figure 6.6; the ECD spectrum of the analogue II (**βE**EQW**βA**RE**βI**GAQ**βL**RR**βM**ADD**βL**NA**βQ**YER**βR**) is shown in Figure 6.7. The spectra show nearly complete sequence coverage with various types of fragments observed, including $a^{\bullet}$, *y, c,* and $z^{\bullet}$ fragments. In agreement with the modified substance P result, no N-C_β bond cleavages were observed for the β-type amino acid residues, but the corresponding α-amino acid residues all provided such cleavages. For example, *c,* and $z^{\bullet}$ fragments are observed at the α-Ala_5, α-$Leu_{12,20}$, and α-Arg_{26} positions (analogue I) but not in the β-Ala_5, β-$Leu_{12,20}$, and β-Arg_{26} positions (analogue II) (Figure 6.8, relevant residues are highlighted). The only N-C_β bond rupture was detected for β-Asp provided by the z_9^{2+} and c_{17}^{2+} fragments (Figure 6.6).

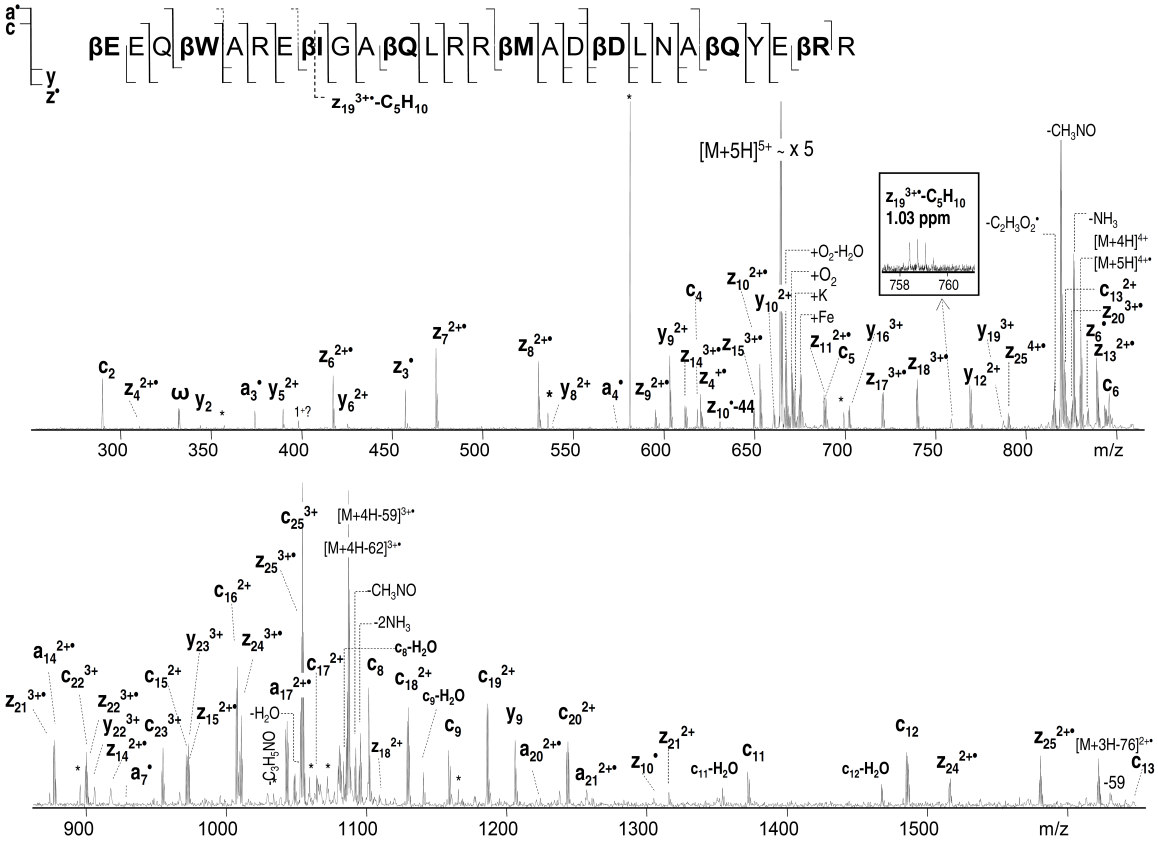

Figure 6.6 ECD of Puma BH_3 protein analogue I.

Interestingly, this is a β-homo aspartic acid; *i.e.* the sidechain carboxylic acid is separated from the backbone β-carbon by one methylene group. Hence, β-Asp side chain carbonyl cannot provide the same stabilization for the C_β radical as in the native isoAsp, and the z_9^{2+} and c_{17}^{2+} fragments were only present at very low abundance.

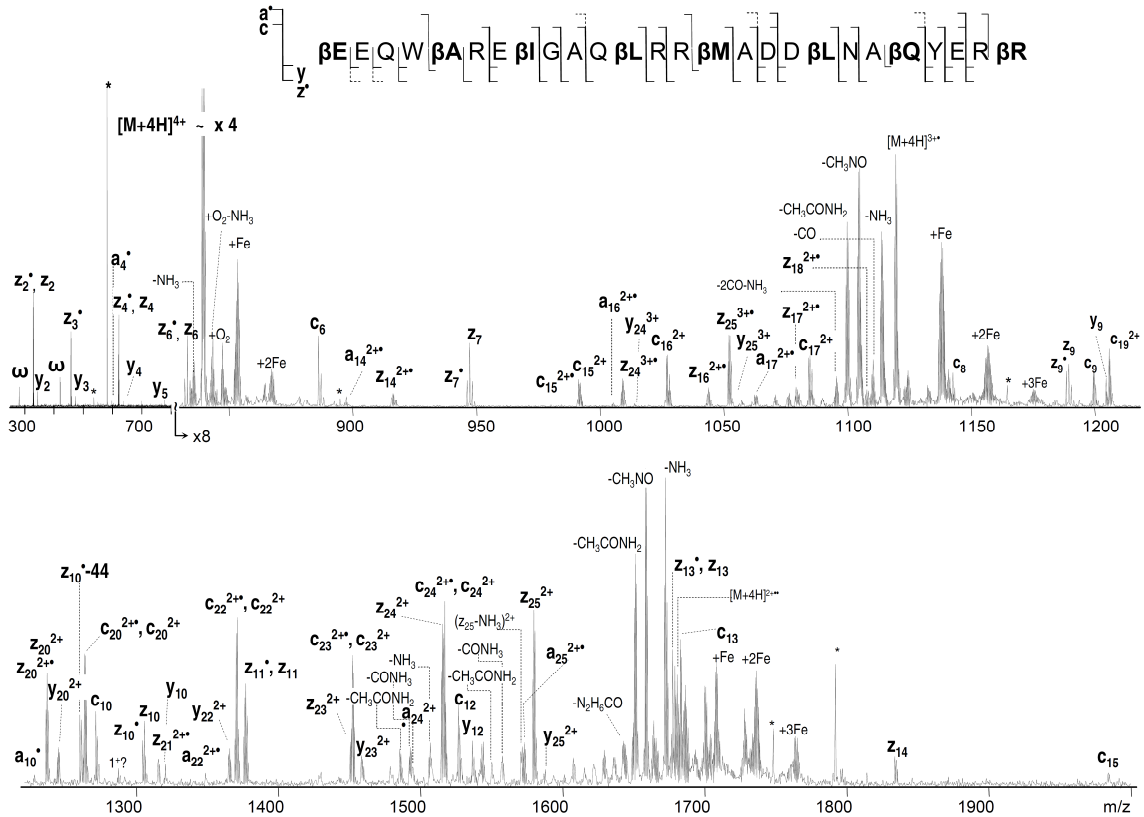

Figure 6.7 ECD of Puma BH_3 protein analogue II.

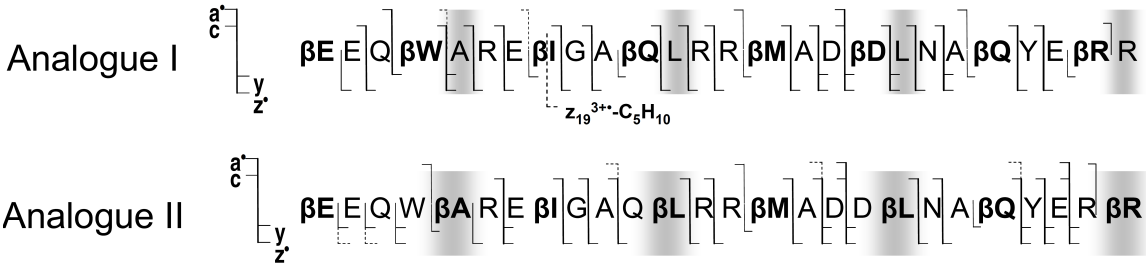

Figure 6.8 ECD cleavage scheme of Puma BH_3 protein analogues I and II.

As was noted earlier, the Puma BH_3 peptides studied here have α-helix like conformations. It is possible that the N-C_β bonds can be cleaved but protected from dissociation due to strong hydrogen bonding within the α-helix as was suggested previously[231] and consistent with the results from ECD mechanistic studies.[69, 71] Yet, there were many *c* and *z*• fragments present except for those missing within β-residues

suggesting that the peptide was relatively unfolded, and thus, the hydrogen bonds should not interfere with the fragment separation. Furthermore, dissociation of the C_α-C_β bond now seems to be an exception rather than the rule for β-amino acid residues as only one peak representing the C_α-C_β cleavage of isoleucine was identified provided by the $z_{19}^{3+\bullet}$-C_5H_{10} fragment ion (Figure 6.6). Indeed, according to Turecek and coworkers[232] who studied the β-alanine N-methyl amide model system, dissociation of the C_α-C_β bond was slow and in competition with other dissociations from the most stable composition with a radical located on the C-terminal amide carbonyl. To conclude, the N-C_β and C_α-C_β backbone cleavages are still possible, but do not represent the dominant channel of fragmentation within β-amino acid residues.

6.3.6 Proposed mechanism

The incorporation of an extra methylene group within the polypeptide backbone increases the flexibility of the molecule. The conformational change is probably not that dramatic, but an increase in internal rotations is expected, resulting in decreased steric hindrance. Thus, the backbone nitrogen may become more exposed for hydrogen bonding. In addition, elongation of the backbone within the β-residue moves the amide nitrogen and the following amide carbonyl apart removing the captodative stabilization effect at the C_β. Therefore, the N-C_β bond dissociation becomes a less favorable process, thus shifting dissociation to other fragmentation channels. One such channel may proceed via backbone nitrogen protonation, leading to increased $a^\bullet$ and *y* fragment ion formation (Figure 6.9) as was proposed in an early ECD paper.[233] The N-C_β bond rupture may still occur, creating *c* fragment and unstable intermediate $z^\bullet$ fragment that, if formed, will probably undergo further rapid dissociation, and is thus not observed.

However, it is more likely, that upon electron capture the radical at the backbone amide hydrogen will induce the homolytic cleavage of the peptide bond and further loss of a CO molecule to produce the more stable $a^{\bullet}$ and *y* fragment ions. It is interesting to note that, unlike the doubly charged Q_{06} peptide, the $a^{\bullet}/y$ fragmentation channel was not observed in the ECD spectrum of the doubly charged β-substance P variant.

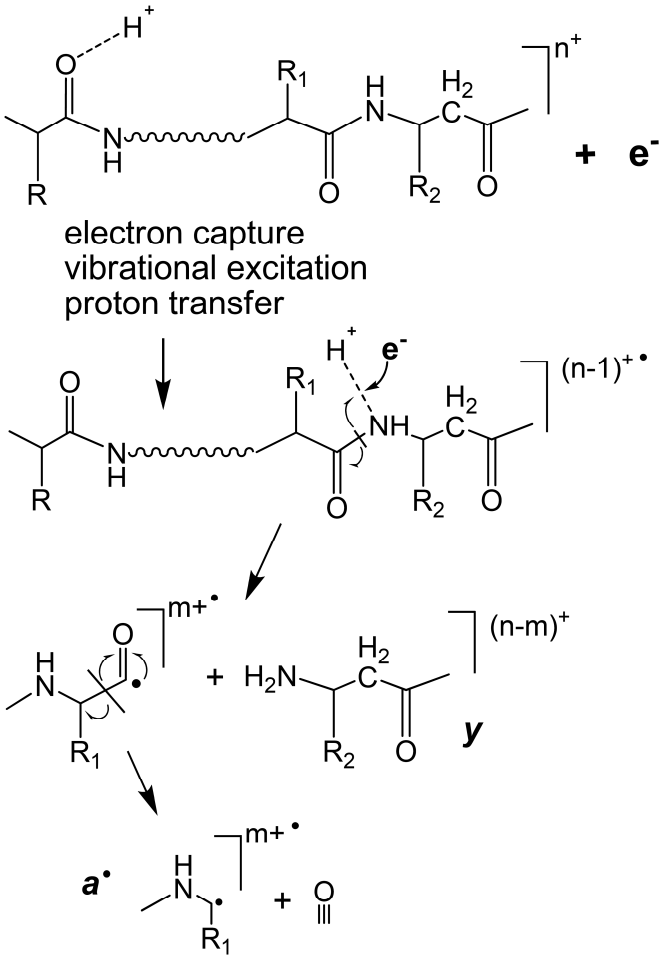

Figure 6.9 ECD mechanism for β-amino acid residues.

A closer look at the Q_{06} β-peptide and the modified substance P revealed that, besides the nature of the amino acids, the clear difference between the peptides is the presence of basic amino acid residues, which could dictate the sites of protonation and

thus the sites of electron capture dissociation. The two charges carried by the substance P peptide would preferably reside at the Arg and Lys sidechains, and are solvated by the carbonyl groups of the peptide. According to the Cornell ECD mechanism,[57] upon electron capture at the protonated site, hydrogen migration to various carbonyl groups would result in N-C_α bond cleavages. Due to arginine being a poor hydrogen donor, backbone fragmentations are most likely initiated by electron capture at the protonated N-terminal or lysine sidechain amino group.[65, 73, 234] In the case of the β-substance P, this process will result in the formation of unstable C_β radicals within the βQ and βL residues, which correlates with their disappearance. On the other hand, in the Q_{06} β-peptide, there are no basic amino acids. As was discussed earlier, the first protonation site would be the N-terminal amine; and the second proton would be mobile within the polypeptide backbone. Thus electron capture would occur at the N-Terminus or on the backbone rather than on the side chain and the electron induced fragmentation of the Q_{06} peptide would occur via a different mechanism to that of substance P. Introducing the third charge to the substance P peptide should lead to the protonation of an additional site within the molecule, which is likely one of the backbone amide nitrogen or carbonyls (see below), since N-terminal amine protonation seems unlikely because of the strong columbic repulsions by the nearby protonated Lys and Arg residues. To test this hypothesis, triply charged β-substance P was subject to the ECD analysis (Figure 6.10). Indeed, many $a^\bullet$ and y fragments now appeared in the spectra. Interestingly, they often were slightly higher in abundance in the modified substance P variant as shown in the inset (Figure 6.10). Nonetheless, all of the $a^\bullet$ and y fragments were observed in both peptides, except for y_2 and $a_9^\bullet$, which were exclusively present in the modified substance P variant. The last two fragments are formed due to

the cleavages within the β-Leu_{10} residue. Note that the N-C_β bond cleavage was not observed within this residue as c_9 and $z_2^{\bullet}$ fragments were still absent (yet present in the non-modified variant). This is consistent with the previous results and supports the proposed hypothesis for the fragmentation within the β-amino acid residues.

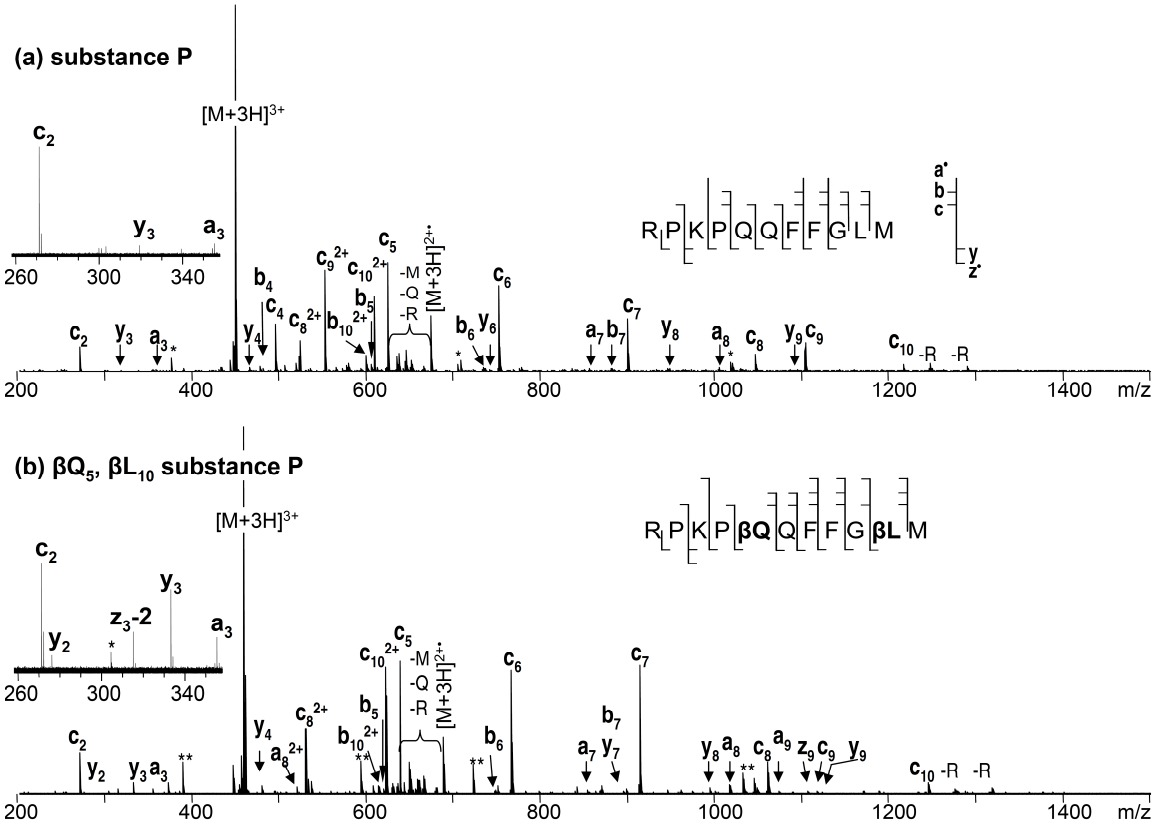

Figure 6.10 ECD of triply charged substance P $[M+3H]^{3+}$: a) unmodified, b) modified at Q_5 and L_{10} to β_3-type amino acids.

The role of backbone nitrogen protonation in ECD has been previously discussed in the literature. In the original ECD study, the $a^{\bullet}$ and *y* ions were proposed to be formed from the backbone nitrogen protonated species.[233] Backbone nitrogen protonation was also suggested to play a role in the formation of *b* ions in ECD. Theoretical investigation by the Uggerud group showed that electron capture by nitrogen protonated N-methyl-

acetamide resulted in rapid amide bond dissociation and production of CH_3CO and NH_2CH_2, corresponding to the $b^{\bullet}$ and *y* ions in peptides.[235] Concomitantly, $b^{\bullet}$ ions can further lose CO to form $a^{\bullet}$ ions. In addition, *b* ions were present in ECD of peptides without basic amino acid residues.[62] It was suggested that upon backbone nitrogen protonation, the peptide bond could be cleaved to form a $b^{\bullet}/y$ ion pair, and the subsequent intra-complex hydrogen atom transfer within this long-lived ion pair could lead to the formation of *b and* $y^{\bullet}$ ions. Backbone amide nitrogen protonation was also invoked to explain the $a^{\bullet}$, *b*, and $b^{\bullet}$ ion formation in nitrated peptides that are either acetylated at the N-terminus, or lacking basic amino acid residues.[236] In the current study, however, neither *b* nor *y* ions observed were radicals. Thus, these *b* ions were most likely formed via the energetic fragmentation of vibrationally excited even-electron charged reduced species.[60]

It should be noted that protonation on the backbone nitrogen is not thermodynamically favorable.[237-239] For instance, for the model system of N-methylacetamide, the proton affinity of the carbonyl oxygen was calculated to be ~60 kJ/mol higher than that of the backbone nitrogen.[238] This is in agreement with the study of the dipeptide Lys-Gly, where the carbonyl oxygen protonated species was calculated to be ~45 kJ/mol more stable than the backbone nitrogen protonated species.[239] Based on these results, peptide fragmentation via protonation of the backbone nitrogen would seem unlikely. However, theoretical investigations have usually been done on very small model systems, which often do not possess extensive intramolecular interactions such as hydrogen bonding and salt bridges that are expected to play a more important role in the fragmentation of larger peptides. Charge solvation by nearby backbone and sidechain groups could appreciably change the relative

stabilities of different protonated species. In β-peptides, the elongation of the backbone may make it better positioned (due to less steric hindrance by the adjacent side chain) for hydrogen bond formation. The addition of an extra methylene group in the backbone can also slightly increases the gas-phase basicity of the amide nitrogen, as the electron withdrawing carbonyl group is replaced by the electron donating alkyl group. Further, electron capture by the precursor ion could increase its internal energy considerably (by several eVs), and less favored protonation sites may become significantly populated as the system relaxes from the initial Rydberg state to low lying electronic states. In other words, the proton may initially reside on the carbonyl oxygen, but could migrate to the backbone amide nitrogen upon excitation. This argument is similar to the one used in the mobile proton model to explain the low energy CAD fragmentation behavior of peptide ions,[237, 240] where it was proposed that the proton initially resides on the thermodynamically more stable sites, such as the lysine sidechain or backbone oxygen, and later migrates to the less favorable sites, including the backbone amide nitrogen upon collisional activation to facilitate fragmentations. Finally, for the β-linked peptides studied here, electron capture at the protonated oxygen site cannot lead to "normal" c/z fragmentation due to the radical instability, which may further drive the migration of the proton to the less preferable backbone nitrogen site that could lead to the formation of $a^{\bullet}$ and *y* ions upon electron capture. In general, the abundance of these unusual ECD fragments was fairly low, as expected from the low population of nitrogen protonated species (Figure 6.10), but they were nonetheless present in competitive abundance when the primary ECD fragmentation channel was blocked within β-amino acid residues.

Further experiments are needed to test the proposed mechanism. In addition, basicity measurements and theoretical investigations specifically for β-amino acid

containing peptides could provide a better understanding on how these $a^{\bullet}$ and *y* type fragments are formed.

6.4 Conclusion

Various peptides containing β-amino acid residues were analyzed in this study. Remarkably, N-C_{β} bond cleavages were rare within the β-residues, and C_{α}-C_{β} cleavages were seldom observed providing no evidence of the β-residues in spite of previous results of the isoaspartic acid. Furthermore, no distinct difference was found for the fragmentation within β_2 vs. β_3-type amino acid residues. Meanwhile, $a^{\bullet}$ and *y* fragments were often produced at β-residues, particularly for the bigger peptides with α-helical like structures. The lack of $z^{\bullet}$ and *c* fragments and increased $a^{\bullet}$ and *y* fragment formation could imply the presence of β-residues in the peptide; however, this is a poor signature, because of the normal appearance of $a^{\bullet}$ and *y* fragments in ExD spectra of α-peptides, and various other reasons that can contribute to the disappearance of $z^{\bullet}$ and *c* fragments. Thus, currently, ExD methods cannot be used to reliably differentiate α- from β- or β_2 from β_3 type amino acids.

The introduction of one extra methylene group into the polypeptide chain destabilizes the C_{β} radical formed by the N-C_{β} bond rupture making this channel of fragmentation less favorable. Thus the fragmentation occurs via alternative channels. The dominant products appear to be the $a^{\bullet}$ and *y* fragments, with the exception when the side chain of the β-residue can provide radical stabilization for the formation of the $z^{\bullet}$ and *c* fragments. It is suggested that appearance of such fragments may require protonation on the backbone amide nitrogen, which is further supported by the charge state-dependent study of modified substance P peptide. The fragmentation mechanism for β-

peptides has been proposed via backbone nitrogen protonation similarly to what was originally proposed for the ECD of α-peptides.

The minor ECD pathway of $a^{\bullet}$ and *y* fragment formations was little studied. Future studies of this fragmentation pathway would help with our understanding of the fragmentation of the β-amino acid containing peptides. Further ExD studies, as well as computational studies and kinetic analysis specifically for the β-amino acids are needed for better characterization of β-peptides.

Chapter 7

In-Source Decay for β-Peptide Analysis

7.1 Introduction

In-source decay (ISD) during the matrix assisted laser desorption ionization (MALDI) process can produce abundant ECD-like fragmentation resulting from the cleavage of the N-C_α bond on the polypeptide backbone.[88] The ISD process is believed to be mediated by hydrogen radical transfer from the matrix to the analyte ions generating aminoketyl radicals to produce *c*- and *z*- type fragments (Figure 7.1.a). The radical nature of the ISD method and its similarity to the ECD process suggest that characterization of β-peptides may lead to no or little fragmentation of C_α-C_β bond due to the lack of C_β radical stabilization based on the results described in the previous chapter. It was recently reported that some novel matrices, such as 5-formylsalicylic acid (5-FSA) and 5-nitrosalicylic acid (5-NSA), can accept a hydrogen from the analyte ions.[91, 92] In this case, the hydrogen abstraction from the peptide results in the formation of an oxidized peptide containing a radical site on the backbone amide nitrogen with subsequent radical-induced cleavage at the C_α-C bond, leading to the formation of *a*- and *x*-type fragments (Figure 7.1.b).

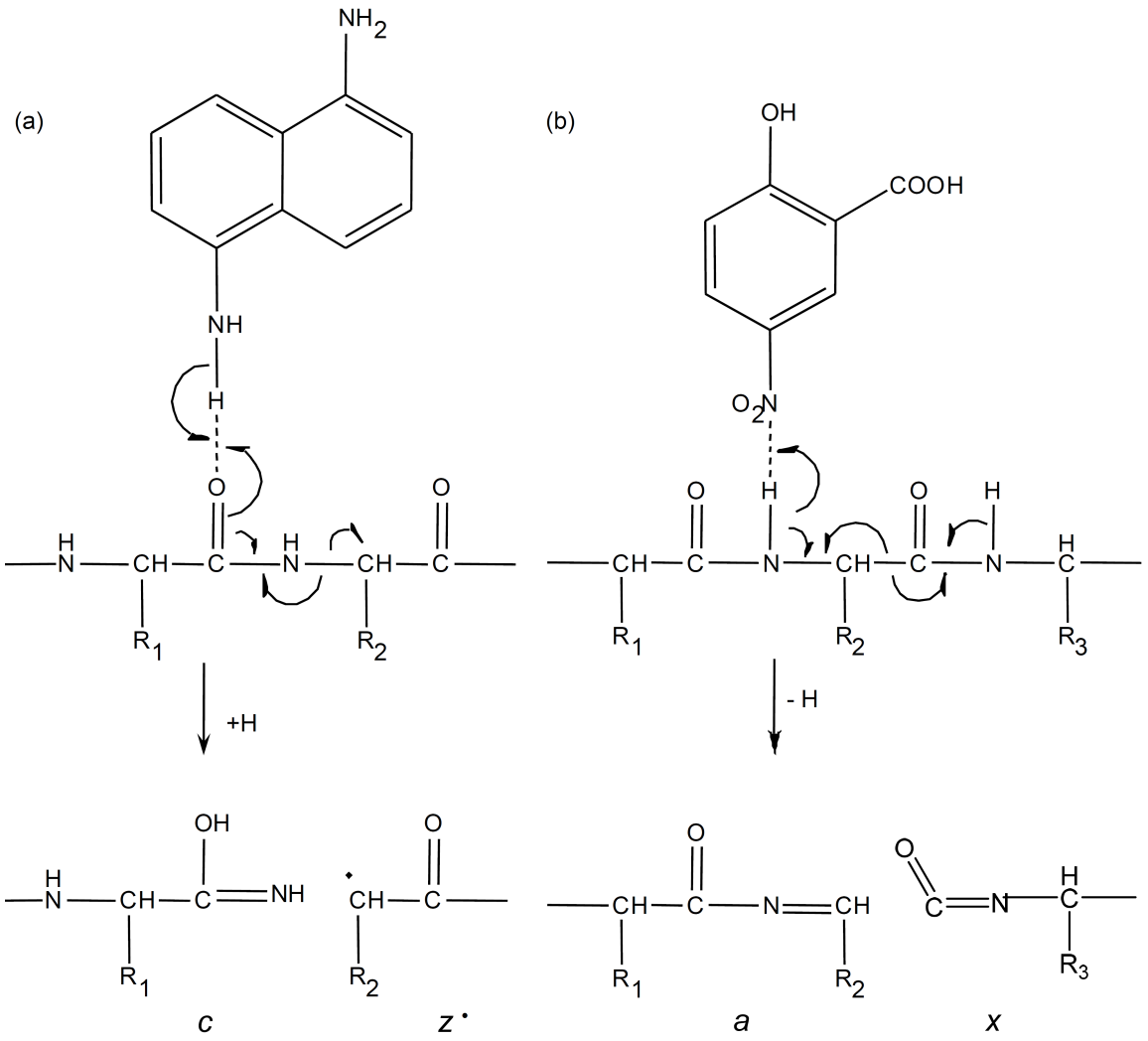

Figure 7.1 Formation of the ISD fragments: (a) *c/z*-type via hydrogen attachment and (b) *a/x*-type via hydrogen abstraction.

In β-amino acids, because of the presence of an extra methylene group between the C_α and the carbonyl C, it is possible that amide nitrogen radical driven fragmentation would result in the cleavage of the C_α-C_β bond. Thus, it is hypothesized that the use of hydrogen accepting matrices in ISD may lead to formation of diagnostic fragments for β-amino acids.

7.2 Experimental section

7.2.1 Peptides and reagents

C-terminally amidated Substance P with two amino acids modified to β_3-type amino acids (RPKPβQQFFGβLM) was custom synthesized by AnaSpec (San Jose, CA, USA). Non-modified Substance P was purchased from Sigma-Aldrich (St. Louis, MO, USA); Formic Acid (FA) was purchased from Thermo Scientific (Rockford, IL, USA). HPLC grade Acetonitrile (ACN) and Methanol (MeOH) were obtained from Fisher Scientific (Fair Lawn, NJ, USA). Deionized water was purified by a Millipore Milli-Q Gradient system (R=18.2 MΩ cm and TOC = 9 – 12 ppb) (Billerica, MA, USA). 5-Aminosalicylic acid (5-NSA, or 2-hydroxy-5-nitrobenzoic acid) matrix was obtained from Sigma Aldrich (St. Louis, MO, USA).

7.2.2 Sample preparation

Peptides were dissolved in 50:50 ACN:H_2O with 0.1 % FA at a concentration of 20 pmol/µl. 5-NSA matrix was dissolved in the same solvent at a concentration of 20 mg/ml. Sample was deposited onto a stainless steel MALDI target in a “sandwich” manner: 1 µl of matrix solution followed by 1 µl of analyte solution and then again 1 µl matrix solution on top, letting the droplet dry each time before spotting the next layer.

7.2.3 Mass Spectrometry

The in-source decay fragmentation was performed on a solariX hybrid Qh-FTICR instrument at the Bruker facility (Bruker Daltonics, Billerica, MA, USA) with a 12 T actively shielded magnet. The laser power was 30 %, 1000 Hz laser frequency, 300

laser shots per scan, 50 scans were accumulated for each spectrum. Data were analyzed using dataAnalysis 4.0 software.

7.3 Results and Discussion

7.3.1 Diagnostic fragments for the C_α-C_β bond cleavage

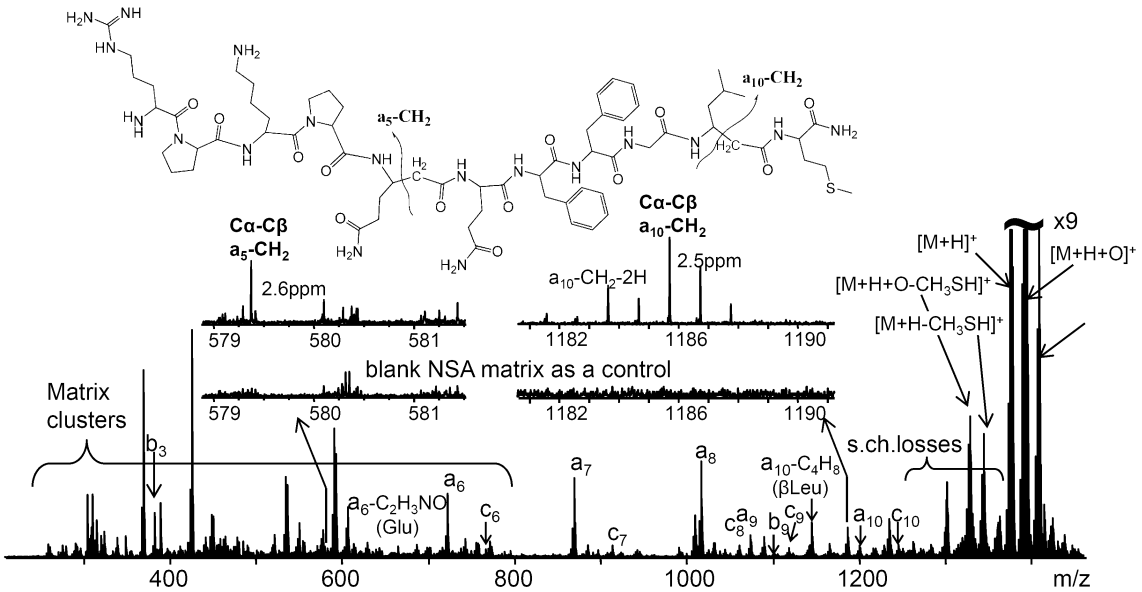

Figure 7.2 MALDI-ISD-FTICR mass spectrum of modified substance Pusing 5-NSA matrix. Data was acquired at the Bruker Daltonics facility, Billerica, MA.

MALDI-ISD experiment was performed on a synthetic substance P analogue with two β-homo-amino acids incorporated at the glutamine-5 and leucine-10 positions. The resulting ISD spectrum is presented in Figure 7.2. The peptide structure is illustrated on top, and the insets show the diagnostic ions, a_5-CH_2 and a_{10}-CH_2, for the two β-amino acid residues present. Characteristic for hydrogen accepting matrices,[91] a peak corresponding to the loss of two hydrogen atoms is also indicated in spectrum

(a_{10}-CH_2-2H). The MALDI spectrum of the blank 5-NSA matrix was acquired at the same conditions as a control (insets).

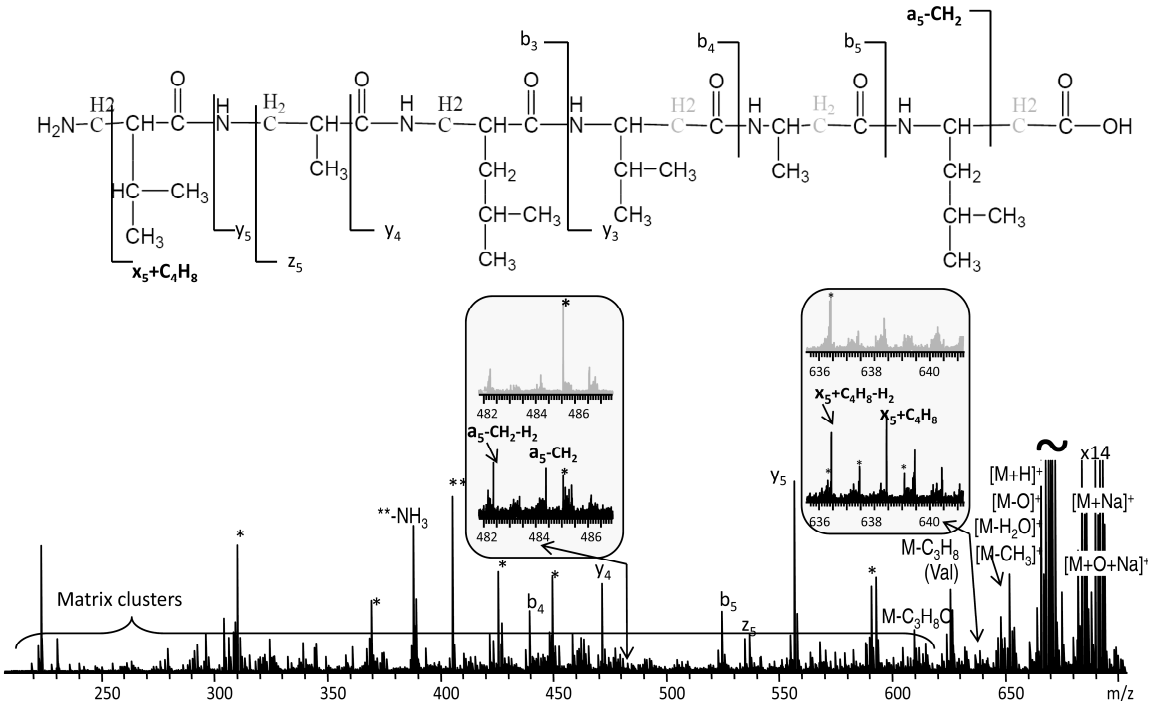

Figure 7.3 MALDI-ISD-FTICR mass spectrum of the β-Q06 peptide. Insets show the diagnostic ions for β_2-valine-1, and β_3-leucine-5 amino acids with corresponding region of a blank matrix as a control on top. * indicates abundant matrix cluster ions, ** indicates unidentified chemical noise peaks.

Another β-peptide, β-Q06, was analyzed with MALDI-ISD (Figure 7.3). For this small peptide, it was very difficult to obtain doubly charged precursor ions required for ECD analysis (Chapter 6). Thus, this peptide seems to be a good case to test the ISD performance. Interestingly, similar to the ECD and ETD data, the ISD spectrum of β-Q_{06} contains mostly *b*- and *y*- fragments, which could be the result of post-source decay mediated by collisions in the hot MALDI plume owing to the high laser power used for the ISD experiment.[90] Nonetheless, as a result of the ISD process, two diagnostic C_α-C_β

cleavages were observed, $x_5^{\bullet}$+C_4H_8 and a_5-CH_2. β-Q_{06} contains both β_2 and β_3 amino acids, and if one can produce the C_α-C_β bond cleavage, it should be possible to distinguish β_2- from β_3-type amino acids. Indeed, a "switch" of the side chain from the C_α to C_β carbon in β_3-type amino acids would provide diagnostic fragments $x^{\bullet}$+[side chain] and *a*-[side chain], whereas for β_2-type amino acids, such fragments would be $x^{\bullet}$+CH_2 and *a*-CH_2. One diagnostic ion of each complementary pair was observed for the β_2-valine-1 and β_3-leucine-5 residues, respectively, with their complementary ions having too small *m/z* value to be detected. In addition, similar to the substance P result, double hydrogen losses were also observed for β-Q_{06}. Mechanisms for the formation of diagnostic fragments within β-amino acids in ISD using hydrogen accepting matrices are proposed in Figure 7.4.

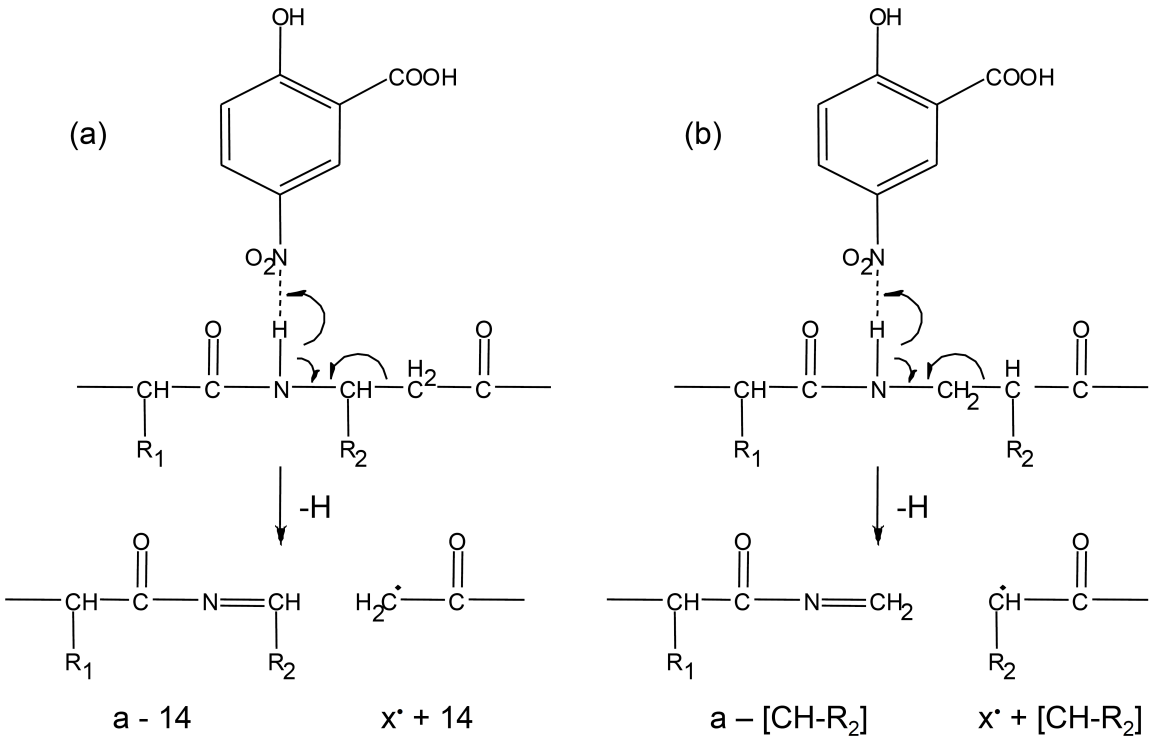

Figure 7.4 Upon the loss of a hydrogen, amide nitrogen radical would cleave the C_α-C_β bond producing diagnostic *a*-14 and *x*•+14 in the case of the β_3-type amino acid (a) and *a*-[side chain] and *x*•+[side chain] in the case of the β_2-type amino acid (b).

7.3.2 Advantages and disadvantages of the proposed method

One of the limitations of the ISD method is that fragmentation occurs during the MS^1 event, and the precursor ion may not be isolated prior to fragmentation as is possible in most tandem MS methods. Therefore, sample purity is essential for successful data interpretation and sample complexity must be reduced, ideally to single species with, for example, HPLC prior to the MALDI-ISD analysis. The matrix amount necessary for successful desorption, ionization, and ISD fragmentation is high (~10 mg/µl). Matrix ions, matrix clusters and analyte-matrix adducts are usually abundant in MALDI spectra and represent dominating peaks below 1000 *m/z* limiting the

analysis of smaller analyte molecules due to the peak interference (Figures 7.2 and 7.3). Therefore, blank matrix spectrum must be used as a control for comparison. In some instruments, such as FTICR and Q-o-TOF, the longer delay between ion formation and detection allows some matrix clusters to fall apart leading to less matrix interference. Higher mass resolving power instruments are highly desirable for this kind of experiments for confident assignment of matrix/analyte peaks.

One of the advantages of the ISD method is its ability to generate ECD-type fragments from singly charged precursor ions, which cannot be analyzed by ECD and most ECD-related techniques due to the charge reduction upon electron capture. Importantly, ISD can produce specific cleavages of the N-C_α, C_α-C, and C_α-C_β bonds of the peptide backbone without loss of the side-chains and PTMs, providing a valuable tool for the analysis of biological samples.

7.4 Conclusion

The in-source decay fragmentation was applied toward the analysis of β-linked amino acid containing peptides. The cleavage of the C_α-C_β bond on the polypeptide backbone was observed providing diagnostic fragments for the β-amino acids. In addition, it was possible to differentiate β_2-type from β_3-type amino acids using ISD, which was not possible with ECD. However, for some C_α-C_β bonds present, diagnostic fragments were not detected. The efficiency of such cleavage may depend on the peptide sequence and various parameters of the experiment, such as the laser power, analyte - matrix concentration ratio, and others. Thus, the method needs to be further optimized for the best results. Nonetheless, ISD seems to be a promising tool for the analysis of β-peptides.

Chapter 8

Conclusion and Future Perspective

8.1 Conclusion

Deamidation and isomerization are two common post translational modifications (PTMs), which accumulate with time and have been associated with a number of diseases. These modifications have garnered a lot of attention from researchers in various biospheres. Much progress has been made toward the analysis and characterization of these PTMs in peptides and proteins, although it still remains a challenging task. Electron capture dissociation (ECD) technique is one of the great recent achievements in this area. In this thesis, the ECD method was applied to characterize specific species, and new and improved methods were suggested in general analysis of deamidation and its products.

Amyloid β (Aβ) peptides are the major components of the vascular and plaque amyloid filaments in individuals with Alzheimer's disease (AD). Isoaspartic acid (isoAsp) was detected in Aβ peptides in the brain of AD patients and, thus, is related to the pathology of AD. In this thesis, ECD was applied to analyze amyloid β protein fragments to differentiate isomerized Asp residues. The most aggregative fragment Aβ42 was successfully characterized by top-down ECD-MS/MS approach. It was further shown that electron ionization/impact dissociation (EID) can also produce diagnostic fragment ion on the example of the tryptic peptide Aβ17-28. This method would benefit the analysis of singly charged small or non-polar peptides, which is not possible with the ECD technique, because of the charge neutralization. Further, N-terminal isoAsp was differentiated in Aβ and other peptides by ECD and electron transfer dissociation (ETD),

collectively known as electron activated dissociation (ExD) methods. New diagnostic fragment ions for N-terminal isoAsp were proposed and demonstrated in peptides with free N-terminus and acetylated one.

Mixed Aβ and other peptides containing Asp, isoAsp, and Asn at one or two positions, including the N-terminal modification, were characterized using reversed-phase (RP) high performance liquid chromatography (HPLC). Although it was shown that HPLC separation alone may lead to erroneous assignment of peptide isomers because of the sequence and separation parameter dependent changes in elution orders, it is an important complementary technique in proteomics analysis. Predictive chromatography was suggested as an aid to isoAsp-containing peptide separations in combination with tandem MS and when ExD methods are not available. Further, the cerebrospinal fluid (CSF) studies on isomerized Aβ peptides were initiated and would bring an interesting addition to the amyloid β research field.

Because isoAsp is a β-type amino acid, the interest appeared in other β-amino acids and β-peptides. β-Amino acids differ from their α-analogues by the presence of an additional methylene group on the polypeptide backbone. This difference leads to the formation of a bigger variety of secondary and tertiary structures in β-peptides, yet the functional side-chain groups of amino acids remain the same. Another important property of β-peptides is their resistance to proteolytic degradation in living organisms. These features make them good candidates for therapeutic agents by mimicking α-peptide's and protein's active sites and allowing prolonged circulation in the body. Despite substantial progress in β-peptide synthesis and understanding of their structure, a fast and accurate analytical method for analysis of β-peptides is lacking. It was proposed in this thesis that ExD methods could be one such technique, based on the

isoAsp analysis results. However, ExD produced no diagnostic fragment ions at β-amino acid residue sites. It appears that formation of isoAsp diagnostic ion is driven by the stability of the C_β radical due to the presence of the isoAsp side-chain's carboxylic group. Such radical stabilization is absent in other β-amino acids, except for β-phenylalanine. Although no diagnostic ions were detected, the fragmentation pattern within β–amino acid residues was somewhat different from that within α-amino acid residues. The characteristic N-C_α bond cleavage was severely diminished or not observed producing little or no *c* and *z* fragments, yet the alternative ECD pathway, in which *a* and *y* ions are formed was activated. These results lead to a better understanding of the ECD mechanism as well as of other fragmentation methods producing ECD-like fragments. One such technique is the in-source decay (ISD). It was proposed that use of hydrogen-accepting matrices in ISD may lead to C_α-C_β bond cleavage in β-amino acids, because the resulting radical ion would be stabilized by the polypeptide backbone carbonyl group irrespective of the amino acid's side-chain. This hypothesis was tested on a few peptides containing β-amino acid residues which showed promising results. β-Amino acid residue-characteristic cleavages of the C_α-C_β bond were generated providing diagnostic fragment ion peaks in the ISD spectra. In addition, characteristic to the use of hydrogen accepting matrices in ISD, the accompanying peaks of double hydrogen loss were also observed, giving an additional confirmation of the result.

In conclusion, the author believes that the results of the work in this thesis have brought a valuable addition to the deamidation and related problems in structural analysis of peptides and proteins by investigating and improving the existing methods of analysis as well as by introducing a new means for β-peptide characterization.

8.2 Future Perspective

Despite the great progress in the development of analytical methods for the characterization of deamidation and isomerization and in biological research of these PTMs, there are ample possibilities for further method improvement and applications. One such interesting project involves protein L-isoaspartyl O-methyltransferase (PIMT) enzyme (registry number: EC 2.1.1.77). PIMT is an isoAsp-repairing enzyme, which catalyzes the conversion of isoAsp back to Asp residue. Deamidation as well as isomerization reaction are highly sequence dependent processes. Deamidation rates are the fastest for the Asn-Gly sequence, followed by the Asn-His, Asn-Ser, and Asn-Ala sequences. It is possible that the specificity of the PIMT enzyme is also sequence dependent. This can be tested by a mechanistic study of isoAsp-containing peptides with varied position of modification within the sequence on the PIMT enzyme reaction rates. In order to do so, one would need to measure the disappearance of PIMT enzyme substrates by, for example, measuring the isoAsp diagnostic fragment abundance in the spectra based on calibrated linear curves of the known isoAsp concentrations.

Proteomic scale analyses of isoAsp peptides have already been performed by means of a “bottom-up” LC-ECD-MS/MS approach.[205] This is a great achievement, although such “bottom-up” analysis has its limitations, such as loss of some peptides because of difference in hydrophobicity in LC separation and ion suppression during ionization process in MS. Further, artifactual deamidation can be introduced to the sample during sample handling. For instance, trypsin digestion commonly used in the bottom-up approach is normally performed at pH ~8 under which condition partial deamidation of Asn in rapid-deamidating sequences such as AsnGly and AsnSer could

occur if performed over 4 hours. On the contrary, in a top-down mode, these limitations are eliminated because the single protein characterization should yield a 100 % sequence coverage and does not require prior digestion. However, the analysis of intact proteins can be quite challenging and has its own limitations such as disrupting the protein 3D structure inside the mass spectrometer for high efficiency fragmentation. Some preliminary work has been done toward this direction but further development would be needed.[241]

Preliminary data have been acquired on the analysis of β-peptides by tandem MS. Although for most β-amino acids studied, diagnostic fragments were not observed using ExD methods, some amino acids yield those in a low abundance. Thus, sequence dependence in formation of diagnostic fragments in β-peptides would provide a better understanding of the fragmentation mechanism. Additional ExD studies, as well as computational studies and kinetic analysis specifically for the β-amino acids are needed for better characterization of β-peptides.

Further, preliminary studies exploring the utility of ISD in β-peptide analysis have been performed, but analysis of a larger number of samples would be necessary for complete method characterization. In biological research, it is important to get quantitative information as the outcome of the analytical investigation. This can be done by using either isotope labeling technique or by creating linear curves of known concentration model peptides similarly as was done for the isoAsp analysis.[178]

Other radical-induced fragmentation methods, such as ultraviolet photodissociation (UVPD),[24] could bring a new complementary method for analysis of both deamidation/isomerization products and β-amino acid-containing peptides.

Bibliography

(1) Karas, M.; Bachmann, D.; Bahr, U.; Hillenkamp, F., Matrix-Assisted Ultraviolet-Laser Desorption of Nonvolatile Compounds, *International Journal of Mass Spectrometry and Ion Processes*, **1987**, *78*, 53-68.

(2) Karas, M.; Hillenkamp, F., Laser Desorption Ionization of Proteins with Molecular Masses Exceeding 10000 Daltons, *Analytical Chemistry*, **1988**, *60*, 2299-2301.

(3) Tanaka, K.; Waki, H.; Ido, Y.; Akita, S.; Yoshida, Y.; Yoshida, T.; Matsuo, T., Protein and polymer analyses up to m/z 100 000 by laser ionization time-of-flight mass spectrometry, *Rapid Communications in Mass Spectrometry*, **1988**, *2*, 151-153.

(4) Aleksandrov, M. L.; Gall, L. N.; Krasnov, N. V.; Nikolaev, V. I.; Pavlenko, V. A.; Shkurov, V. A.; Baram, G. I.; Grachev, M. A.; Knorre, V. D.; Kusner, Y. S., Direct Coupling of a Microcolumn Liquid Chromatograph and a Mass-Spectrometer, **1984**, *10*, 710-712.

(5) Fenn, J. B.; Mann, M.; Meng, C. K.; Wong, S. F.; Whitehouse, C. M., Electrospray Ionization for Mass-Spectrometry of Large Biomolecules, *Science*, **1989**, *246*, 64-71.

(6) Yamashita, M.; Fenn, J. B., Electrospray Ion-Source - Another Variation on the Free-Jet Theme, *Journal of Physical Chemistry*, **1984**, *88*, 4451-4459.

(7) Schier, G. M.; Halpern, B.; Milne, G. W., Characterization of dipeptides by electron impact and chemical ionization mass spectrometry, *Biomed Mass Spectrom*, **1974**, *1*, 212-218.

(8) Davis, R.; Frearson, M. *Mass Spectrometry: Analytical Chemistry by Open Learning*; John Wiley & Sons, London, 1987.

(9) Hoffmann, E.; Stroobant, V. *Mass Spectrometry: Principles and Applications*, Third ed.; John Wiley & Sons, Ltd, 2007.

(10) Siuzdak, G., Ion Sources and Sample Introduction Mass Spectrometry for Biotechnology; *Academic Press*: San Diego, 1996, pp 4-31.

(11) Gaskell, S. J., Electrospray: Principles and practice, *Journal of Mass Spectrometry*, **1997**, *32*, 677-688.

(12) Loo, J. A., Studying noncovalent protein complexes by electrospray ionization mass spectrometry, *Mass Spectrometry Reviews*, **1997**, *16*, 1-23.

(13) Carroll, D. I.; Dzidic, I.; Stillwell, R. N.; Haegele, K. D.; Horning, E. C., Atmospheric-Pressure Ionization Mass-Spectrometry - Corona Discharge Ion-Source for Use in Liquid Chromatograph Mass Spectrometer-Computer Analytical System, *Analytical Chemistry*, **1975**, *47*, 2369-2373.

(14) Zenobi, R.; Knochenmuss, R., Ion formation in MALDI mass spectrometry, *Mass Spectrometry Reviews*, **1998**, *17*, 337-366.

(15) Jaskolla, T. W.; Karas, M., Compelling evidence for Lucky Survivor and gas phase protonation: the unified MALDI analyte protonation mechanism, *Journal of the American Society for Mass Spectrometry*, **2011**, *22*, 976-988.

(16) Bienvenut, W. V. *Acceleration and Improvement of Protein Identification by Mass Spectrometry*; Springer-Verlag New York Inc.: New York, 2005.

(17) Stafford, G. C.; Kelley, P. E.; Syka, J. E. P.; Reynolds, W. E.; Todd, J. F. J., Recent Improvements in and Analytical Applications of Advanced Ion Trap Technology, *International Journal of Mass Spectrometry and Ion Processes*, **1984**, *60*, 85-98.

(18) Douglas, D. J.; Frank, A. J.; Mao, D., Linear ion traps in mass spectrometry, *Mass Spectrometry Reviews*, **2005**, *24*, 1-29.

(19) Pitteri, S. J.; Chrisman, P. A.; Hogan, J. M.; McLuckey, S. A., Electron transfer ion/ion reactions in a three-dimensional quadrupole ion trap: Reactions of doubly and triply protonated peptides with SO2 center dot, *Analytical Chemistry*, **2005**, *77*, 1831-1839.

(20) Wolff, M. M.; Stephens, W. E., A Pulsed Mass Spectrometer with Time Dispersion, *Review of Scientific Instruments*, **1953**, *24*, 616-617.

(21) Brown, R. S.; Lennon, J. J., Mass resolution improvement by incorporation of pulsed ion extraction in a matrix-assisted laser desorption/ionization linear time-of-flight mass spectrometer, *Analytical Chemistry*, **1995**, *67*, 1998-2003.

(22) Mamyrin, B. A.; Karataev, V. I.; Shmikk, D. V.; Zagulin, V. A., The mass-reflectron, a new nonmagnetic time-of-flight mass spectrometer with high resolution, *Soviet Physics JETP*, **1973**, *37*, 45-48.

(23) Vestal, M. L.; Campbell, J. M., Tandem time-of-flight mass spectrometry, *Methods in Enzymology*, **2005**, *402*, 79-108.

(24) Reilly, J. P., Ultraviolet photofragmentation of biomolecular ions., *Mass Spectrometry Reviews*, **2009**, *28*, 425-447.

(25) Comisarow, M. B.; Marshall, A. G., Fourier-Transform Ion-Cyclotron Resonance Spectroscopy, *Chemical Physics Letters*, **1974**, *25*, 282-283.

(26) Guan, S.; Marshall, A. G., Ion traps for Fourier transform ion cyclotron resonance mass spectrometry: principles and design of geometric and electric configurations, *International Journal of Mass Spectrometry and Ion Processes*, **1995**, *146-147*, 261-296.

(27) Marshall, A. G.; Hendrickson, C. L.; Jackson, G. S., Fourier transform ion cyclotron resonance mass spectrometry: a primer, *Mass Spectrometry Reviews*, **1998**, *17*, 1-35.

(28) Beu, S. C.; Hendrickson, C. L.; Marshall, A. G., Design Considerations for External Ion Injection FT-ICR MS at 21 Tesla, *The 58th ASMS Conference on Mass Spectrometry and Allied Topics*, Salt Lake City, UT, USA, 2010.

(29) Hakansson, K.; Cooper, H. J.; Hudgins, R. R.; Nilsson, C. L., High resolution tandem mass spectrometry for structural biochemistry, *Current Organic Chemistry*, **2003**, *7*, 1503-1525.

(30) Marshall, A. G.; Hendrickson, C. L., Fourier transform ion cyclotron resonance detection: principles and experimental configurations, *International Journal of Mass Spectrometry*, **2002**, *215*, 59-75.

(31) Amster, I. J., Fourier transform mass spectrometry, *Journal of Mass Spectrometry*, **1996**, *31*, 1325-1337.

(32) Shen, Y.; Tolic, N.; Masselon, C.; Pasa-Tolic, L.; Camp Ii, D. G.; Lipton, M. S.; Anderson, G. A.; Smith, R. D., Nanoscale proteomics, *Analytical and Bioanalytical Chemistry*, **2004**, *378*, 1037-1045.

(33) Zubarev, R. A.; Kelleher, N. L.; McLafferty, F. W., Electron capture dissociation of multiply charged protein cations. A nonergodic process., *Journal of the American Chemical Society*, **1998**, *120*, 3265-3266.

(34) Gauthier, J. W.; Trautman, T. R.; Jacobson, D. B., Sustained off-resonance irradiation for collision-activated dissociation involving Fourier-transform mass spectrometry. Collision-activated dissociation technique that emulates infrared multiphoton dissociation, *Analytica Chimica Acta*, **1991**, *246*, 211-225.

(35) Little, D. P.; Speir, J. P.; Senko, M. W.; O'Connor, P. B.; McLafferty, F. W., Infrared multiphoton dissociation of large multiply charged ions for biomolecule sequencing, *Analytical Chemistry*, **1994**, *66*, 2809-2815.

(36) Marshall, A. G., Milestones in Fourier transform ion cyclotron resonance mass spectrometry technique development, *International Journal of Mass Spectrometry*, **2000**, *200*, 331-356.

(37) Bogdanov, B.; Smith, R. D., Proteomics by FTICR mass spectrometry: Top down and bottom up, *Mass Spectrometry Reviews*, **2005**, *24*, 168-200.

(38) Marshall, A. G.; Hendrickson, C. L.; Shi, S. D. H., Scaling MS plateaus with high-resolution FT-ICRMS, *Analytical Chemistry*, **2002**, *74*, 253A-259A.

(39) Makarov, A., Electrostatic axially harmonic orbital trapping: a high-performance technique of mass analysis, *Analytical Chemistry*, **2000**, *72*, 1156-1162.

(40) Lewis, R. R., Motion of Ions in the Kingdon Trap, *Journal of Applied Physics*, **1982**, *53*, 3975-3980.

(41) Hu, Q. Z.; Noll, R. J.; Li, H. Y.; Makarov, A.; Hardman, M.; Cooks, R. G., The Orbitrap: a new mass spectrometer, *Journal of Mass Spectrometry*, **2005**, *40*, 430-443.

(42) Scigelova, M.; Makarov, A., Orbitrap mass analyzer--overview and applications in proteomics, *Proteomics*, **2006**, *6 Suppl 2*, 16-21.

(43) Zeller, M.; Crone, C.; Mueller, M.; Damoc, E.; Denisov, E.; Makarov, A.; Nolting, D.; Moehring, T., Increased analytical performance on a hybrid iontrap-FTMS mass spectrometer with a compact orbitrap mass analyzer, *The 59th ASMS Conference on Mass Spectrometry and Allied Topics*, Denver, CO, USA, 2011.

(44) Denisov, E.; Damoc, E.; Makarov, A.; Lange, O., Orbitrap mass spectrometry with resolving powers above 500,000 and 1,000,000 on chromatographic time scale, *The 59th ASMS Conference on Mass Spectrometry and Allied Topics*, Denver, CO, USA, 2011.

(45) Damoc, E.; Denisov, E.; Lange, O.; Moehring, T.; Makarov, A., Improving protein analysis in Orbitrap mass spectrometry, *The 59th ASMS Conference on Mass Spectrometry and Allied Topics*, Denver, CO, USA, 2011.

(46) Makarov, A.; Scigelova, M., Coupling liquid chromatography to Orbitrap mass spectrometry, *Journal of Chromatography A*, **2010**, *1217*, 3938-3945.

(47) Scigelova, M.; Makarov, A., Advances in bioanalytical LC-MS using the Orbitrap mass analyzer, *Bioanalysis*, **2009**, *1*, 741-754.

(48) McAlister, G. C.; Berggren, W. T.; Griep-Raming, J.; Horning, S.; Makarov, A.; Phanstiel, D.; Stafford, G.; Swaney, D. L.; Syka, J. E.; Zabrouskov, V.; Coon, J. J., A proteomics grade electron transfer dissociation-enabled hybrid linear ion trap-orbitrap mass spectrometer, *Journal of Proteome Research*, **2008**, *7*, 3127-3136.

(49) Roepstorff, P.; Fohlman, J., Proposal for a common nomenclature for sequence ions in mass spectra of peptides, *Biomedical Mass Spectrometry*, **1984**, *11*, 601.

(50) Senko, M. W.; Speir, J. P.; McLafferty, F. W., Collisional activation of large multiply charged ions using Fourier transform mass spectrometry., *Analytical Chemistry*, **1994**, *66*, 2801-2808.

(51) Johnson, R. S.; Martin, S. A.; Biemann, K.; Stults, J. T.; Watson, J. T., Novel fragmentation process of peptides by collision- induced decomposition in a tandem mass spectrometer: differentiation of leucine and isoleucine., *Analytical Chemistry*, **1987**, *59*, 2621-2625.

(52) Cooper, H. J.; Hakansson, K.; Marshall, A. G., The role of electron capture dissociation in biomolecular analysis, *Mass Spectrometry Reviews*, **2005**, *24*, 201-222.

(53) Leymarie, N.; Costello, C. E.; O'Connor, P. B., Electron capture dissociation initiates a free radical reaction cascade, *Journal of the American Chemical Society*, **2003**, *125*, 8949-8958.

(54) Turecek, F., N-C-alpha bond dissociation energies and kinetics in amide and peptide radicals. Is the dissociation a non-ergodic process?, *Journal of the American Chemical Society*, **2003**, *125*, 5954-5963.

(55) Breuker, K.; Oh, H. B.; Lin, C.; Carpenter, B. K.; McLafferty, F. W., Nonergodic and conformational control of the electron capture dissociation of protein cations, *Proceedings of the National Academy of Sciences of the United States of America*, **2004**, *101*, 14011-14016.

(56) Baba, T.; Hashimoto, Y.; Hasegawa, H.; Hirabayashi, A.; Waki, I., Electron capture dissociation in a radio frequency ion trap, *Analytical Chemistry*, **2004**, *76*, 4263-4266.

(57) McLafferty, F. W.; Horn, D. M.; Breuker, K.; Ge, Y.; Lewis, M. A.; Cerda, B.; Zubarev, R. A.; Carpenter, B. K., Electron capture dissociation of gaseous multiply charged ions by Fourier-transform ion cyclotron resonance, *Journal of the American Society for Mass Spectrometry*, **2001**, *12*, 245-249.

(58) Syrstad, E. A.; Turecek, F., Toward a general mechanism of electron capture dissociation, *Journal of the American Society for Mass Spectrometry*, **2005**, *16*, 208-224.

(59) Li, X.; Lin, C.; Han, L.; Costello, C. E.; O'Connor, P. B., Charge remote fragmentation in electron capture and electron transfer dissociation, *Journal of the American Society for Mass Spectrometry*, **2010**, *21*, 646-656.

(60) Cooper, H. J., Investigation of the presence of b ions in electron capture dissociation mass spectra., *Journal of the American Society for Mass Spectrometry*, **2005**, *16*, 1932-1940.

(61) Tsybin, Y. O.; Haselmann, K. F.; Emmett, M. R.; Hendrickson, C. L.; Marshall, A. G., Charge location directs electron capture dissociation of peptide dications., *Journal of the American Society for Mass Spectrometry*, **2006**, *17*, 1704-1711.

(62) Liu, H. C.; Hakansson, K., Abundant b-type ions produced in electron capture dissociation of peptides without basic amino acid residues., *Journal of the American Society for Mass Spectrometry*, **2007**, *18*, 2007-2013.

(63) Li, X. J.; Cournoyer, J. J.; Lin, C.; O'Connor, P. B., The effect of fixed charge modifications on electron capture dissociation, *Journal of the American Society for Mass Spectrometry*, **2008**, *19*, 1514-1526.

(64) Ben Hamidane, H.; He, H.; Tsybin, O. Y.; Emmett, M. R.; Hendrickson, C. L.; Marshall, A. G.; Tsybin, Y. O., Periodic sequence distribution of product Ion abundances in electron capture dissociation of amphipathic peptides and proteins, *Journal of the American Society for Mass Spectrometry*, **2009**, *20*, 1182-1192.

(65) Chen, X. H.; Turecek, F., The arginine anomaly: Arginine radicals are poor hydrogen atom donors in electron transfer induced dissociations, *Journal of the American Chemical Society*, **2006**, *128*, 12520-12530.

(66) Zubarev, R. A.; Haselmann, K. F.; Budnik, B.; Kjeldsen, F.; Jensen, F., Towards an understanding of the mechanism of electron-capture dissociation: a historical perspective and modern ideas, *European Journal of Mass Spectrometry*, **2002**, *8*, 337-349.

(67) Zubarev, R. A., Reactions of polypeptide ions with electrons in the gas phase, *Mass Spectrometry Reviews*, **2003**, *22*, 57-77.

(68) Turecek, F.; Syrstad, E. A., Mechanism and energetics of intramolecular hydrogen transfer in amide and peptide radicals and cation-radicals, *Journal of the American Chemical Society*, **2003**, *125*, 3353-3369.

(69) O'Connor, P. B.; Lin, C.; Cournoyer, J. J.; Pittman, J. L.; Belyayev, M.; Budnik, B. A., Long-lived electron capture dissociation product ions experience radical migration via hydrogen abstraction, *Journal of the American Society for Mass Spectrometry*, **2006**, *17*, 576-585.

(70) Savitski, M. M.; Kjeldsen, F.; Nielsen, M. L.; Zubarev, R. A., Hydrogen rearrangement to and from radical z fragments in electron capture dissociation of peptides, *Journal of the American Society for Mass Spectrometry*, **2007**, *18*, 113-120.

(71) Lin, C.; Cournoyer, J. J.; O'Connor, P. B., Probing the gas-phase folding kinetics of peptide ions by IR activated DR-ECD, *Journal of the American Society for Mass Spectrometry*, **2008**, *19*, 780-789.

(72) Turecek, F.; Chen, X. H.; Hao, C. T., Where does the electron go? Electron distribution and reactivity of peptide cation radicals formed by electron transfer in the gas phase, *Journal of the American Chemical Society*, **2008**, *130*, 8818-8833.

(73) Panja, S.; Nielsen, S. B.; Hvelplund, P.; Turecek, F., Inverse hydrogen migration in arginine-containing peptide ions upon electron transfer, *Journal of the American Society for Mass Spectrometry*, **2008**, *19*, 1726-1742.

(74) Sohn, C. H.; Chung, C. K.; Yin, S.; Ramachandran, P.; Loo, J. A.; Beauchamp, J. L., Probing the mechanism of electron capture and electron transfer dissociation using tags with variable electron affinity, *Journal of the American Chemical Society*, **2009**, *131*, 5444-5459.

(75) Frison, G.; van der Rest, G.; Turecek, F.; Besson, T.; Lemaire, J.; Maitre, P.; Chamot-Rooke, J., Structure of electron-capture dissociation fragments from charge-tagged peptides probed by tunable infrared multiple photon dissociation, *Journal of the American Chemical Society*, **2008**, *130*, 14916.

(76) Simons, J., Mechanisms for S-S and N-C-alpha bond cleavage in peptide ECD and ETD mass spectrometry, *Chemical Physics Letters*, **2010**, *484*, 81-95.

(77) Syka, J. E. P.; Coon, J. J.; Schroeder, M. J.; Shabanowitz, J.; Hunt, D. F., Peptide and protein sequence analysis by electron transfer dissociation mass spectrometry, *Proceedings of the National Academy of Sciences of the United States of America*, **2004**, *101*, 9528-9533.

(78) Fung, Y. M. E.; Adams, C. M.; Zubarev, R. A., Electron ionization dissociation of singly and multiply charged peptides., *Journal of the American Chemical Society*, **2009**, *131*, 9977-9985.

(79) Enyenihi, A. A.; Baba, T.; Glish, G. L. *57th ASMS Conference*, Electron Ionization Dissociation in a Radio Frequency Linear Ion Trap, *Proceedings of the 57th ASMS Conference*, Philadelphia, PA, June 1 - 5, 2009.

(80) Lioe, H.; O'Hair, R. A., Comparison of collision-induced dissociation and electron-induced dissociation of singly protonated aromatic amino acids, cystine and related simple peptides using a hybrid linear ion trap-FT-ICR mass spectrometer, *Analytical and Bioanalytical Chemistry*, **2007**, *389*, 1429-1437.

(81) Wolff, J. J.; Laremore, T. N.; Aslam, H.; Linhardt, R. J.; Amster, I. J., Electron-induced dissociation of glycosaminoglycan tetrasaccharides, *Journal of the American Society for Mass Spectrometry*, **2008**, *19*, 1449-1458.

(82) Liang, X. L. R.; Liu, J.; Leblanc, Y.; Covey, T.; Ptak, A. C.; Brenna, J. T.; McLuckey, S. A., Electron transfer dissociation of doubly sodiated glycerophosphocholine lipids, *Journal of the American Society for Mass Spectrometry*, **2007**, *18*, 1783-1788.

(83) Yang, J.; Mo, J. J.; Adamson, J. T.; Hakansson, K., Characterization of oligodeoxynucleotides by electron detachment dissociation Fourier-transform ion cyclotron resonance mass spectrometry, *Analytical Chemistry*, **2005**, *77*, 1876-1882.

(84) Zubarev, R. A.; Horn, D. M.; Fridriksson, E. K.; Kelleher, N. L.; Kruger, N. A.; Lewis, M. A.; Carpenter, B. K.; McLafferty, F. W., Electron capture dissociation for structural characterization of multiply charged protein cations, *Analytical Chemistry*, **2000**, *72*, 563-573.

(85) Mikesh, L. M.; Ueberheide, B.; Chi, A.; Coon, J. J.; Syka, J. E. P.; Shabanowitz, J.; Hunt, D. F., The utility of ETD mass spectrometry in proteomic analysis, *Biochimica et Biophysica Acta-Proteins and Proteomics*, **2006**, *1764*, 1811-1822.

(86) Brown, R. S.; Lennon, J. J., Sequence-Specific Fragmentation of Matrix-Assisted Laser-Desorbed Protein Peptide Ions, *Analytical Chemistry*, **1995**, *67*, 3990-3999.

(87) Lennon, J. J.; Walsh, K. A., Direct sequence analysis of proteins by in-source fragmentation during delayed ion extraction, *Protein Science*, **1997**, *6*, 2446-2453.

(88) Takayama, M., N-C-alpha bond cleavage of the peptide backbone via hydrogen abstraction, *Journal of the American Society for Mass Spectrometry*, **2001**, *12*, 1044-1049.

(89) Kocher, T.; Engstrom, A.; Zubarev, R. A., Fragmentation of peptides in MALDI in-source decay mediated by hydrogen radicals, *Analytical Chemistry*, **2005**, *77*, 172-177.

(90) Demeure, K.; Quinton, L.; Gabelica, V.; De Pauw, E., Rational selection of the optimum MALDI matrix for top-down proteomics by in-source decay, *Analytical Chemistry*, **2007**, *79*, 8678-8685.

(91) Asakawa, D.; Takayama, M., C(alpha) - C Bond Cleavage of the Peptide Backbone in MALDI In-Source Decay Using Salicylic Acid Derivative Matrices, *Journal of the American Society for Mass Spectrometry*, **2011**, *22*, 1224-1233.

(92) Asakawa, D.; Takayama, M., Specific cleavage at peptide backbone C(alpha)-C and CO-N bonds during matrix-assisted laser desorption/ionization in-source decay mass spectrometry with 5-nitrosalicylic acid as the matrix, *Rapid Communications in Mass Spectrometry*, **2011**, *25*, 2379-2383.

(93) Smargiasso, N.; Demeure, K.; De Pauw, E., New MALDI matrices inducing radical mediated In-Source Decay of peptides and proteins, *The 59th ASMS Conference on Mass Spectrometry and Allied Topics*, Denver, CO, USA, 2011.

(94) Jagannadham, M. V.; Nagaraj, R., Detecting the site of phosphorylation in phosphopeptides without loss of phosphate group using MALDI TOF mass spectrometry, *Analytical Chemistry Insights*, **2008**, *3*, 21-29.

(95) Soltwisch, J.; Dreisewerd, K., Discrimination of isobaric leucine and isoleucine residues and analysis of post-translational modifications in peptides by MALDI in-source decay mass spectrometry combined with collisional cooling, *Analytical Chemistry*, **2010**, *82*, 5628-5635.

(96) Demeure, K.; Gabelica, V.; De Pauw, E. A., New Advances in the Understanding of the In-Source Decay Fragmentation of Peptides in MALDI-TOF-MS, *Journal of the American Society for Mass Spectrometry*, **2010**, *21*, 1906-1917.

(97) Scheffler, K.; Arrey, T.; Strupat, K., A-, B-, C-, D-, W-, Y- and Z-Ions of Peptides and Proteins Generated Simultaneously by MALDI In-Source Decay, *The 59th*

ASMS Conference on Mass Spectrometry and Allied Topics, Denver, CO, USA, 2011.

(98) Bache, N.; Rand, K. D.; Roepstorff, P.; Jorgensen, T. J., Gas-phase fragmentation of peptides by MALDI in-source decay with limited amide hydrogen (1H/2H) scrambling, *Analytical Chemistry*, **2008**, *80*, 6431-6435.

(99) Zimmerman, T. A.; Debois, D.; Mazzucchelli, G.; Bertrand, V.; De Pauw-Gillet, M. C.; De Pauw, E., An Analytical Pipeline for MALDI In-Source Decay Mass Spectrometry Imaging, *Analytical Chemistry*, **2011**, *83*, 6090-6097.

(100) O'Connor, P. B.; Pittman, J. L.; Thomson, B. A.; Budnik, B. A.; Cournoyer, J. C.; Jebanathirajah, J.; Lin, C.; Moyer, S.; Zhao, C., A new hybrid electrospray Fourier-transform mass spectrometer: design and performance characteristics, *Rapid Communications in Mass Spectrometry*, **2006**, *20*, 259-266.

(101) Tsybin, Y. O.; Hakansson, P.; Budnik, B. A.; Haselmann, K. F.; Kjeldsen, F.; Gorshkov, M.; Zubarev, R. A., Improved low-energy electron injection systems for high rate electron capture dissociation in Fourier transform ion cyclotron resonance mass spectrometry, *Rapid Communications in Mass Spectrometry*, **2001**, *15*, 1849-1854.

(102) Jebanathirajah, J. A.; Pittman, J. L.; Thomson, B. A.; Budnik, B. A.; Kaur, P.; Rape, M.; Kirschner, M.; Costello, C. E.; O'Connor, P. B., Characterization of a new qQq-FTICR mass spectrometer for post-translational modification analysis and top-down tandem mass spectrometry of whole proteins., *Journal of the American Society for Mass Spectrometry*, **2005**, *16*, 1985-1999.

(103) Tsybin, Y. O.; Witt, M.; Baykut, G.; Kjeldsen, F.; Hakansson, P., Combined infrared multiphoton dissociation and electron capture dissociation with a hollow electron beam in Fourier transform ion cyclotron resonance mass spectrometry, *Rapid Communications in Mass Spectrometry*, **2003**, *17*, 1759-1768.

(104) Alpert, A. J., Hydrophilic-interaction chromatography for the separation of peptides, nucleic acids and other polar compounds, *Journal of Chromatography*, **1990**, *499*, 177-196.

(105) Alpert, A. J., Electrostatic repulsion hydrophilic interaction chromatography for isocratic separation of charged solutes and selective isolation of phosphopeptides, *Analytical Chemistry*, **2008**, *80*, 62-76.

(106) Molnar, I.; Horvath, C., Reverse-phase chromatography of polar biological substances: separation of catechol compounds by high-performance liquid chromatography, *Clinical Chemistry*, **1976**, *22*, 1497-1502.

(107) Annesley, T. M., Ion suppression in mass spectrometry, *Clinical Chemistry*, **2003**, *49*, 1041-1044.

(108) Clarke, S., Propensity for spontaneous succinimide formation from aspartyl and asparaginyl residues in cellular proteins, *International Journal of Peptide and Protein Research*, **1987**, *30*, 808-821.

(109) Geiger, T.; Clarke, S., Deamidation, isomerization, and racemization at asparaginyl and aspartyl residues in peptides-succinimide-linked reactions that contribute to protein-degradation., *Journal of Biological Chemistry*, **1987**, *262*, 785-794.

(110) Harris, R. J.; Kabakoff, B.; Macchi, F. D.; Shen, F. J.; Kwong, M.; Andya, J. D.; Shire, S. J.; Bjork, N.; Totpal, K.; Chen, A. B., Identification of multiple sources of charge heterogeneity in a recombinant antibody, *Journal of Chromatography B*, **2001**, *752*, 233-245.

(111) Xiao, G.; Bondarenko, P. V.; Jacob, J.; Chu, G. C.; Chelius, D., O-18 labeling method for identification and quantification of succinimide in proteins, *Analytical Chemistry*, **2007**, *79*, 2714-2721.

(112) Robinson, N. E.; Robinson, A. B., Molecular clocks, *Proceedings of the National Academy of Sciences of the United States of America*, **2001**, *98*, 944-949.

(113) Stephenson, R. C.; Clarke, S., Succinimide formation from aspartyl and asparaginyl peptides as a model for the spontaneous degradation of proteins, *The Journal of Biological Chemistry*, **1989**, *264*, 6164-6170.

(114) Ritz-Timme, S.; Collins, M. J., Racemization of aspartic acid in human proteins, *Ageing Research Reviews*, **2002**, *1*, 43-59.

(115) Robinson, N. E.; Robinson, Z. W.; Robinson, B. R.; Robinson, A. L.; Robinson, J. A.; Robinson, M. L.; Robinson, A. B., Structure-dependent nonenzymatic deamidation of glutaminyl and asparaginyl pentapeptides, *Journal of Peptide Research*, **2004**, *63*, 426-436.

(116) Peters, B.; Trout, B. L., Asparagine deamidation: pH-dependent mechanism from density functional theory, *Biochemistry*, **2006**, *45*, 5384-5392.

(117) Wakankar, A. A.; Borchardt, R. T., Formulation considerations for proteins susceptible to asparagine deamidation and aspartate isomerization, *Journal of Pharmaceutical Sciences*, **2006**, *95*, 2321-2336.

(118) Fujii, N.; Ishibashi, Y.; Satoh, K.; Fujino, M.; Harada, K., Simultaneous racemization and isomerization at specific aspartic acid residues in alpha B-crystallin from the aged human lens, *Biochim Biophys Acta*, **1994**, *1204*, 157-163.

(119) Roher, A. E.; Lowenson, J. D.; Clarke, S.; Wolkow, C.; Wang, R.; Cotter, R. J.; Reardon, I. M.; Zurcherneely, H. A.; Heinrikson, R. L.; Ball, M. J.; Greenberg, B. D., Structural alterations in the peptide backbone of beta-amyloid core protein may account for its deposition and stability in Alzheimer's disease., *Journal of Biological Chemistry*, **1993**, *268*, 3072-3083.

(120) Shimizu, T.; Matsuoka, Y.; Shirasawa, T., Biological significance of isoaspartate and its repair system, *Biological & Pharmaceutical Bulletin*, **2005**, *28*, 1590-1596.

(121) Nilsson, M. R.; Driscoll, M.; Raleigh, D. P., Low levels of asparagine deamidation can have a dramatic effect on aggregation of amyloidogenic peptides: Implications for the study of amyloid formation, *Protein Science*, **2002**, *11*, 342-349.

(122) Deverman, B. E.; Cook, B. L.; Manson, S. R.; Niederhoff, R. A.; Langer, E. M.; Rosova, I.; Kulans, L. A.; Fu, X. Y.; Weinberg, J. S.; Heinecke, J. W.; Roth, K. A.; Weintraub, S. J., Bcl-X-L deamidation is a critical switch in the regulation of the response to DNA damage, *Cell*, **2002**, *111*, 51-62.

(123) Shimizu, T.; Watanabe, A.; Ogawara, M.; Mori, H.; Shirasawa, T., Isoaspartate formation and neurodegeneration in Alzheimer's disease, *Archives of Biochemistry and Biophysics*, **2000**, *381*, 225-234.

(124) Noguchi, S., Structural changes induced by the deamidation and isomerization of asparagine revealed by the crystal structure of Ustilago sphaerogena ribonuclease U2B, *Biopolymers*, **2010**, *93*, 1003-1010.

(125) Rehder, D. S.; Chelius, D.; McAuley, A.; Dillon, T. M.; Xiao, G.; Crouse-Zeineddini, J.; Vardanyan, L.; Perico, N.; Mukku, V.; Brems, D. N.; Matsumura, M.; Bondarenko, P. V., Isomerization of a single aspartyl residue of anti-epidermal growth factor receptor immunoglobulin gamma2 antibody highlights the role avidity plays in antibody activity, *Biochemistry*, **2008**, *47*, 2518-2530.

(126) Hambly, D. M.; Banks, D. D.; Scavezze, J. L.; Siska, C. C.; Gadgil, H. S., Detection and quantitation of IgG 1 hinge aspartate isomerization: a rapid degradation in stressed stability studies, *Analytical Chemistry*, **2009**, *81*, 7454-7459.

(127) Kameoka, D.; Ueda, T.; Imoto, T., A method for the detection of asparagine deamidation and aspartate isomerization of proteins by MALDI/TOF-mass spectrometry using endoproteinase Asp-N, *Journal of Biochemistry*, **2003**, *134*, 129-135.

(128) Lapko, V. N.; Purkiss, A. G.; Smith, D. L.; Smith, J. B., Deamidation in human gamma S-crystallin from cataractous lenses is influenced by surface exposure, *Biochemistry*, **2002**, *41*, 8638-8648.

(129) Zhang, W.; Czupryn, J. M.; Boyle, P. T., Jr.; Amari, J., Characterization of asparagine deamidation and aspartate isomerization in recombinant human interleukin-11, *Pharmaceutical Research*, **2002**, *19*, 1223-1231.

(130) Johnson, B. A.; Aswad, D. W., Fragmentation of isoaspartyl peptides and proteins by carboxypeptidase Y: release of isoaspartyl dipeptides as a result of internal and external cleavage, *Biochemistry*, **1990**, *29*, 4373-4380.

(131) Clarke, S., Aging as war between chemical and biochemical processes: protein methylation and the recognition of age-damaged proteins for repair, *Ageing Research Reviews*, **2003**, *2*, 263-285.

(132) Reissner, K. J.; Aswad, D. W., Deamidation and isoaspartate formation in proteins: unwanted alterations or surreptitious signals?, *Cellular and Molecular Life Sciences*, **2003**, *60*, 1281-1295.

(133) Kim, E.; Lowenson, J. D.; MacLaren, D. C.; Clarke, S.; Young, S. G., Deficiency of a protein-repair enzyme results in the accumulation of altered proteins, retardation of growth, and fatal seizures in mice, *Proceedings of the National Academy of Sciences of the United States of America*, **1997**, *94*, 6132-6137.

(134) Madan, A.; El-Ferzli, G.; Carlson, S. M.; Whitin, J. C.; Schilling, J.; Najmi, A.; Yu, T. T.; Lau, K.; Dimmitt, R. A.; Cohen, H. J., A potential biomarker in the cord blood of preterm infants who develop retinopathy of prematurity, *Pediatric Research*, **2007**, *61*, 215-221.

(135) Curnis, F.; Sacchi, A.; Gasparri, A.; Longhi, R.; Bachi, A.; Doglioni, C.; Bordignon, C.; Traversari, C.; Rizzardi, G. P.; Corti, A., Isoaspartate-glycine-arginine: a new tumor vasculature-targeting motif, *Cancer Research*, **2008**, *68*, 7073-7082.

(136) Manning, M. C.; Patel, K.; Borchardt, R. T., Stability of protein pharmaceuticals, *Pharmaceutical Research*, **1989**, *6*, 903-918.

(137) Zomber, G.; Reuveny, S.; Garti, N.; Shafferman, A.; Elhanany, E., Effects of spontaneous deamidation on the cytotoxic activity of the Bacillus anthracis protective antigen, *Journal of Biological Chemistry*, **2005**, *280*, 39897-39906.

(138) Seebach, D.; Overhand, M.; Kuhnle, F. N. M.; Martinoni, B.; Oberer, L.; Hommel, U.; Widmer, H., Beta-peptides: Synthesis by Arndt-Eistert homologation with concomitant peptide coupling. Structure determination by NMR and CD spectroscopy and by X-ray crystallography. Helical secondary structure of a beta-hexapeptide in solution and its stability towards pepsin, *Helvetica Chimica Acta*, **1996**, *79*, 913-941.

(139) Appella, D. H.; Christianson, L. A.; Karle, I. L.; Powell, D. R.; Gellman, S. H., beta-peptide foldamers: Robust Helix formation in a new family of beta-amino acid oligomers, *Journal of the American Chemical Society*, **1996**, *118*, 13071-13072.

(140) Seebach, D.; Matthews, J. L., Beta-peptides: a surprise at every turn, *Chemical Communications*, **1997**, 2015-2022.

(141) Disney, M. D.; Hook, D. F.; Namoto, K.; Seeberger, P. H.; Seebach, D., N-linked glycosylated beta-peptides are resistant to degradation by glycoamidase A, *Chemistry & Biodiversity*, **2005**, *2*, 1624-1634.

(142) Seebach, D.; Beck, A. K.; Bierbaum, D. J., The world of beta- and gamma-peptides comprised of homologated proteinogenic amino acids and other components, *Chemistry & Biodiversity*, **2004**, *1*, 1111-1239.

(143) Weiss, H. M.; Wirz, B.; Schweitzer, A.; Amstutz, R.; Perez, M. I. R.; Andres, H.; Metz, Y.; Gardiner, J.; Seebach, D., ADME investigations of unnatural peptides: Distribution of a C-14-labeled beta(3)-octaarginine in rats, *Chemistry & Biodiversity*, **2007**, *4*, 1413-1437.

(144) Seebach, D.; Gardiner, J., Beta-peptidic peptidomimetics, *Accounts of Chemical Research*, **2008**, *41*, 1366-1375.

(145) Kritzer, J. A.; Lear, J. D.; Hodsdon, M. E.; Schepartz, A., Helical beta-peptide inhibitors of the p53-hDM2 interaction, *Journal of the American Chemical Society*, **2004**, *126*, 9468-9469.

(146) Namoto, K.; Gardiner, J.; Kimmerlin, T.; Seebach, D., Investigation of the interactions of beta-peptides with DNA duplexes by circular dichroism spectroscopy, *Helvetica Chimica Acta*, **2006**, *89*, 3087-3103.

(147) Porter, E. A.; Wang, X.; Lee, H. S.; Weisblum, B.; Gellman, S. H., Non-haemolytic beta-amino-acid oligomers, *Nature*, **2000**, *404*, 565.

(148) Selkoe, D. J., Normal and abnormal biology of the beta-amyloid precursor protein, *Annual Review of Neuroscience*, **1994**, *17*, 489-517.

(149) Glenner, G. G.; Wong, C. W., Alzheimer's disease: initial report of the purification and characterization of a novel cerebrovascular amyloid protein., *Biochemical and Biophysical Research Communications*, **1984**, *120*, 885-890.

(150) Masters, C. L.; Simms, G.; Weinman, N. A.; Multhaup, G.; McDonald, B. L.; Beyreuther, K., Amyloid plaque core protein in Alzheimer disease and Down syndrome, *Proceedings of the National Academy of Sciences of the United States of America*, **1985**, *82*, 4245-4249.

(151) Hardy, J.; Selkoe, D. J., Medicine - The amyloid hypothesis of Alzheimer's disease: Progress and problems on the road to therapeutics, *Science*, **2002**, *297*, 353-356.

(152) Roher, A. E.; Esh, C. L.; Kokjohn, T. A.; Castano, E. M.; Van Vickle, G. D.; Kalback, W. M.; Patton, R. L.; Luehrs, D. C.; Daugs, I. D.; Kuo, Y. M.; Emmerling, M. R.; Soares, H.; Quinn, J. F.; Kaye, J.; Connor, D. J.; Silverberg, N. B.; Adler, C. H.; Seward, J. D.; Beach, T. G.; Sabbagh, M. N., Amyloid beta peptides in

human plasma and tissues and their significance for Alzheimer's disease, *Alzheimers & Dementia*, **2009**, *5*, 18-29.

(153) Capasso, S., Thermodynamic parameters of the reversible isomerization of aspartic residues via a succinimide derivative, *Thermochimica Acta*, **1996**, *286*, 41-50.

(154) Aswad, D. W.; Paranandi, M. V.; Schurter, B. T. *3rd Symposium on the Analysis of Well Characterized Biotechnology Pharmaceuticals*, Isoaspartate in peptides and proteins: formation, significance, and analysis, *3rd Symposium on the Analysis of Well Characterized Biotechnology Pharmaceuticals*, Washington, D.C., January, 07, 1999; Pergamon-Elsevier Science Ltd; 1129-1136.

(155) Bohme, L.; Bar, J. W.; Hoffmann, T.; Manhart, S.; Ludwig, H. H.; Rosche, F.; Demuth, H. U., Isoaspartate residues dramatically influence substrate recognition and turnover by proteases, *5th General Meeting of the International-Proteolysis-Society*, Patras, Greece, Oct 20-24, 2007; Walter De Gruyter & Co; 1043-1053.

(156) Grabowski, T. J.; Cho, H. S.; Vonsattel, J. P. G.; Rebeck, G. W.; Greenberg, S. M., Novel amyloid precursor protein mutation in an Iowa family with dementia and severe cerebral amyloid angiopathy, *Annals of Neurology*, **2001**, *49*, 697-705.

(157) Wakutani, Y.; Watanabe, K.; Adachi, Y.; Wada-Isoe, K.; Urakami, K.; Ninomiya, H.; Saido, T. C.; Hashimoto, T.; Iwatsubo, T.; Nakashima, K., Novel amyloid precursor protein gene missense mutation (D678N) in probable familial Alzheimer's disease, *Journal of Neurology Neurosurgery and Psychiatry*, **2004**, *75*, 1039-1042.

(158) Shin, Y.; Cho, H. S.; Fukumoto, H.; Shimizu, T.; Shirasawa, T.; Greenberg, S. M.; Rebeck, G. W., A beta species, including IsoAsp23 A beta, in Iowa-type familial cerebral amyloid angiopathy, *Acta Neuropathologica*, **2003**, *105*, 252-258.

(159) Fukuda, H.; Shimizu, T.; Nakajima, M.; Mori, H.; Shirasawa, T., Synthesis, aggregation, and neurotoxicity of the Alzheimer's A beta 1-42 amyloid peptide and its isoaspartyl isomers, *Bioorganic & Medicinal Chemistry Letters*, **1999**, *9*, 953-956.

(160) Murakami, K.; Uno, M.; Masuda, Y.; Shimizu, T.; Shirasawa, T.; Irie, K., Isomerization and/or racemization at Asp23 of A beta 42 do not increase its

aggregative ability, neurotoxicity, and radical productivity in vitro, *Biochemical and Biophysical Research Communications*, **2008**, *366*, 745-751.

(161) Fonseca, M. I.; Head, E.; Velazquez, P.; Cotman, C. W.; Tenner, A. J., The presence of isoaspartic acid in beta-amyloid plaques indicates plaque age, *Experimental Neurology*, **1999**, *157*, 277-288.

(162) Gonzalez, L. J.; Shimizu, T.; Satomi, Y.; Betancourt, L.; Besada, V.; Padron, G.; Orlando, R.; Shirasawa, T.; Shimonishi, Y.; Takao, T., Differentiating alpha- and beta-aspartic acids by electrospray ionization and low-energy tandem mass spectrometry, *Rapid Communications in Mass Spectrometry*, **2000**, *14*, 2092-2102.

(163) Castet, S.; Enjalbal, C.; Fulcrand, P.; Guichou, J. F.; Martinez, J.; Aubagnac, J. L., Characterization of aspartic acid and beta-aspartic acid in peptides by fast-atom bombardment mass spectrometry and tandem mass spectrometry, *Rapid Communications in Mass Spectrometry*, **1996**, *10*, 1934-1938.

(164) Lehmann, W. D.; Schlosser, A.; Erben, G.; Pipkorn, R.; Bossemeyer, D.; Kinzel, V., Analysis of isoaspartate in peptides by electrospray tandem mass spectrometry, *Protein Science*, **2000**, *9*, 2260-2268.

(165) Chelius, D.; Rehder, D. S.; Bondarenko, P. V., Identification and characterization of deamidation sites in the conserved regions of human Immunoglobulin Gamma antibodies, *Analytical Chemistry*, **2005**, *77*, 6004-6011.

(166) Barnes, C. A. S.; Lim, A., Applications of mass spectrometry for the structural characterization of recombinant protein pharmaceuticals, *Mass Spectrometry Reviews*, **2007**, *26*, 370-388.

(167) Takata, T.; Shimo-Oka, T.; Kojima, M.; Miki, K.; Fujii, N., Differential analysis of D-beta-Asp-containing proteins found in normal and infrared irradiated rabbit lens, *Biochemical and Biophysical Research Communications*, **2006**, *344*, 263-271.

(168) De Boni, S.; Oberthur, C.; Hamburger, M.; Scriba, G. K. E., Analysis of aspartyl peptide degradation products by high-performance liquid chromatography and high-performance liquid chromatography-mass spectrometry, *Journal of Chromatography A*, **2004**, *1022*, 95-102.

(169) Adams, C. M.; Zubarev, R. A., Distinguishing and quantifying peptides and proteins containing D-amino acids by tandem mass spectrometry, *Analytical Chemistry*, **2005**, *77*, 4571-4580.

(170) Winter, D.; Pipkorn, R.; Lehmann, W. D., Separation of peptide isomers and conformers by ultra performance liquid chromatography, *Journal of Separation Science*, **2009**, *32*, 1111-1119.

(171) Ni, W.; Dai, S.; Karger, B. L.; Zhou, Z. S., Analysis of isoaspartic Acid by selective proteolysis with Asp-N and electron transfer dissociation mass spectrometry, *Analytical Chemistry*, **2010**, *82*, 7485-7491.

(172) Teshima, G.; Porter, J.; Yim, K.; Ling, V.; Guzzetta, A., Deamidation of Soluble Cd4 at Asparagine-52 Results in Reduced Binding-Capacity for the Hiv-1 Envelope Glycoprotein Gp120, *Biochemistry*, **1991**, *30*, 3916-3922.

(173) Terashima, I.; Koga, A.; Nagai, H., Identification of deamidation and isomerization sites on pharmaceutical recombinant antibody using (H2O)-O-18, *Analytical Biochemistry*, **2007**, *368*, 49-60.

(174) Liu, P. R.; Regnier, F. E., Recognizing single amino acid polymorphism in proteins, *Analytical Chemistry*, **2003**, *75*, 4956-4963.

(175) Alfaro, J. F.; Gillies, L. A.; Sun, H. G.; Dai, S. J.; Zang, T. Z.; Klaene, J. J.; Kim, B. J.; Lowenson, J. D.; Clarke, S. G.; Karger, B. L.; Zhou, Z. S., Chemo-enzymatic detection of protein isoaspartate using protein Isoaspartate methyltransferase and hydrazine trapping, *Analytical Chemistry*, **2008**, *80*, 3882-3889.

(176) Cournoyer, J. J.; Pittman, J. L.; Ivleva, V. B.; Fallows, E.; Waskell, L.; Costello, C. E.; O'Connor, P. B., Deamidation: Differentiation of aspartyl from isoaspartyl products in peptides by electron capture dissociation, *Protein Science*, **2005**, *14*, 452-463.

(177) Cournoyer, J. J.; Lin, C.; O'Connor, P. B., Detecting deamidation products in proteins by electron capture dissociation, *Analytical Chemistry*, **2006**, *78*, 1264-1271.

(178) Cournoyer, J. J.; Lin, C.; Bowman, M. J.; O'Connor, P. B., Quantitating the relative abundance of isoaspartyl residues in deamidated proteins by electron

capture dissociation, *Journal of the American Society for Mass Spectrometry*, **2007**, *18*, 48-56.

(179) Cooper, H. J.; Hudgins, R. R.; Hakansson, K.; Marshall, A. G., Secondary fragmentation of linear peptides in electron capture dissociation, *Symposium in Honor of Helmut Schwaz*, Berlin, Germany, Aug, 2003; Elsevier Science Bv; 723-728.

(180) Falth, M.; Savitski, M. M.; Nielsen, M. L.; Kjeldsen, F.; Andren, P. E.; Zubarev, R. A., Analytical utility of small neutral losses from reduced species in electron capture dissociation studied using SwedECD database, *Analytical Chemistry*, **2008**, *80*, 8089-8094.

(181) Tsybin, Y. O.; He, H.; Emmett, M. R.; Hendrickson, C. L.; Marshall, A. G., Ion activation in electron capture dissociation to distinguish between N-terminal and C-terminal productions, *Analytical Chemistry*, **2007**, *79*, 7596-7602.

(182) Lin, C.; O'Connor, P. B.; Cournoyer, J. J., Use of a double resonance electron capture dissociation experiment to probe fragment intermediate lifetimes, *Journal of the American Society for Mass Spectrometry*, **2006**, *17*, 1605-1615.

(183) Li, X. J.; Cournoyer, J. J.; Lin, C.; O'Cormora, P. B., Use of O-18 labels to monitor deamidation during protein and peptide sample processing, *Journal of the American Society for Mass Spectrometry*, **2008**, *19*, 855-864.

(184) Portelius, E.; Tran, A. J.; Andreasson, U.; Persson, R.; Brinkmalm, G.; Zetterberg, H.; Blennow, K.; Westman-Brinkmalm, A., Characterization of amyloid beta peptides in cerebrospinal fluid by an automated immunoprecipitation procedure followed by mass spectrometry, *Journal of Proteome Research*, **2007**, *6*, 4433-4439.

(185) Roher, A. E.; Lowenson, J. D.; Clarke, S.; Woods, A. S.; Cotter, R. J.; Gowing, E.; Ball, M. J., Beta-Amyloid-(1-42) is a major component of cerebrovascular amyloid deposits: implications for the pathology of Alzheimer disease, *Proceedings of the National Academy of Sciences of the United States of America*, **1993**, *90*, 10836-10840.

(186) Kuo, Y. M.; Emmerling, M. R.; VigoPelfrey, C.; Kasunic, T. C.; Kirkpatrick, J. B.; Murdoch, G. H.; Ball, M. J.; Roher, A. E., Water-soluble A beta (N-40, N-42) oligomers in normal and Alzheimer disease brains, *Journal of Biological Chemistry*, **1996**, *271*, 4077-4081.

(187) Huang, L.; Lu, J.; Wroblewski, V. J.; Beals, J. M.; Riggin, R. M., In vivo deamidation characterization of monoclonal antibody by LC/MS/MS, *Analytical Chemistry*, **2005**, *77*, 1432-1439.

(188) Sadakane, Y.; Yamazaki, T.; Nakagomi, K.; Akizawa, T.; Fujii, N.; Tanimura, T.; Kaneda, M.; Hatanaka, Y., Quantification of the isomerization of Asp residue in recombinant human alpha A-crystallin by reversed-phase HPLC, *Journal of Pharmaceutical and Biomedical Analysis*, **2003**, *30*, 1825-1833.

(189) Johnson, B. A.; Shirokawa, J. M.; Hancock, W. S.; Spellman, M. W.; Basa, L. J.; Aswad, D. W., Formation of Isoaspartate at 2 Distinct Sites During Invitro Aging of Human Growth-Hormone, *Journal of Biological Chemistry*, **1989**, *264*, 14262-14271.

(190) Krokhin, O. V.; Antonovici, M.; Ens, W.; Wilkins, J. A.; Standing, K. G., Deamidation of -Asn-Gly- sequences during sample preparation for proteomics: Consequences for MALDI and HPLC-MALDI analysis, *Analytical Chemistry*, **2006**, *78*, 6645-6650.

(191) Sargaeva, N. P.; Goloborodko, A.; Ivanov, A. R.; al, e., UPLC/HPLC combined with Electron Capture Dissociation FTICR MS detection of apsartic acid isomerisation located at different sites within a peptide sequence, *35th Symposium on Liquid Chromatography and Related Topics HPLC-2010*, Boston, MA, USA, June 21-24, 2010.

(192) Babushok, V. I.; Zenkevich, I. G., Retention Characteristics of Peptides in RP-LC: Peptide Retention Prediction, *Chromatographia*, **2010**, *72*, 781-797.

(193) Baczek, T.; Kaliszan, R., Predictions of peptides' retention times in reversed-phase liquid chromatography as a new supportive tool to improve protein identification in proteomics, *Proteomics*, **2009**, *9*, 835-847.

(194) Gorshkov, A. V.; Tarasova, I. A.; Evreinov, V. V.; Savitski, M. M.; Nielsen, M. L.; Zubarev, R. A.; Gorshkov, M. V., Liquid chromatography at critical conditions: Comprehensive approach to sequence-dependent retention time prediction, *Analytical Chemistry*, **2006**, *78*, 7770-7777.

(195) Gorshkov, A. V.; Evreinov, V. V.; Tarasova, I. A.; Gorshkov, M. V., Applicability of the critical chromatography concept to proteomics problems: Dependence of retention time on the sequence of amino acids, *Polymer Science Series B*, **2007**, *49*, 93-107.

(196) Tarasova, I. A.; Gorshkov, A. V.; Evreinov, V. V.; Adams, K.; Zubarev, R. A.; Gorshkov, M. V., Applicability of the critical chromatography concept to proteomics problems: Experimental study of the dependence of peptide retention time on the sequence of amino acids in the chain, *Polymer Science Series A*, **2008**, *50*, 309-321.

(197) Gorshkov, A. V.; Evreinov, V. V.; Tarasova, I. A.; Gorshkov, M. V., Critical Chromatography of Macromolecules as a Tool for Reading the Amino Acid Sequence of Biomacromolecules: Reality or Science Fiction?, *Journal of Analytical Chemistry*, **2010**, *65*, 2-11.

(198) Perlova, T. Y.; Goloborodko, A. A.; Margolin, Y.; Pridatchenko, M. L.; Tarasova, I. A.; Gorshkov, A. V.; Moskovets, E.; Ivanov, A. R.; Gorshkov, M. V., Retention time prediction using the model of liquid chromatography of biomacromolecules at critical conditions in LC-MS phosphopeptide analysis, *PROTEOMICS*, **2010**, *10*, 3458-3468.

(199) Di Donato, A.; Ciardiello, M. A.; de Nigris, M.; Piccoli, R.; Mazzarella, L.; D'Alessio, G., Selective deamidation of ribonuclease A. Isolation and characterization of the resulting isoaspartyl and aspartyl derivatives, *Journal of Biological Chemistry*, **1993**, *268*, 4745-4751.

(200) Zhang, W.; Czupryn, M. J., Analysis of isoaspartate in a recombinant monoclonal antibody and its charge isoforms, *Journal of Pharmaceutical and Biomedical Analysis*, **2003**, *30*, 1479-1490.

(201) Yamazaki, Y.; Fujii, N.; Sadakane, Y., Differentiation and semiquantitative analysis of an isoaspartic acid in human alpha-Crystallin by postsource decay in a curved field reflectron, *Analytical Chemistry*, **2010**, *82*, 6384-6394.

(202) Sargaeva, N. P.; Lin, C.; O'Connor, P. B., Identification of aspartic and isoaspartic acid residues in amyloid beta peptides, Including A beta 1-42, using electron-ion reactions, *Analytical Chemistry*, **2009**, *81*, 9778-9786.

(203) Chan, W. Y. K.; Chan, T. W. D.; O'Connor, P. B., Electron transfer dissociation with supplemental activation to differentiate aspartic and isoaspartic residues in doubly charged peptide cations, *Journal of the American Society for Mass Spectrometry*, **2010**, *21*, 1012-1015.

(204) O'Connor, P. B.; Cournoyer, J. J.; Pitteri, S. J.; Chrisman, P. A.; McLuckey, S. A., Differentiation of aspartic and isoaspartic acids using electron transfer

dissociation, *Journal of the American Society for Mass Spectrometry*, **2006**, *17*, 15-19.

(205) Yang, H. Q.; Fung, E. Y. M.; Zubarev, A. R.; Zubarev, R. A., Toward proteome-scale identification and quantification of isoaspartyl residues in biological samples, *Journal of Proteome Research*, **2009**, *8*, 4615-4621.

(206) Mukherjee, R.; Adhikary, L.; Khedkar, A.; Iyer, H., Probing deamidation in therapeutic immunoglobulin gamma (IgG1) by 'bottom-up' mass spectrometry with electron transfer dissociation, *Rapid Communications in Mass Spectrometry*, **2010**, *24*, 879-884.

(207) Andreazza, H. J.; Wang, T.; Bagley, C. J.; Hoffmann, P.; Bowie, J. H., Negative ion fragmentations of deprotonated peptides. The unusual case of isoAsp: a joint experimental and theoretical study. Comparison with positive ion cleavages, *Rapid Communications in Mass Spectrometry*, **2009**, *23*, 1993-2002.

(208) Sargaeva, N. P.; Goloborodko, A. A.; Moskovets, E.; Gorshkov, M. V.; O'Connor, P. B., Sequence-specific predictive chromatography to assist mass spectrometric analysis of asparagine deamidation and aspartate isomerization in peptides, *Electrophoresis*, **2011**, *32*, 1962-1969.

(209) Robinson, N. E.; Robinson, A. B., Prediction of protein deamidation rates from primary and three-dimensional structure, *Proceedings of the National Academy of Sciences of the United States of America*, **2001**, *98*, 4367-4372.

(210) Horn, D. M.; Ge, Y.; McLafferty, F. W., Activated ion electron capture dissociation for mass spectral sequencing of larger (42 kDa) proteins, *Analytical Chemistry*, **2000**, *72*, 4778-4784.

(211) Swaney, D. L.; McAlister, G. C.; Wirtala, M.; Schwartz, J. C.; Syka, J. E. P.; Coon, J. J., Supplemental activation method for high-efficiency electron-transfer dissociation of doubly protonated peptide precursors, *Analytical Chemistry*, **2007**, *79*, 477-485.

(212) Grundke-Iqbal, I.; Iqbal, K.; Tung, Y. C.; Quinlan, M.; Wisniewski, H. M.; Binder, L. I., Abnormal phosphorylation of the microtubule-associated protein tau (tau) in Alzheimer cytoskeletal pathology, *Proceedings of the National Academy of Sciences of the United States of America*, **1986**, *83*, 4913-4917.

(213) Gouras, G. K.; Tsai, J.; Naslund, J.; Vincent, B.; Edgar, M.; Checler, F.; Greenfield, J. P.; Haroutunian, V.; Buxbaum, J. D.; Xu, H.; Greengard, P.; Relkin, N. R., Intraneuronal Abeta42 accumulation in human brain, *American Journal of Pathology*, **2000**, *156*, 15-20.

(214) De Meyer, G.; Shapiro, F.; Vanderstichele, H.; Vanmechelen, E.; Engelborghs, S.; De Deyn, P. P.; Coart, E.; Hansson, O.; Minthon, L.; Zetterberg, H.; Blennow, K.; Shaw, L.; Trojanowski, J. Q., Diagnosis-independent Alzheimer disease biomarker signature in cognitively normal elderly people, *Archives of Neurology*, **2010**, *67*, 949-956.

(215) Mattsson, N.; Zetterberg, H.; Hansson, O.; Andreasen, N.; Parnetti, L.; Jonsson, M.; Herukka, S. K.; van der Flier, W. M.; Blankenstein, M. A.; Ewers, M.; Rich, K.; Kaiser, E.; Verbeek, M.; Tsolaki, M.; Mulugeta, E.; Rosen, E.; Aarsland, D.; Visser, P. J.; Schroder, J.; Marcusson, J.; de Leon, M.; Hampel, H.; Scheltens, P.; Pirttila, T.; Wallin, A.; Jonhagen, M. E.; Minthon, L.; Winblad, B.; Blennow, K., CSF biomarkers and incipient Alzheimer disease in patients with mild cognitive impairment, *The Journal of the American Medical Association*, **2009**, *302*, 385-393.

(216) Sargaeva, N. P.; Yao, C. X.; Lin, T. Y.; Cui, W. D.; Aizikov, K.; Li, X. J.; Lin, C.; O'Connor, P. B., ECD and EID of Amyloid beta and synthetic beta-peptides., *The 57th ASMS Conference on Mass Spectrometry and Allied Topics*, Philadelphia, PA, May 31 - June 4, 2009.

(217) Sargaeva, N. P.; Lin, C.; O'Connor, P. B., Differentiating N-terminal aspartic and isoaspartic acid residues in peptides, *Analytical Chemistry*, **2011**, *83*, 6675-6682.

(218) Sargaeva, N. P.; Cournoyer, J. J.; Yao, C. X.; Lin, C.; O'Connor, P. B., ECD and IRMPD of amyloid beta protein fragment 1-40 and synthetic beta-linked peptides., *The 56th ASMS Conference on Mass Spectrometry and Allied Topics*, Denver, CO, USA, June 1 - 5, 2008.

(219) Sargaeva, N. P.; Lin, C.; O'Connor, P. B., Is this a trend or coincidence? Unusual fragmentation of beta - amino acid containing peptides., *The 7th Uppsala Conference on Electron Capture and Transfer Dissociation*, Nara, Japan, December 8-10, 2009.

(220) Ben Hamidane, H.; Vorobyev, A.; Larregola, M.; Lukaszuk, A.; Tourwe, D.; Lavielle, S.; Karoyan, P.; Tsybin, Y. O., Radical stability directs electron capture and transfer dissociation of beta-amino acids in peptides, *Chemistry-a European Journal*, **2010**, *16*, 4612-4622.

(221) Cooper, H. J.; Hudgins, R. R.; Marshall, A. G., Electron capture dissociation Fourier-transform ion cyclotron resonance mass spectrometry of cyclodepsipeptides, branched peptides, and epsilon-peptides, *International Journal of Mass Spectrometry*, **2004**, *234*, 23-35.

(222) Lamos, S. M.; Shortreed, M. R.; Frey, B. L.; Belshaw, P. J.; Smith, L. M., Relative quantification of carboxylic acid metabolites by liquid chromatography - mass spectrometry using isotopic variants of cholamine., *Analytical Chemistry*, **2007**, *79*, 5143-5149.

(223) Iavarone, A. T.; Jurchen, J. C.; Williams, E. R., Supercharged protein and peptide ions formed by electrospray ionization, *Analytical Chemistry*, **2001**, *73*, 1455-1460.

(224) Kjeldsen, F.; Giessing, A. M. B.; Ingrell, C. R.; Jensen, O. N., Peptide sequencing and characterization of post-translational modifications by enhanced ion-charging and liquid chromatography electron-transfer dissociation tandem mass spectrometry, *Analytical Chemistry*, **2007**, *79*, 9243-9252.

(225) Liu, H.; Hakansson, K., Electron capture dissociation of tyrosine O-sulfated peptides complexed with divalent metal cations, *Analytical Chemistry*, **2006**, *78*, 7570-7576.

(226) Hunt, D. F., Innovative mass spectrometry for the study of protein post-translational modifications., *The 7th Uppsala Conference on Electron Capture and Transfer Dissociation*, Nara, Japan, December 8-10, 2009.

(227) Xia, Y.; Gunawardena, H. P.; Erickson, D. E.; McLuckey, S. A., Effects of cation charge-site identity and position on electron-transfer dissociation of polypeptide cations, *Journal of the American Chemical Society*, **2007**, *129*, 12232-12243.

(228) Jensen, C. S.; Holm, A. I. S.; Zettergren, H.; Overgaard, J. B.; Hvelplund, P.; Nielsen, S. B., On the charge partitioning between c and z fragments formed after electron-capture induced dissociation of charge-tagged Lys-Lys and Ala-Lys dipeptide dications, *Journal of the American Society for Mass Spectrometry*, **2009**, *20*, 1881-1889.

(229) Li, X. J.; Lin, C.; O'Connor, P. B., Glutamine deamidation: differentiation of glutamic acid and gamma-glutamic acid in peptides by electron capture dissociation, *Journal of the American Society for Mass Spectrometry*, **2010**, *in press*.

(230) Horne, W. S.; Boersma, M. D.; Windsor, M. A.; Gellman, S. H., Sequence-based design of alpha/beta-peptide foldamers that mimic BH3 domains, *Angewandte Chemie-International Edition*, **2008**, *47*, 2853-2856.

(231) Skurski, P.; Sobczyk, M.; Jakowski, J.; Simons, J., Possible mechanisms for protecting N-C-alpha bonds in helical peptides from electron-capture (or transfer) dissociation, *International Journal of Mass Spectrometry*, **2007**, *265*, 197-212.

(232) Yao, C. X.; Syrstad, E. A.; Turecek, F., Electron transfer to protonated beta-alanine N-methylamide in the gas phase: An experimental and computational study of dissociation energetics and mechanisms, *Journal of Physical Chemistry A*, **2007**, *111*, 4167-4180.

(233) Zubarev, R. A.; Kruger, N. A.; Fridriksson, E. K.; Lewis, M. A.; Horn, D. M.; Carpenter, B. K.; McLafferty, F. W., Electron capture dissociation of gaseous multiply-charged proteins is favored at disulfide bonds and other sites of high hydrogen atom affinity, *Journal of the American Chemical Society*, **1999**, *121*, 2857-2862.

(234) Hayakawa, S.; Matsubara, H.; Panja, S.; Hvelplund, P.; Nielsen, S. B.; Chen, X. H.; Turecek, F., Experimental evidence for an inverse hydrogen migration in arginine radicals., *Journal of the American Chemical Society*, **2008**, *130*, 7645-7654.

(235) Bakken, V.; Helgaker, T.; Uggerud, E., Models of fragmentations induced by electron attachment to protonated peptides, *European Journal of Mass Spectrometry*, **2004**, *10*, 625-638.

(236) Jones, A. W.; Cooper, H. J., Probing the mechanisms of electron capture dissociation mass spectrometry with nitrated peptides, *Physical Chemistry Chemical Physics*, **2010**, *12*, 13394-13399.

(237) Paizs, B.; Suhai, S., Fragmentation pathways of protonated peptides, *Mass Spectrometry Reviews*, **2005**, *24*, 508-548.

(238) Syrstad, E. A.; Stephens, D. D.; Turecek, F., Hydrogen atom adducts to the amide bond. Generation and energetics of amide radicals in the gas phase, *Journal of Physical Chemistry A*, **2003**, *107*, 115-126.

(239) Csonka, I. P.; Paizs, B.; Lendvay, G.; Suhai, S., Proton mobility and main fragmentation pathways of protonated lysylglycine, *Rapid Communications in Mass Spectrometry*, **2001**, *15*, 1457-1472.

(240) Dongre, A. R.; Jones, J. L.; Somogyi, A.; Wysocki, V. H., Influence of peptide composition, gas-phase basicity, and chemical modification on fragmentation efficiency: Evidence for the mobile proton model, *Journal of the American Chemical Society*, **1996**, *118*, 8365-8374.

(241) Li, X.; Yu, X.; Lin, C.; Costello, C. E.; O'Connor, P. B., Top-down study of beta-2-microglobulin deamidation, *Manuscript in preparation*.

Curriculum vitae

Nadezda P. Sargaeva

Address: 6103 Stearns Hill Road, Waltham, MA 02451

Email: sargaeva@bu.edu

Year of Birth: 1981

Education

Ph.D. Biochemistry

Boston University School of Medicine, Boston, MA, anticipated May 2012

Thesis title: "Deamidation and related problems in structural analysis of peptides and proteins"

Advisor: Professor Peter B. O'Connor

M.Sc. and B.S. in Physical Electronics

St-Petersburg State Polytechnical University, Russia, 2002, 2004

Concentration: Physics of Medical Technologies

Advisor: Professor Oleg Y. Tsybin

Additional education:

Integrated course of Liquid Separation and Mass Spectrometry, Uppsala University, Sweden, 2003

CUSO PhD Summer School "Frontiers in Mass Spectrometry", EPFL, Switzerland, 2009

Research and Professional Experience

2006 Research assistant, Chemistry department, Joensuu University, Finland. Prof. Pirjo Vainiotalo

2004-2006 Graduate Research Assistant, St-Petersburg State Polytechnical University, Russia. Prof. Oleg Y. Tsybin

2003-2004 Exchange Graduate Research Assistant, the Angstrom Laboratory, Uppsala University, Sweden. Prof. Per Hakansson

2002-2003 Research Assistant, BioAnalytical Center "CSU Analytical Spectrometry", St.-Petersburg, Russia

Selected Publications

- **Sargaeva, N.P**., Yu, X., Costello, C. E., O'Connor, P.B., Lin, C., et.al. In source decay fragmentation can cleave the C_α-C_β bond in peptides producing the diagnostic fragment for isoaspartic acid as well as β-amino acid residues (manuscript in preparation).
- **Sargaeva, N.P**., Lin, C., O'Connor, P.B., Identification of the N-terminal isoaspartic acid residue in peptides, *Analytical Chemistry**,*** **2011,** 83 (17), pp 6675–6682.
- **Sargaeva, N.P**., Lin, C., O'Connor, P.B., Unusual Fragmentation of β-Linked Peptides by ExD Tandem Mass Spectrometry, *Journal of the American Society for Mass Spectrometry*, **2011**, 22 (3), pp 480-491.
- **Sargaeva, N.P**., Goloborodko, A.A., O'Connor, P.B., Moskovets, E., Gorshkov, M.V., Sequence-specific predictive chromatography to assist mass spectrometric analysis of asparagine deamidation and aspartate isomerization in peptides, *Electrophoresis*, **2011**, 32 (15), pp 1962–1969.
- **Sargaeva, N.P**., Lin, C., O'Connor, P.B., Identification of Aspartic and Isoaspartic Acid Residues in Amyloid beta Peptides, Including A*beta* 1-42, Using Electron-Ion Reactions, *Analytical Chemistry**,*** **2009,** 81 (23), pp 9778–9786.
- **Sargaeva N.P.**, Tsybin Y.O., Tsybin O.Y., Hakansson P. "Low-energy electron injection system in Fourier transform ion cyclotron resonance mass spectrometry", *Nauchnoe Priborostroenie (Scientific Instrumentation),* vol.15 (4*)*, **2005**, 51-55 (publication in Russian).

Honors and awards

2010 - Myrna and Carl Franzblau Student Travel Award, invited speaker to the Uppsala Conference on Electron Capture and Transfer Dissociation, Nara, Japan

2004 - The best scientific diploma work within Universities of Russia